Buden

BDM

A Ford Aerospace Company

NEW CONCEPTS FOR COMPACT SPACE REACTOR POWER SYSTEMS FOR SPACE BASED RADAR APPLICATIONS: A Feasibility Study

U4459

Accession Number: 4459

Publication Date: Dec 01, 1989

Title: New Concepts For Compact Space Reactor Power Systems For Space Based Radar Applications: A Feasibility Study

Personal Author: Khan, E.U.; Parlos, A.G.

Corporate Author Or Publisher: BDM International, Inc., 7915 Jones Branch Drive, McLean, VA 22102-339

Descriptors, Keywords: Concept Space Reactor Power System Based Radar Application

Pages: 00100

Cataloged Date: Apr 21, 1993

Document Type: HC

Number of Copies In Library: 000001

Record ID: 26713

BDM INTERNATIONAL, INC.
7915 JONES BRANCH DRIVE
McLEAN, VIRGINIA 22102-3396
(703) 848-5000

A Ford Aerospace Company

NEW CONCEPTS FOR COMPACT SPACE REACTOR POWER SYSTEMS FOR SPACE BASED RADAR APPLICATIONS: A Feasibility Study

Dr. Ehsan U. Khan
Dr. Alexander G. Parlos

December 1989

EXECUTIVE SUMMARY

This report contains the results of a feasibility study on new concepts for compact space reactor power systems for space based radar applications. Notwithstanding the limited scope and duration of the study, the results, which include innovative space reactor configurations and associated technologies indicate promising avenues for the development of compact space reactors. The goal of this work focused on development of new and innovative reactor concepts. Consequently, existing reactor designs, such as the SP-100, are not discussed here, although such power systems are also candidates for space based radar applications.

Ongoing studies on potential future military missions indicate that extremely compact nuclear reactor systems with low specific mass will be required to provide power in the tens to hundreds of kilowatts electric range.

Three new compact reactor concepts are described in this report. These concepts have emerged from an attempt to produce reactor designs that require minimum volume and mass, while making maximum use of available technology. Of the three concepts, two (Concepts A and B) include energy storage subsystems and one does not (Concept C). Concepts A and B involve operation at high power levels for short durations during which energy is stored and then rejected via radiation during the remainder of the orbit cycle. In Concept C the reactor operates continually.

Concept A involves only the use of off-the-shelf technologies. For example, conventional fuel technology (uranium dioxide), conventional thermionic conversion technology, conventional heat pipe technology and proven energy storage technology. Since the materials and technology for this concept have been tested extensively in prototypical environments, this concept would require a relatively small amount of development and testing. Concept B involves use of an advanced fuel (Americium oxide, Am_2O_3) and advanced thermionic conversion. Concept C involves use of an advanced fuel (Americium oxide, Am_2O_3), but conventional thermionic energy conversion technology, no energy storage and conventional heat pipe technology for heat rejection. In the studies undertaken thus far, Concept C has not been investigated to the same degree as Concepts A and B. The reactor volume for Concept C is very small as compared to Concepts A and B which themselves are competitive with existing space nuclear reactor designs. It is important to note that if the Americium oxide fuel (Am_2O_3), in Concept C is replaced by conventional fuel such as UC, the reactor volume is only slightly larger than for Concept C, yet significantly lower than other concepts.

It is recommended that development of Concept B should not be continued since only small gains in mass and volume reduction are achieved but a new fuel and thermionic technology development program is required. In contrast Concept C would result in very significant reductions in reactor mass and volume using conventional thermionic technology and so one could justify a new fuels development

12/8/89
1-7268-89/J-I

program. However note that the use of conventional fuels (UN, UO_2, UC) does not increase the volume of Concept C significantly (see column 8 in Table 1.2 on page 1.5).

It has also been found that compact reactors of the size of Concepts B and C cannot be effectively controlled using in-core control rods. This is because of significant radial neutron leakage and the transparency of the control rods to neutrons. Use of reflector control, on the other hand, would result in an unacceptably large reactor size. To address the issue of reactor control for these new compact reactor concepts, two new control schemes have been introduced which in combination can be effectively used for reactor control. The first scheme involves separating the reactor into two halves and varying the distance between them to provide adequate reactor control. The second scheme employs two rotating control discs at the middle of the reactor.

The new reactor fuel, Am_2O_3, appears to provide a number of benefits which include: low initial fuel loading (for example, one design contains a mixture of about three kilograms of Am_2O_3 and three kilograms of UO_2), low initial activity (about 60% of Pu^{238} activity), potential for using Am^{241} as a burnable poison that converts into fissile Am^{242} , as well as the additional safety margin provided by the use Am^{241} (mixed with Am^{242}) at the launch pad.

In summary, one new concept that uses off-the-shelf technology and energy storage and another new concept that does not use energy storage are proposed and a preliminary feasibility assessment is presented. All of the concepts are shown to be competitive with the most promising alternate designs in the 10 to 30 KW_e power range. Furthermore, Concept C is found to be the most attractive among all candidates as a result of its very low initial fuel loading and very small total system volume. Even though an advanced fuel has been used for this concept, initial results indicate that use of conventional fuels, such as UO_2, UC, and UN, instead of advanced fuels (Am_2O_3) do not substantially diminish its superior advantages. It is recommended that this concept be further developed.

TABLE OF CONTENTS

Section		Page
	EXECUTIVE SUMMARY	i
	TABLE OF CONTENTS	iii
	LIST OF FIGURES	iv
	LIST OF TABLES	vi
	ACKNOWLEDGMENT	vii
1.0	INTRODUCTION	1.1
2.0	CONCEPT DESCRIPTION AND DEVELOPMENT	2.1
	2.1 Fundamental Scoping Studies	2.1
	2.2 Concept Description	2.10
	2.3 Concept Development	2.26
	2.3.1 Reactor Neutronics and Control	2.26
	2.3.2 Off-the-Shelf-Concept Calculations	2.26
	2.3.3 Advanced Concept	2.33
3.0	IDENTIFICATION OF KEY FEASIBILITY ISSUES AND PROGRAM PLAN FOR CONCEPT DEVELOPMENT	3.1
Appendix		
A	(SCOTT NEGRON - TEXAS A&M)	A-1
B	RELEVANT PROPERTIES OF ZIRCONIUM HYDRIDE AND OTHER METAL HYDRIDES	B.1

LIST OF FIGURES

Figure		Page
2.1	Model Used in Scoping Studies	2.3
2.2	Fuel Volume vs. M/F	2.4
2.3	Fuel Volume vs. M/F for AM_2O_3	2.5
2.4	Fuel Volume vs. Moderator to Fuel Ratio for PuC	2.6
2.5	Critical Mass of Bare 100% Homogeneous Spheres of U^{235} Moderated by Be as a Function of Radius and Moderator to U Atom Ratio	2.7
2.6	Total Volume vs. BeO Thickness	2.8
2.7	Fuel Volume vs. BeO Thickness	2.9
2.8	Model for Studying Separation Control Technique	2.11
2.9	k_{eff} vs. Gap for PuC Fuel	2.12
2.10	k_{eff} vs. Gap for Americium Oxide Fuel in a Circular Geometry	2.13
2.11	Schematic Showing Relative Zones of Three Reactor Concepts	2.14
2.12	Schematic Showing Relative Zones of OTS Reactor Concept	2.15
2.13	Typical Dimensions of Conventional TFE and Heat Storage Material	2.16
2.14	Receiver Tube Configuration	2.18
2.15	Garrett Space Station Receiver	2.19
2.16	Schematic Showing Zones of Advanced Energy Storage Concept	2.21
2.17	k_{eff} vs. Enrichment for 61 Rods	2.23
2.18	AM_2O_3 Fueled Reactor Core with No Energy Storage (Concept C)	2.24
2.19	Variation of k_{eff} with Separation and Rotation	2.25
2.20	Off-the-Shelf Technology Core Configuration	2.27
2.21	Equivalent UC or UO_2 Fuel Cell	2.29
2.22	k_{eff} vs. Enrichment for UC Cell	2.31
2.23	Advanced Energy Storage Core Configuration	2.34
2.24	Equivalent AM_2O_3 Fuel Cell	2.35
2.25	k_{eff} vs. Enrichment for AM_2O_3	2.38

LIST OF FIGURES (CONTINUED)

Figure		Page
2.26	k_{eff} vs. Separation Distance for Advanced AM_2O_3	2.41
2.27	Thermal Fuse	2.42
2.28	Side Cutaway View	2.43
2.29	Schematic of a Neutron Disk	2.44
2.30	Availability and Irradiation Experience	2.47
2.31	Americium and Curium Phase Relationships	2.48
2.32	Curium (Cm 2-03) Material Properties	2.49
2.33	Curium (CM_2O_3) Compatibility	2.50
2.34	Thermionic Energy Conversion Principles	2.51
2.35	Thermionic Energy Conversion Characteristics	2.52
2.36	Thermionic Energy Conversion Efficiency	2.53
2.37	Efficiency Improvement for Lower Barrier Index	2.54
2.38	Schematic of In-Core Cell	2.55
2.39	Schematic of In-Core Thermionic Fuel Element (TFE)	2.56
2.40	Thermionic Fuel Element (TFE) Verification Program	2.57
2.41	Thermionic Fuel Element (TFE) Verification Program	2.58
2.42	TFE Verification Program Technical Approach	2.59
2.43	TFE Verification Program Technical Approach (Continued)	2.60
2.44	TFE Verification Program Summary of Technology Findings	2.61
3.1	Generic Program Development Plan	3.4
3.2	Development Schedule for OTS Reactor (Concept A)	3.5

LIST OF TABLES

Table		Page
1.1	NASA TECHNOLOGY MATURITY LEVELS	1.3
1.2	SUMMARY OF KEY REACTOR SYSTEM CHARACTERISTICS	1.5
2.1	RANGE OF SYSTEM PARAMETERS	2.2
2.2	OTS REACTOR (CONCEPT A) PERFORMANCE PARAMETERS	2.20
2.3	FUEL CELL ATOM DENSITIES	2.30
2.4	UC CORE SCENARIOS	2.32
2.5	FUEL CELL ATOM DENSITIES	2.36
2.6	AMERICIUM CORE SCENARIOS	2.39
2.7	AM_2O_3 ADVANCED CORE CONTROL USING SEPARATION	2.45
3.1	KEY TECHNICAL FEASIBILITY ISSUES FOR CONCEPTS A AND C	3.2
3.2	EARLIER PROGRAMS AIDING OTS THERMIONIC REACTOR PROGRAM	3.3

ACKNOWLEDGMENT

The authors sincerely thank Thomas Hunt of Eerim Corporation for valuable discussions on the AMTEC. Tom is an internationally recognized expert on heat engines. The help and contributions of the following individuals are also greatly appreciated: Dr. Rick Moats and Dr. J. N. Burch of BDM International, and Professor K. L. Peddicord, and Messrs. Kelly Thomas, Scott Negron and Richard Frymire of Texas A&M. Dr. E. Abed provided considerable support on evaluation of control systems for compact reactors and Mr. John Uber reviewed the document and provided many useful suggestions.

We appreciate the support of Mr. Richard Verga of the Strategic Defense Initiative Organization for supporting this study.

SECTION 1.0
INTRODUCTION

BDM International has conducted a number of studies for the U.S. Air Force and the Strategic Defense Initiative Organization on the strategy and use of nuclear reactor power sources for space applications. A recent reactor power systems applications study lists a number of potential missions that could be enabled or enhanced by the use of space nuclear power systems. These potential missions include Space Based Radar, the Boost Surveillance and Tracking System (BSTS), the Space Surveillance and Tracking System (SSTS), and others. The Space Based Radar application appears to require higher power levels than those required by the BSTS or SSTS missions. Based on studies that are currently being conducted and that have been recently performed on the integration of a nuclear power system into the SBR and the SSTS spacecraft, certain requirements for nuclear reactor power systems have evolved. These requirements include: minimization of the volume and specific mass (<< 140 Kg/KWe at 20KWe) of the power system, no potential for single point failure, multiple restart capability, enhanced survivability (as compared to a solar power system), minimum heat rejection radiator area, high reliability, adequate safety margin, ease of integration with spacecraft/payload, and reasonable cost and schedule risk. The key requirement appears to be the minimization of the allocation of total mass and volume of the power system in the design of the spacecraft. The purpose of this preliminary study is to develop compact space reactor configurations and to understand the key considerations in the development of a concept for a compact Space Nuclear Power System (SNPS) for a Space Based Radar application.

Ongoing studies on the integration of a Space Based Radar with a nuclear power system show that the radar would probably be located in a 900-4000 mile orbit, with orbit periods from one to several hours. The SBR constellation may consist of a total of 7 to 14 spacecraft operating in orbits with different inclinations. If an SBR is deployed in the mid-90s it will probably employ a solar power source and a large stack of batteries. The solar power system (SPS) continually charges the batteries until the radar is activated, at which point the batteries provide hundreds of kilowatts of electric power to the radar. Battery mass considerations limit the period of operation of the radar to a few minutes in each orbit. The orbit duty cycle is anywhere between 5 and 12 percent. One advantage of using a SNPS could be to increase the orbit duty cycle to 100 percent (with a continually operating reactor) or to increase the orbit duty cycle by a factor of 2 to 3, yet decrease the mass and volume of the power source by the use of a nuclear system rather than a solar power system. The scope of the present study is limited to development of compact nuclear reactor power system configurations that can provide a duty cycle that is several times better than

that of a solar system and at the same time is significantly smaller and lighter than a solar power system. The design of a supercompact reactor power system that can operate continually (100 percent duty cycle) at the peak power required by a radar has been initiated. Some preliminary results are presented here although this work was not within the originally defined scope of this study.

The present approach for developing a compact space reactor power source to replace the solar power system on an SBR spacecraft is fundamental in nature. It required investigating a large number of energy conversion systems and reactor types to determine which systems would best suit the need of the spacecraft. The energy conversion systems investigated include: thermoelectric, thermionic, Rankine/Brayton/Stirling engines and Alkali Metal Thermoelectric Convertors (AMTEC). Reactor types investigated include: actively and passively cooled reactors with a fast, thermal or an epithermal neutron energy spectrum. Based on preliminary studies it was found that energy conversion schemes such as Rankine, Brayton, Stirling or AMTEC may require an actively cooled reactor system (with potential for single point failure); in addition they would require heat transport loops, pumps and/or compressors, accumulators, heat exchangers, valves as well as a large number of other active and passive components which would make the power system bulky and massive. Although the AMTEC technology is extremely promising, there are some key unresolved technical feasibility issues, one of which relates to the operation of AMTEC in close proximity of a nuclear reactor. In other words, it is not clear how exposure to the radiation environment would affect the life and operating capabilities of key components of AMTEC such as the electrode and the BETA-ALUMINA. The in-core thermionic (direct) energy conversion system was selected because it can be packaged in a compact configuration in a reactor that can be passively cooled by heat pipes. The proposed approach consists of an in-core thermionic reactor system that continually operates at low power, except for short periods of time (10 to 20 minutes) when the reactor power is several times the steady state power. The excess heat generated during the high power operations is absorbed in a material with high heat capacity and latent heat of fusion. The heat stored in this material is then gradually dissipated in the remainder of the orbit by heat pipes. Two alternative configurations have been developed. The first is the SNPS that uses only "off-the-shelf" technologies, the technologies for this system have been separately proven at least at the NASA level 3 or 4 (Table 1.1). The second is the SNPS that uses advanced technologies for thermionic energy conversion and advanced reactor fuels in an effort to make the reactor power system even more compact.

The concept that uses off-the-shelf technologies (referred to as the OTS concept vs. the advanced concept) uses proven reactor fuels and materials technologies, proven thermionics technology, energy storage technology that has been hardware tested in the space environment at

TABLE 1.1. NASA TECHNOLOGY MATURITY LEVELS

LEVEL 7 ENGINEERING MODEL TESTED IN SPACE

LEVEL 6 PROTOTYPE/ENGINEERING MODEL TEST IN RELEVANT ENVIRONMENT

LEVEL 5 COMPONENT/BREADBOARD TESTED IN RELEVANT ENVIRONMENT

LEVEL 4 CRITICAL FUNCTION/CHARACTERISTIC DEMONSTRATION

LEVEL 3 CONCEPTUAL DESIGN TESTED ANALYTICALLY OR EXPERIMENTALLY

LEVEL 2 CONCEPTUAL DESIGN FORMULATED

LEVEL 1 BASIC PRINCIPLES OBSERVED AND REPORTED

NASA-Lewis for multiple cycle operations [as the Solar-Dynamic heat receiver module], and proven heat pipe technology. The advanced concept requires advancement in thermionics and fuels technologies. The purpose of investigating the advanced concept is to determine to what extent the OTS concept can be further reduced in size using advanced technologies and then to evaluate the benefits vs. cost of doing this.

Table 1.2 shows a comparison between the relative sizes of conventional thermionic reactor designs and the proposed advanced concept designs. The TOPAZ reactors are actively cooled and thus the total volume does not include the volume of the pumps, heat exchangers, primary heat transport loop, and radiators. The STAR-C and Romashka reactors are conductively cooled, and consequently cannot provide hundreds of kilowatts of electric power without a significant increase in volume and mass. The proposed energy storage space reactor power systems are much more compact than the conventional systems and are extrapolable to much higher power levels. However, as discussed in the next section, the advanced energy storage space reactor power system - a system that uses advanced fuel with energy storage and advanced thermionic energy conversion - is not recommended for further development. The use of advanced fuel in a continually operating in-core thermionics reactor that uses no energy storage and conventional thermionics technology led to the lowest volume system (last column in Table 2). It is recommended that this system be further pursued.

This was a four man-month study to develop compact space reactor configurations and to identify the important factors in the development of a compact nuclear power system for Space Based Radar Application. These factors have been identified and preliminary results have been obtained on compact space nuclear reactor configurations for Space Based Radar Application. These results and a description of the configurations are given in detail in Chapter 2. Chapter 3 identifies the key technology feasibility issues and a program plan for concept development .

TABLE 1.2. SUMMARY OF KEY REACTOR SYSTEM CHARACTERISTICS

PARAMETERS	*TOPAZ*	*TOPAZ*	*STAR-C*	*ROMASHKA*	*MODERATED IN-CORE THERMIONICS*	*PROPOSED SYSTEM*			
						ENERGY STORAGE		*NO ENERGY STORAGE*	
FUEL	UO_2	UO_2	UC_2	UC_2	UZrH	UC**	Am_2O_3	UC	Am_2O_3
DIAMETER (cm) (INCLUDING REFLECTORS)	51	51	66	49	58	86.5	52	32	28
LENGTH (cm)	30	40	144*	40	N.A.	73.5*	46*	32*	28*
FUEL MASS (kg)	35	46	175.5	N.A.	75	497.0	18	18	6.2
TOTAL VOLUME (cc)	61,285	81,713	493,000	75,430	N.A.	432,000	97,000	25,000	16,935
MAXIMUM POWER (KWe)	10	30	30	0.8	30	40	20	30	30

m9-1-MCL1-7268-01

* INCLUDES END REFLECTORS

** RESULTS FOR UO_2 FUEL ARE SIMILAR

SECTION 2.0
CONCEPT DESCRIPTION AND DEVELOPMENT

This section first describes the fundamental scoping studies that were conducted to identify the necessary possible combinations of fuel and materials that would yield compact reactor configurations. Two compact space nuclear power concepts that use energy storage are described in detail, and one of these two concepts is recommended for further development. Initial results on a promising supercompact space nuclear power concept are also given. It is recommended that this concept be further developed.

2.1 FUNDAMENTAL SCOPING STUDIES

Once it was clear that in-core thermionic energy conversion is the most suitable alternative for developing a compact, passive reactor power system, a wide range of system parameters (fuels, materials and reactor control techniques) were investigated to determine which of their combinations would lead to the optimal compact reactor configuration. These parameters and materials are shown in Table 2.1.

Three types of scoping studies were conducted. First, results of studies to estimate the fuel volume and/or mass vs. the moderator-to-fuel ratio for various combinations of the fuel and surrounding moderator are shown in Figure 2.1. The purpose of these fundamental scoping studies is to establish trends on reactor size, reflector thickness, and control separation distances using the simplest possible models. The neutronic models assume a homogeneous fuel lump. Figures 2.2 through 2.4 show typical plots of the variation of Am_2O_3 (Americium Oxide) and PuC fuels with moderator to fuel ratio. It is clear that Am_2O_3 fuel volumes are significantly lower than those required for PuC. Americium Oxide (Am_2O_3) was selected as the fuel of choice over Curium Oxide because of its large neutron fission cross-sections, relative ease of production, and significantly lower cost. Other benefits of Am_2O_3 (specifically Am^{242}) over the alternative transuranic fuels are discussed in Section 2.2. Figure 2.5 shows the variation of the mass of an enriched base 100 percent dense sphere of U^{235} as a function of radius, for different moderator to U atom ratios. Similar parametric studies were also conducted using Am_2O_3 and U^{235} fuel, and ZrH and LiF moderators. The key conclusion derived from these studies is the identification of Am_2O_3 as a promising fuel for compact reactor configurations. The critical mass of the fuel was found to be as low as 6-8 kg in combination with the ZrH moderator.

The second study was conducted to determine the minimum reflector thickness necessary for a small compact reactor core. Figures 2.6 and 2.7 show the variation of the fuel volume and total

TABLE 2.1. RANGE OF SYSTEM PARAMETERS

POWER PRODUCED: 20 - 40 KWe

TIME OF FULL POWER OPERATION:10 -15 MINS IN A (2 -4) HR ORBIT

CONVERSION EFFICIENCY: 8 - 33%

LINE POWER LOSS: 20%

RANGE OF MATERIALS AND DESIGNS INVESTIGATED

FUEL:	**UO_2, UZrC, UN, Am_2O_3, PuC, UC**
CONVERTER:	**CONVENTIONAL, ADVANCED THERMIONICS**
STORAGE:	**LIF, LiH, LiF-CaF**
CONTROL:	**RODS, REFLECTORS**
ADVANCED CONTROL:	**DISCS, SEPARATION**
CLADDING:	**INCONEL, Nb-1Zr**
REFLECTOR:	**BeO**
MODERATOR:	**LIF, ZrH, D_2O**
INTERSTITIAL:	**ZrH, LiH, C**
HEAT PIPE:	**Na, K, NaK**

m9-1-MCL1-7268-02

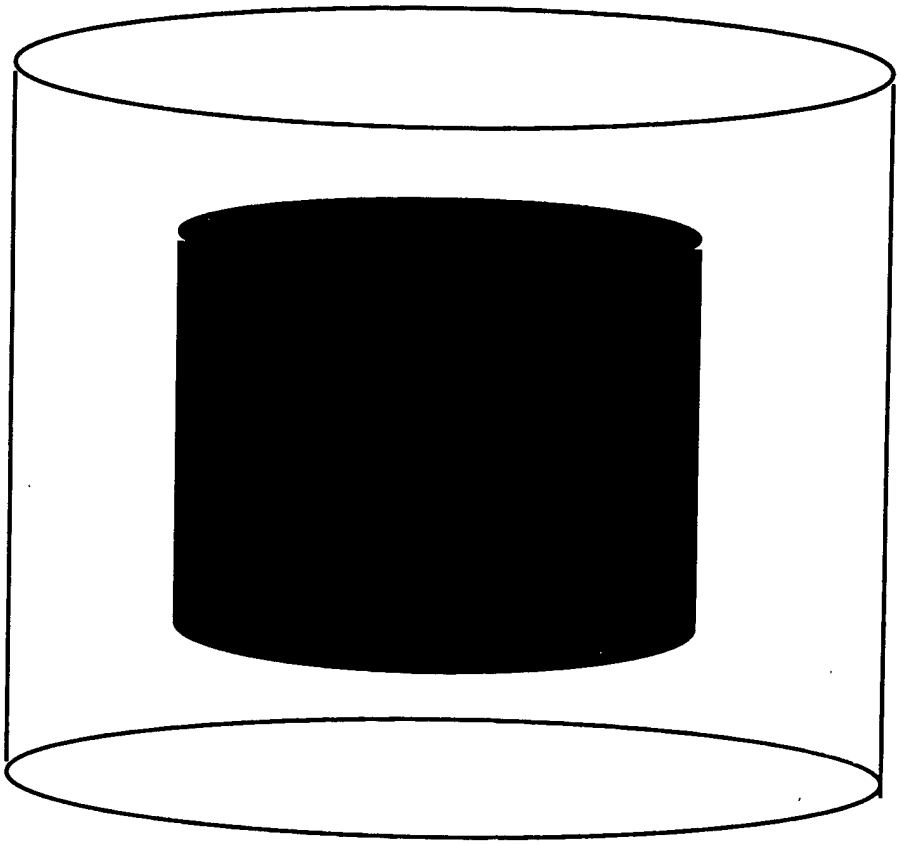

The blackened region is the fuel region surrounded by a moderator region. Above and below the fuel region are two centimeters of moderator.

Figure 2.1. Model Used in Scoping Studies

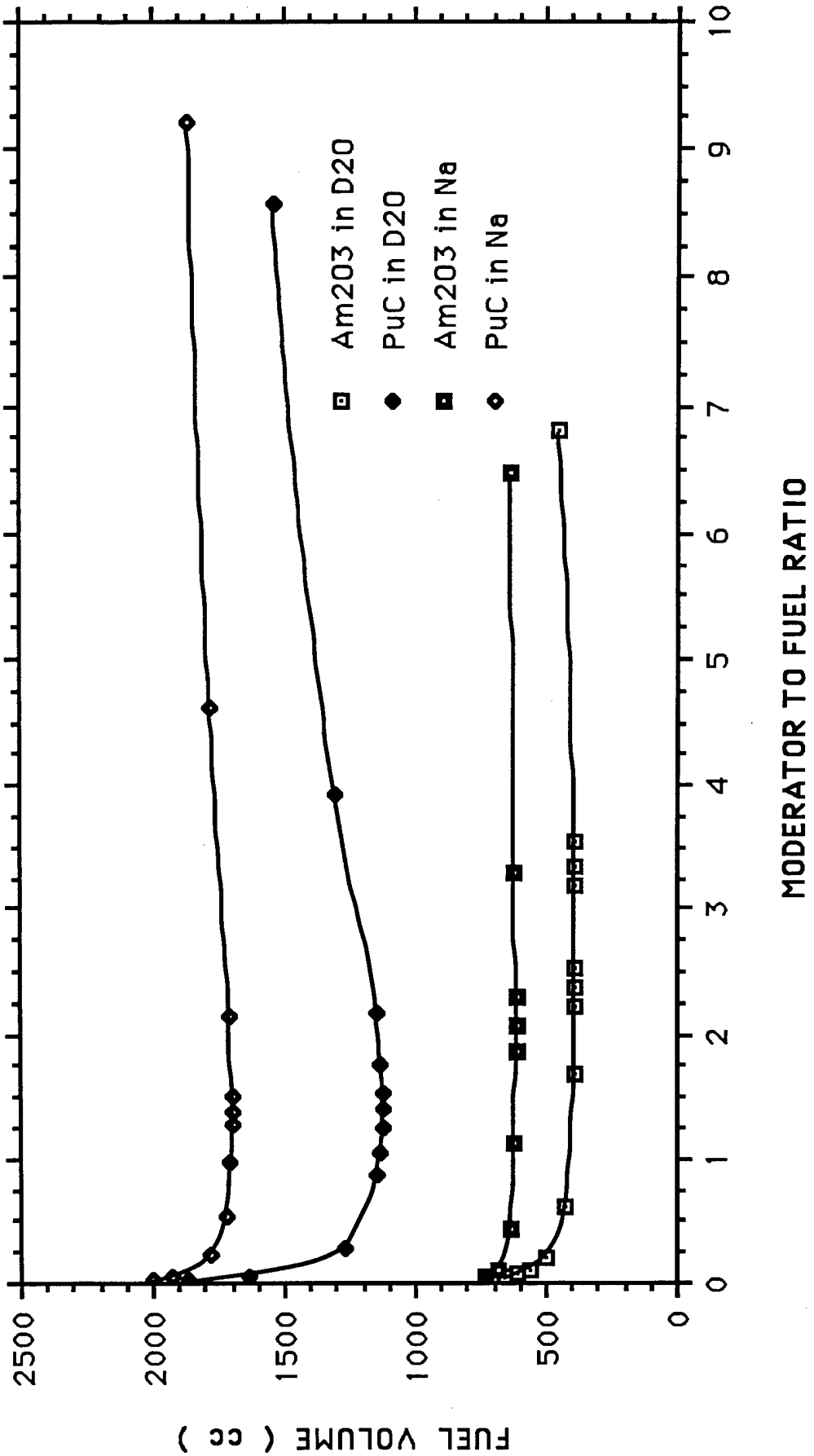

Figure 2.2. Fuel Volume vs. M/F

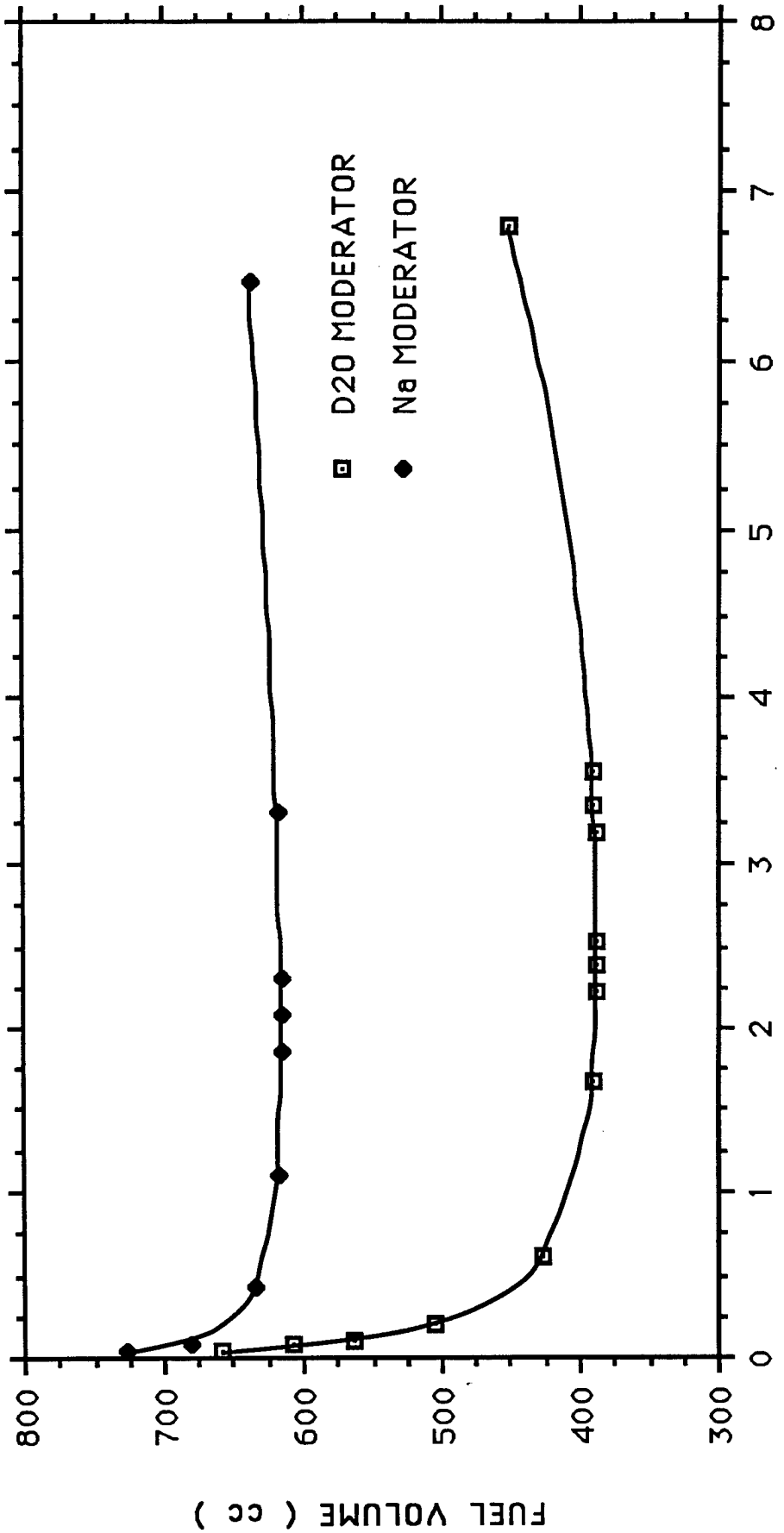

Figure 2.3. Fuel Volume vs. M/F for Am_2O_3Fuel

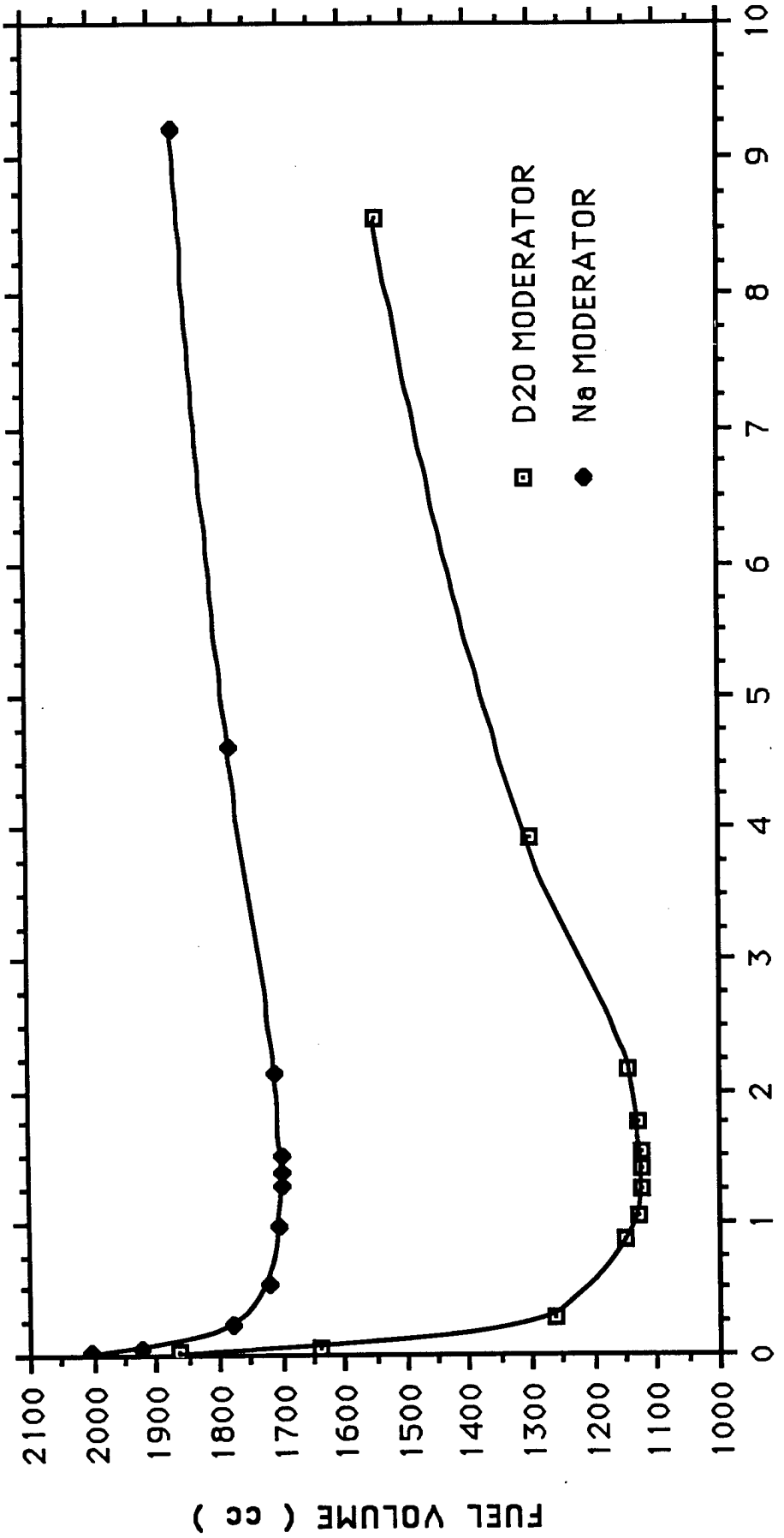

Figure 2.4. Fuel Volume vs. Moderator to Fuel Ratio for PuC

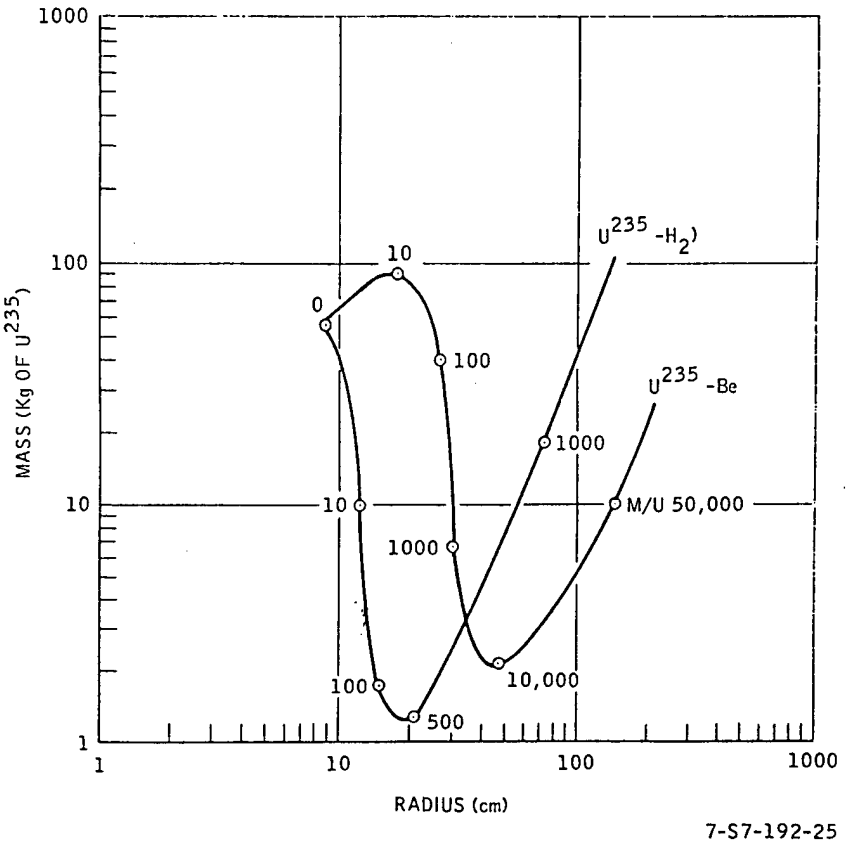

Figure 2.5. Critical Mass of Bare 100% Dense Homogeneous Spheres of U^{235} Moderated by Water and by Be as a Function of Radius and Moderator to U Atom Ratio

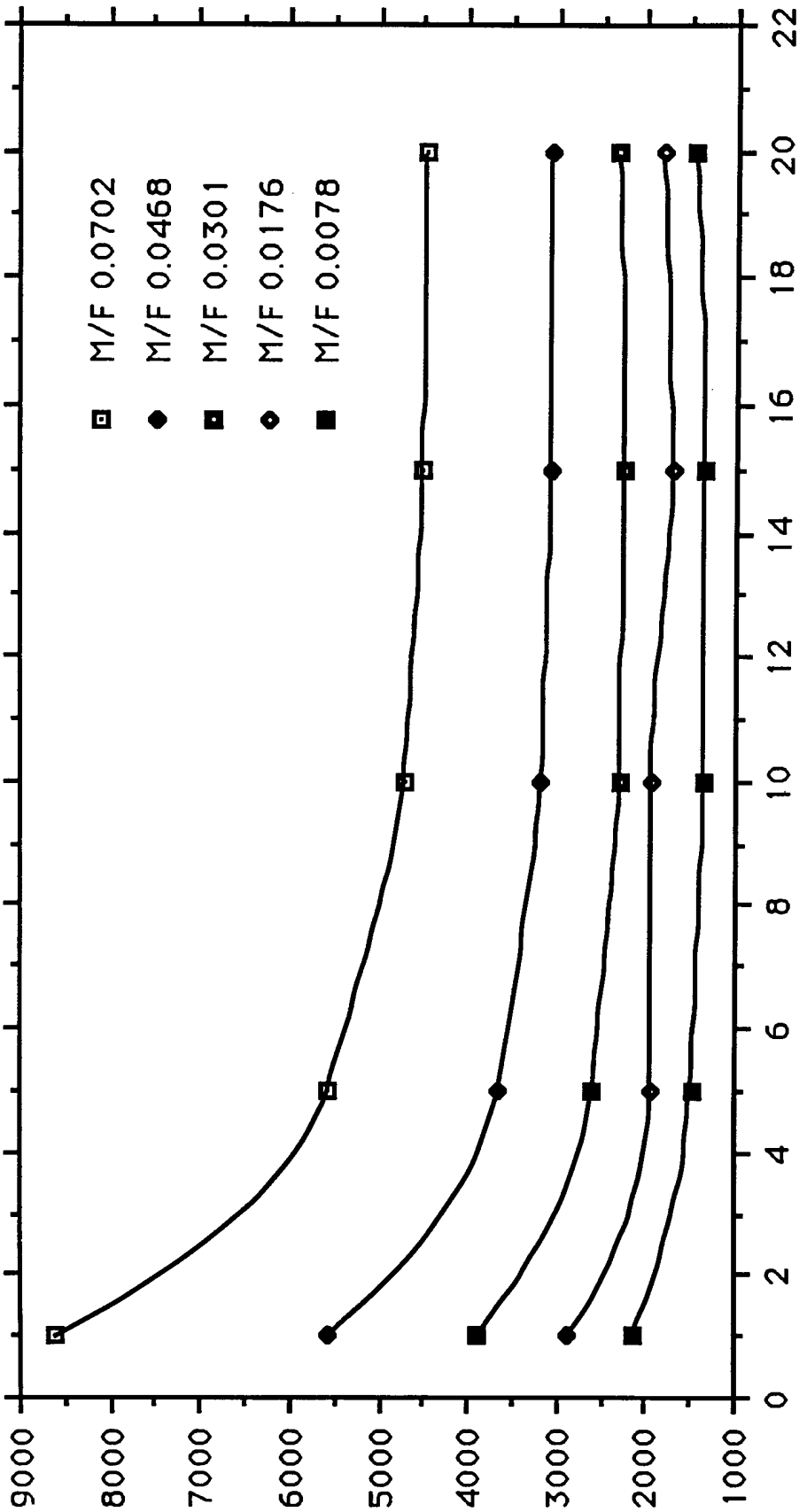

Figure 2.6. Total Volume vs. BeO Thickness

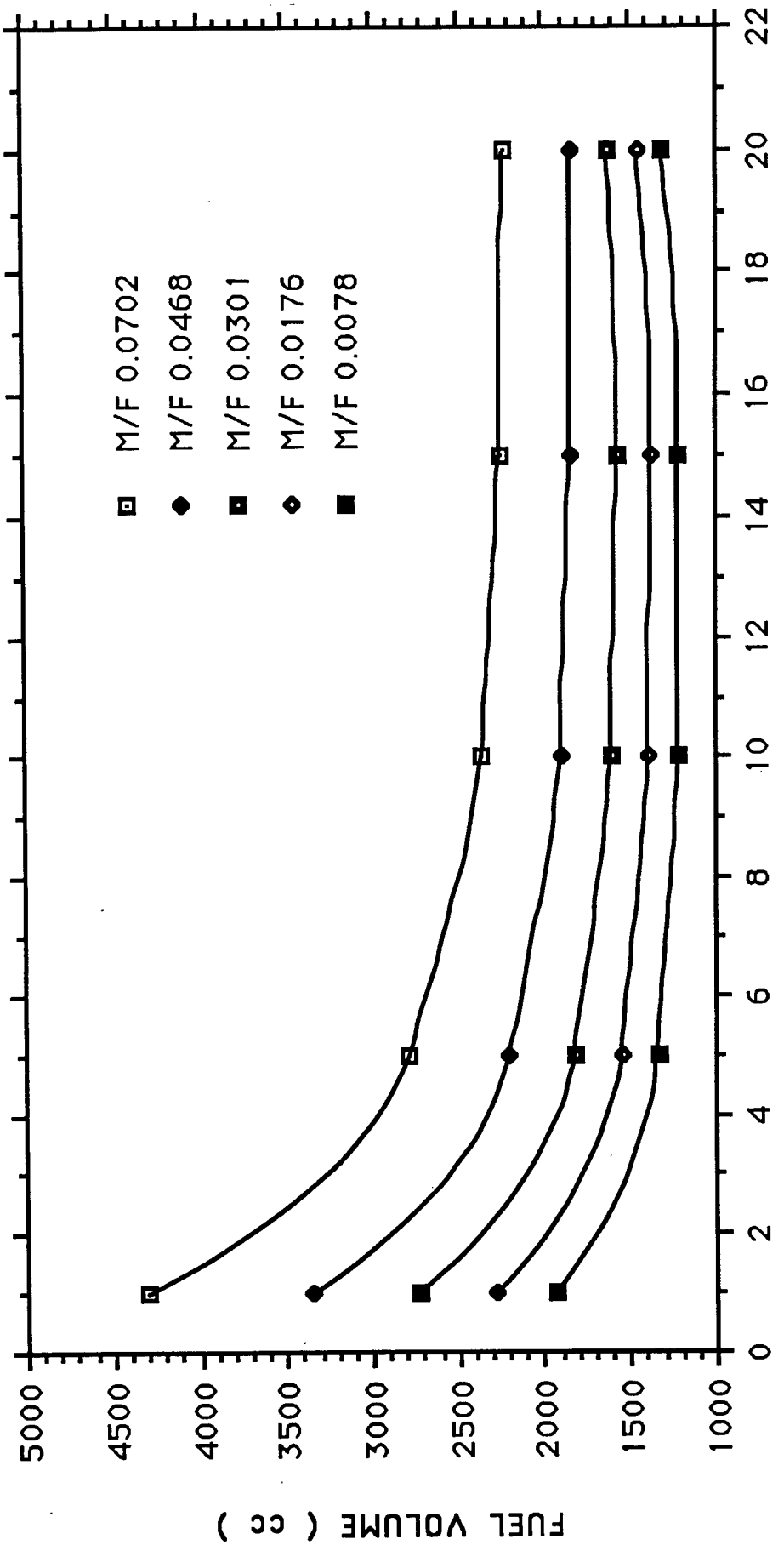

Figure 2.7. Fuel Volume vs. BeO Thickness

reactor volume with the BeO reflector thickness for various moderator to fuel ratios. It was found that a 5 cm thickness of the BeO reflector is adequate, and that further increases in thickness provide only marginal gains in fuel volume, especially for lower values of moderator to fuel ratio.

A third study was conducted to evaluate a new control technique where the two halves of the core are separated at their center until the geometry of the core has changed the reactivity of the fuel to a desired level. It is believed that this control technique is essential to the design because control cylinders typically being used to control space reactors would make the reactor system too bulky. Figure 2.8 shows the geometry used to evaluate the control technique. Figures 2.9 and 2.10 show the variation of k_{eff} with separation distance for different geometric configurations. It is interesting to note that k_{eff} does not change rapidly with varying gap distance, showing that the technique is quite promising.

An interesting experiment has been recently conducted at Texas A&M University. The Texas A&M experiment involved the use of two cylindrical rotating disks that could attenuate neutron energies and thereby offer a compact means of power regulation over a wide range of power. The control disks are centrally located within the reactor core to ensure symmetric flux profiles. Two disks made of a neutron absorbing material, and having identically machined surface hole patterns are coupled such that rotation of one can cause the holes of the pair to open and close. This attenuates neutron activity incident to the disk surface. The use of disks to control power in a compact fission reactor core is described in detail in Appendix A. The combination of rotating disk control and reactor separation control was evaluated as a potential means of providing two distinct and independent means of reactor control.

2.2 CONCEPT DESCRIPTION

Figure 2.11 is a schematic drawing contrasting the three reactor concepts, two of which use energy storage (the third does not have an energy storage mechanism).

Concept A in Figure 2.13 was developed utilizing mainly off-the-shelf components. This concept is also illustrated in Figure 2.12. It consists of a total of 169 elements, arranged in a triangular array with 121 of these elements being thermionic fuel elements (TFE's) that have energy storage material surrounding them. There are 12 control elements and 36 heat transfer pipes. The reactor is surrounded by reflectors and radiation shield materials. Figure 2.13 shows the typical dimensions of a conventional TFE surrounded by heat storage material. The fuel is $U0_2$ or UC, surrounded by a Tungsten emitter, a (tri-layer) collector and a cladding material. This TFE fits into a cylindrical ring containing LiF-CaF as the energy storage medium. This element is in a matrix of ZrH. The dimensions of the TFE and the surrounding container are such that they create a good fit under high power operating conditions.

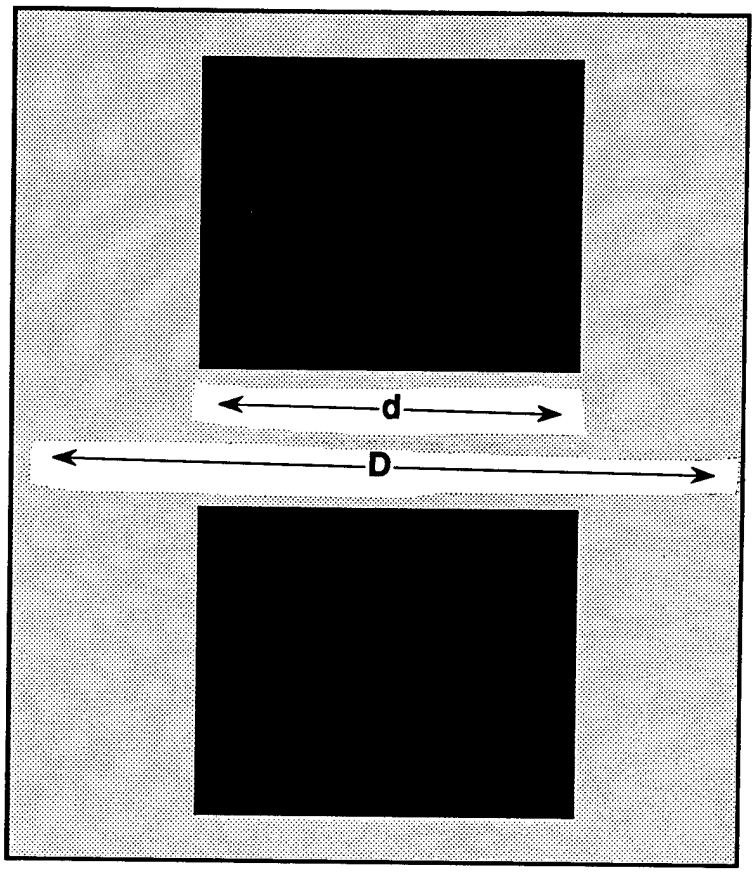

This illustrates the reactor control. The cylinder is separated from the center until the geometry has changed the reactivity to the necessary level.

Figure 2.8. Model for Studying Separation Control Technique

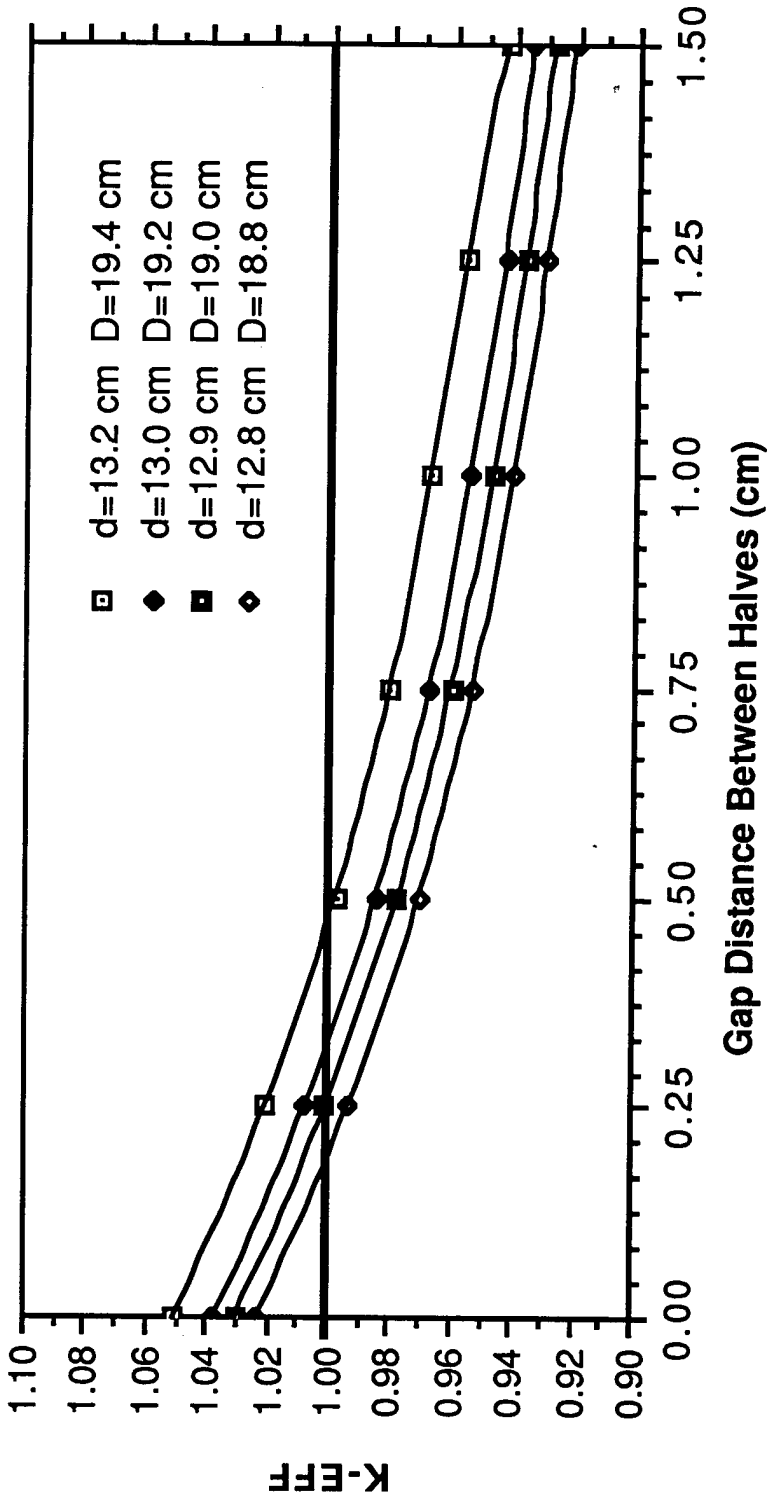

Figure 2.9. k_{eff} vs. Gap for PuC Fuel

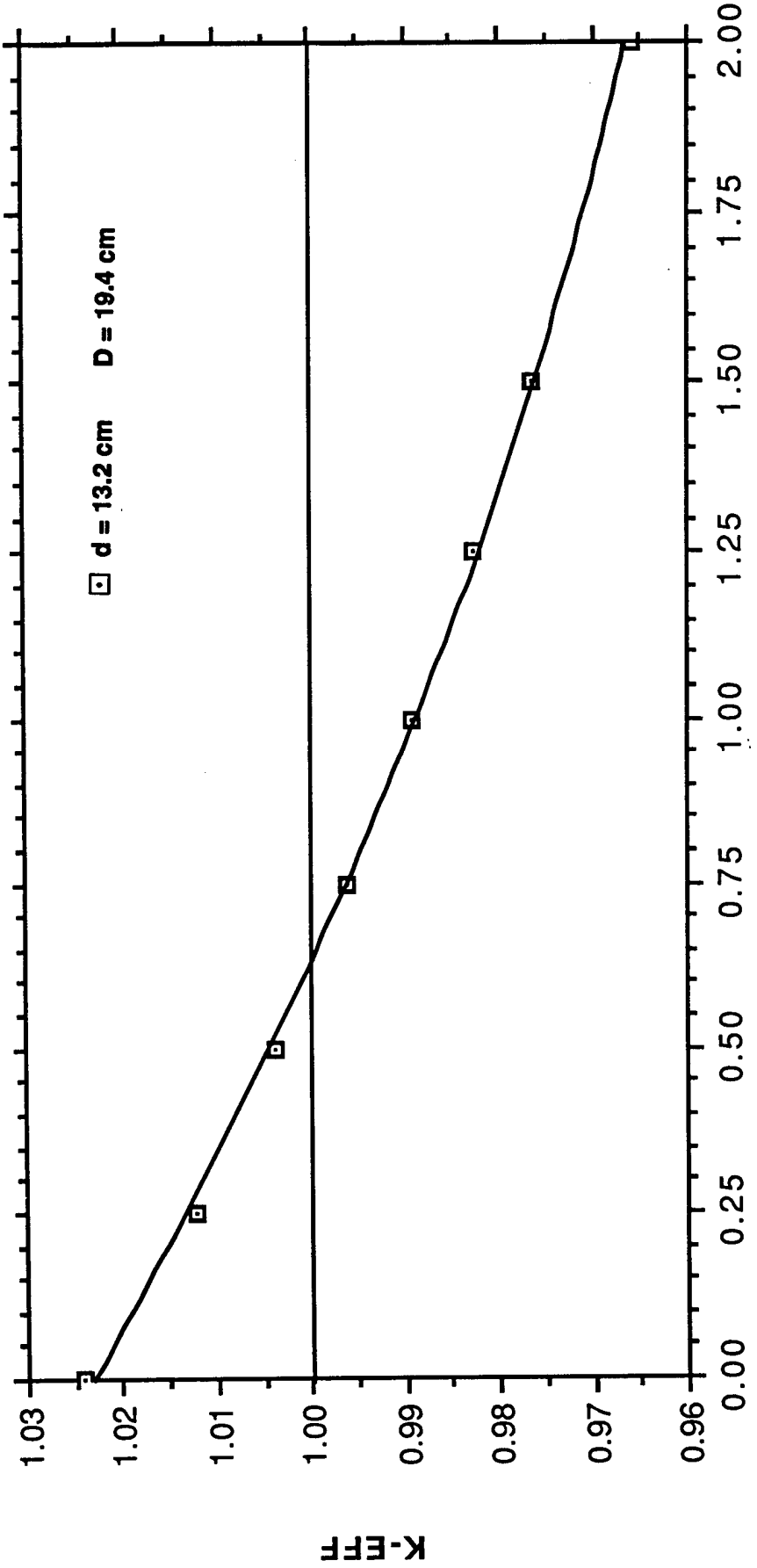

Figure 2.10. k_{eff} vs. Gap for Americium Oxide Fuel in a Circular Geometry

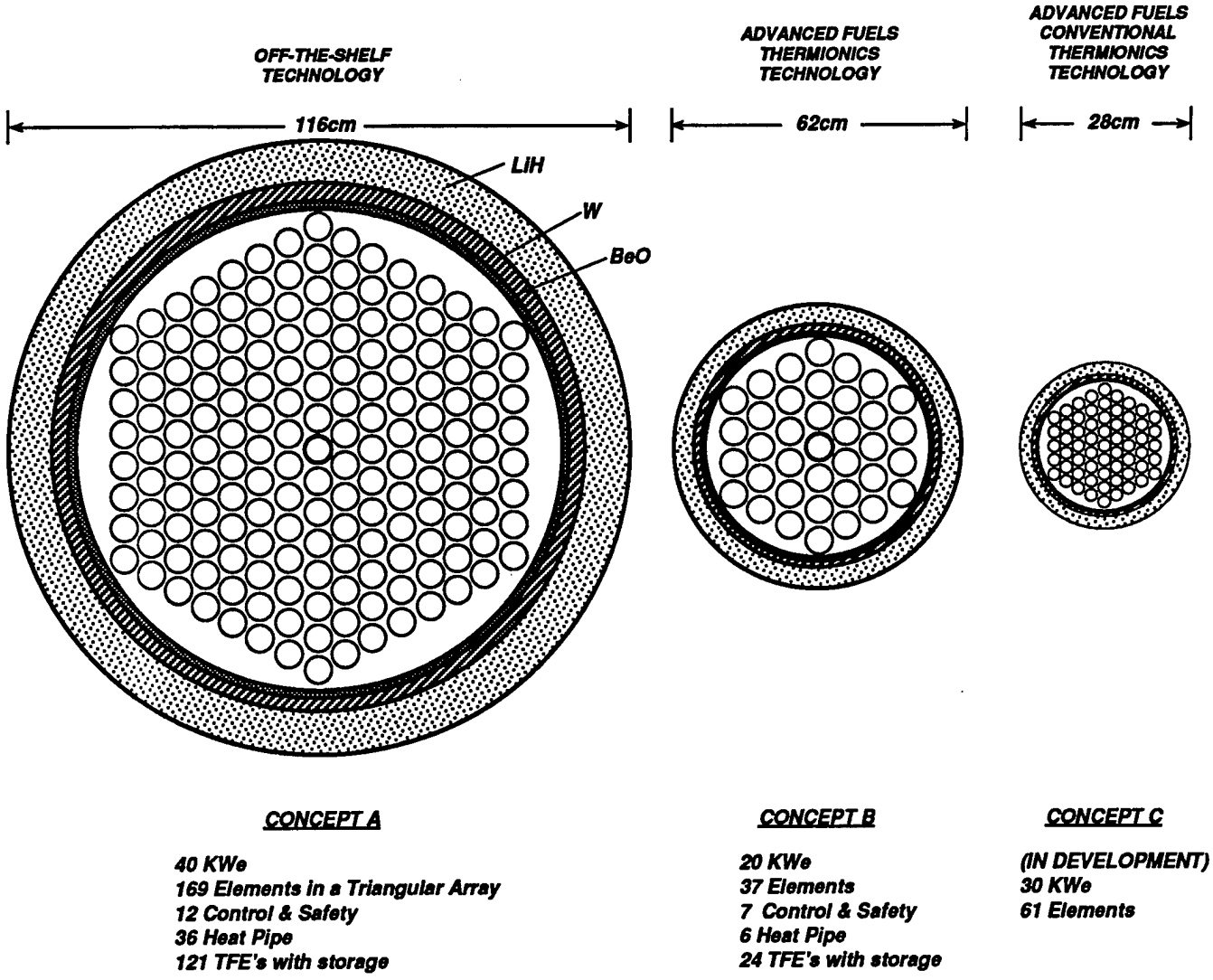

Figure 2.11. Schematic Showing Relative Zones of Three Reactor Concepts

CONVENTIONAL REACTOR CONFIGURATION

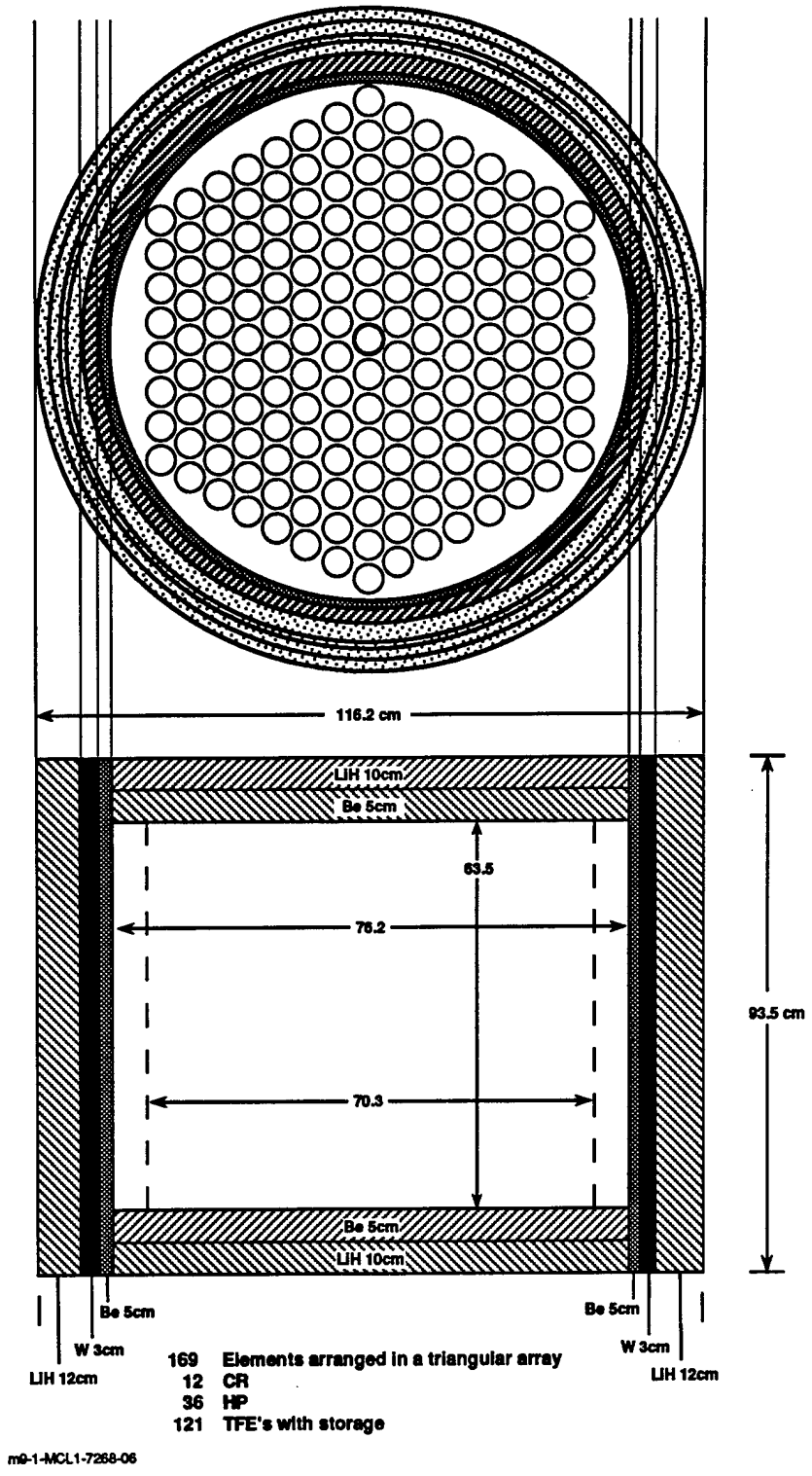

Figure 2.12. Schematic Showing Relative Zones of OTS Reactor Concept

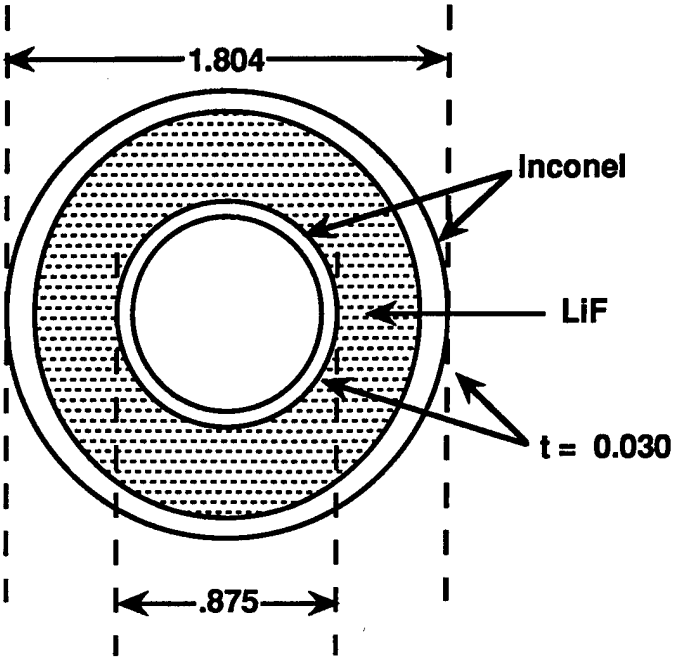

Thermonic Fuel Element

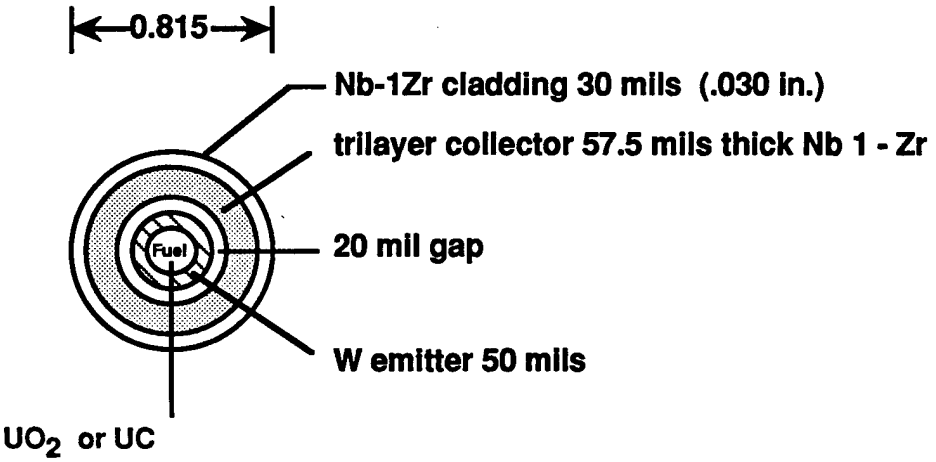

Figure 2.13. Typical Dimensions of Conventional TFE and Heat Storage Material

The major components of this reactor are: the TFE, the energy storage container, the reactor fuel and the heat transfer pipes. The TFE's are made up of conventional TFE elements that are now being tested in the TRIGA, EBR-2 and FFTF reactors. The life of these TFE elements has already been proven to be in excess of three years. The irradiation of the materials under prototypical reactor operating conditions is continuing, and a seven year life of the TFE is anticipated. A description of the thermionic energy conversion along with a brief discussion of the ongoing TFE Verification Program is given in Section 2.3

The energy storage compartment surrounding the TFE is sequenced into one-inch long sections which contains an LiF-CaF_2 eutectic Phase Change Material. This component is similar in design to the Space Station Solar Dynamic Heat Receiver as developed by Garrett for the Solar Dynamic Power Generation system. Figure 2.14 shows the heat receiver tube configuration, and Figure 2.15 shows the overall configuration of the heat receiver, a key component of the Solar Dynamic Power Generation System. Under solar flux conditions the heat receiver temperature rises and the heat is stored in the PCM material. During the solar eclipse, a gas is passed through the inner tube which when heated becomes the working fluid for a Brayton cycle that produces power. Instead of passing the gas through the inside of the canister, a TFE is placed within it. A receiver of this type has been tested in a prototype vacuum environment over a large number of heating/cooling cycles.

Both UO_2 and UC fuels were used in the design of the OTS reactor power system. There is a long history associated with the development of the UO_2 fuel for the Liquid Metal Reactor Program. This fuel has been extensively tested and has been qualified for commercial applications. Although UC has not been as extensively used or tested as UO_2, sufficient in-pile tests on UC have been conducted to qualify it as an acceptable alternative fuel in this design.

There are 36 stainless steel heat pipes in the reactor. There is a large amount of data on both sodium and potassium, stainless steel heat pipes that have been tested in a reactor at high neutron fluence levels. The heat pipe technology is quite mature, and very little further development is necessary. The key performance parameters for the OTS reactor are given in Table 2.2.

Concept B in Figure 2.11 outlines the advanced thermionic concept with energy storage while Figure 2.16 shows a layout of this concept. It contains 37 elements arranged in a triangular array including 24 advanced TFEs with energy storage, 6 heat pipe elements, with the rest being control safety elements. The control elements are shown to be cylindrical rods in Figure 2.16. This was initially used to evaluate their effectiveness, and the results are presented later. It was found that for this design effective control can only be achieved by separation and disc rotation control techniques. This reactor was designed to give a peak 20Kwe (net) at a 33 percent thermionic conversion efficiency using the Americium Oxide fuel (Am_2O_3). As seen in Figure 2.16, the size of this reactor is

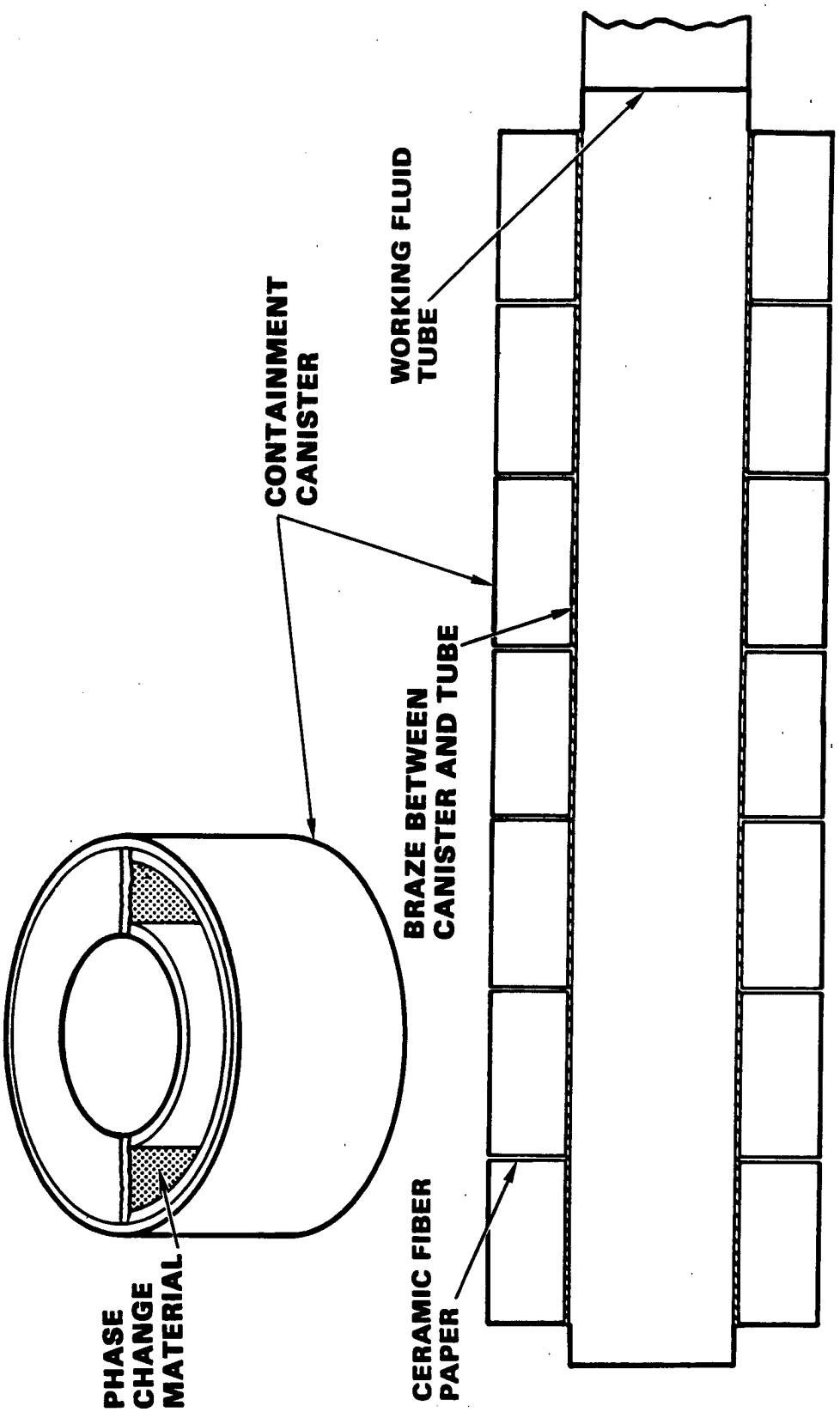

Figure 2.14. Receiver Tube Configuration

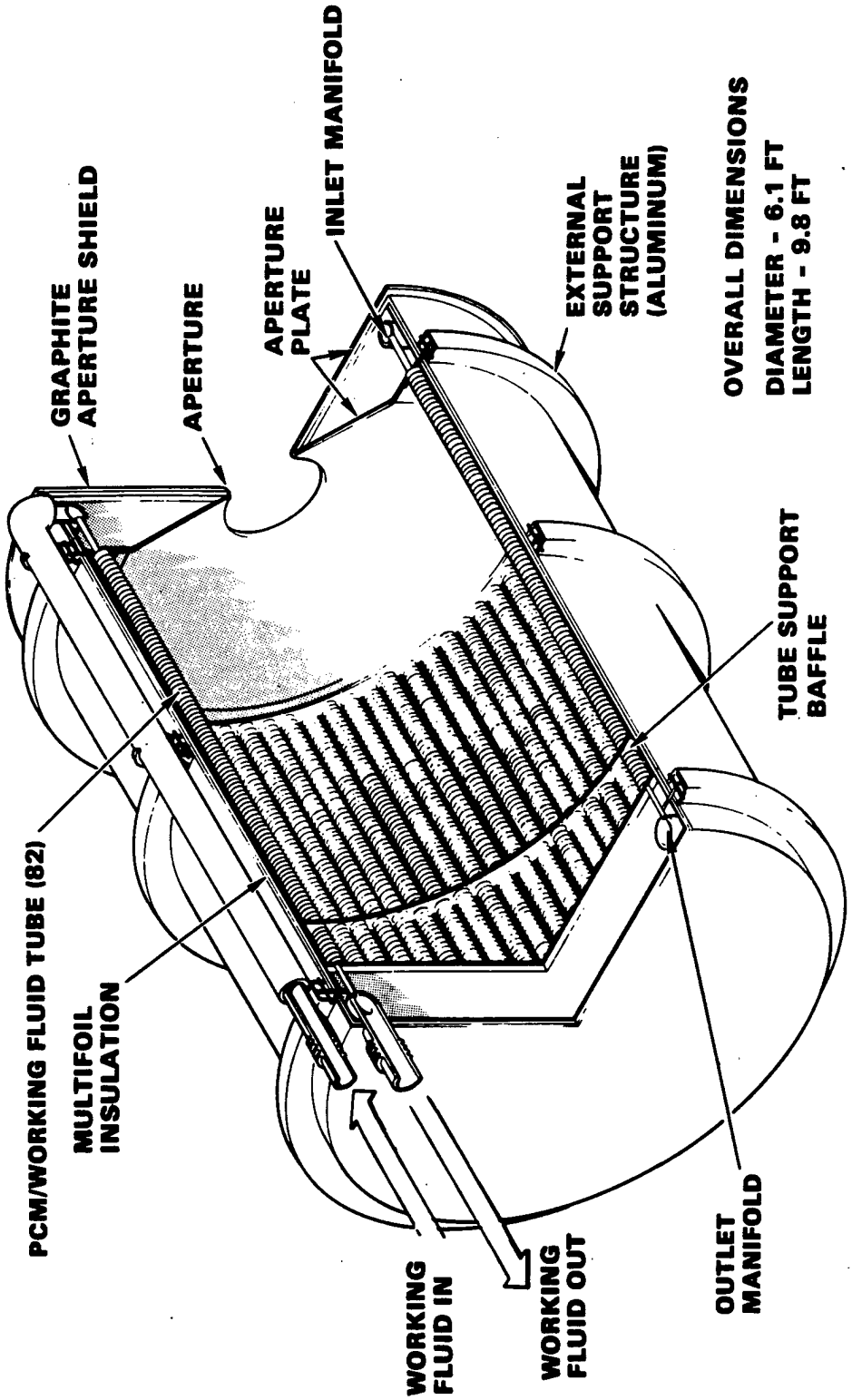

Figure 2.15. Garrett Space Station Receiver

TABLE 2.2. OTS REACTOR (CONCEPT A) PERFORMANCE PARAMETERS

	PEAK CONDITION	*NORMAL CONDITION*
POWER (KWe)		
NET BOL	**40**	**8**
THERMAL POWER (KW)	**450**	**210**
DURATION	**900 SEC**	**REMAINDER OF ORBIT**
TEMPERATURE (°K)		
EMITTER	**1935° K**	**–**
COLLECTOR	**1336° K**	**–**
STORAGE	**1100° K**	**–**
ZrH	**990° K**	**–**
HEAT PIPE WALL	**900° K**	**–**

m9-1-MCL1-7268-08

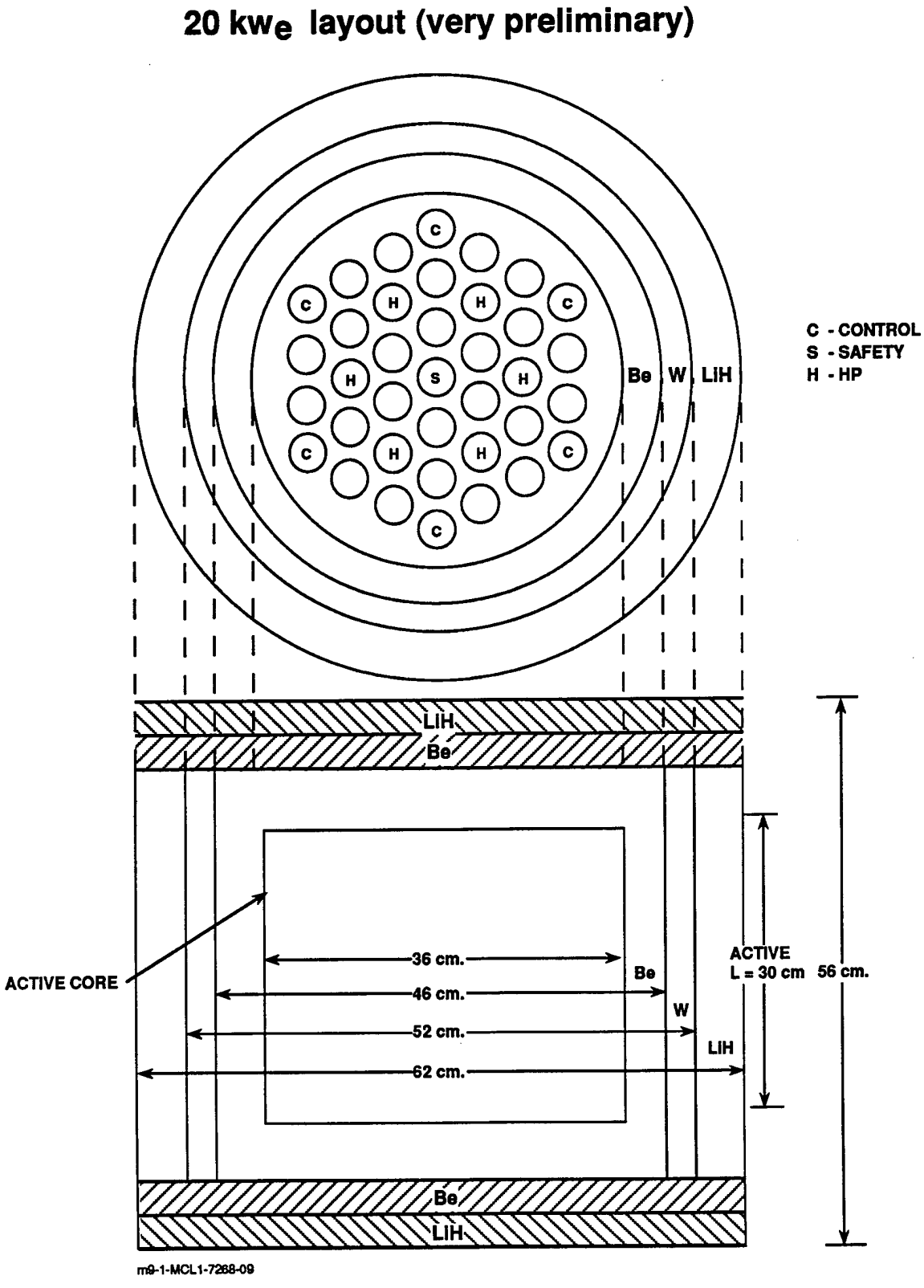

Figure 2.16. Schematic Showing Zones of Advanced Energy Storage Concept

fairly small, although there is a considerable amount of energy storage material within the core. It is recommended, however, that this design should not be further pursued for a variety of reasons.

Although the critical mass of Am_2O_3 is very small (<10kg), the minimum size of this reactor is limited by a need to have a minimum amount of energy storage material and not by the minimum mass of fuel needed to make the reactor critical. Moreover, with a several fold increase in volume, one could use a more conventional fuel and save the significant cost resulting from the qualification of a new advanced fuel. The cost and time required to qualify a new fuel can be substantial and for this particular type of design it is not cost-effective.

Although only preliminary results have been obtained on the third concept (shown in Figure C), is highly recommended for further development. This concept uses conventional TFE technology, no energy storage ZrH moderator and advanced Am_2O_3 fuel. The volume of this reactor, as shown in Table 1.2, is significantly lower than for any of the other reactors. This is possible primarily by the use of Am_2O_3 fuel, which as a very high fission cross section, and hence a low critical mass. Parametric studies are being conducted to determine the required fuel rod and TFE diameters, their number, the pitch to diameter ratio, and the enrichment of Am_2O_3 needed in the fuel. The pitch to diameter ratio is the most dominating factor because as p/d increases the moderator (ZrH) volume fraction increases and the k_{eff} increases as shown in Figure 2.17. This figure also shows that Am_2O_3 mixed with 93% enriched UO_2 can also provide a wide variety of acceptable designs. The minimum core volume occurs when the fuel is fully enriched with Am_2O_3 (Am^{242}). At 30Kwe the mass of fully enriched Am_2O_3 in the core is about 7 kg and the total core volume is about 17 liters. One acceptable core configuration contains 61 rods (at a p/d of 1.248) where the total length of the reactor (including reflectors) is 28 cm, and it contains 61 heat pipes. Thermionic power is generated at 8 W/cm^2.

One of the key considerations in the design of small compact reactors is the development of diverse, independent control mechanisms that do not substantially increase the size of the core. A conventional control mechanism for a space reactor consists of cylinders of BeO about 15 cm in diameter (a portion of which contains the poison control material). For a small reactor core that is about 18 cm in diameter, a BeO reflector that is five cm in thickness is adequate, and the addition of any other surrounding BeO cylinders would increase the reactor diameter substantially without much benefit. This necessitated that the separation and 'disk' types of control schemes be used for the supercompact reactors. Figure 2.18 shows how these control schemes can be functionally adapted to Concept C. Figure 2.19 shows the variation of k_{eff} with axial separation and concentric rotation of the disks. It is important to note that the results shown in Figure 2.19 for k_{eff} show only a typical trend, and not the absolute number for keff.

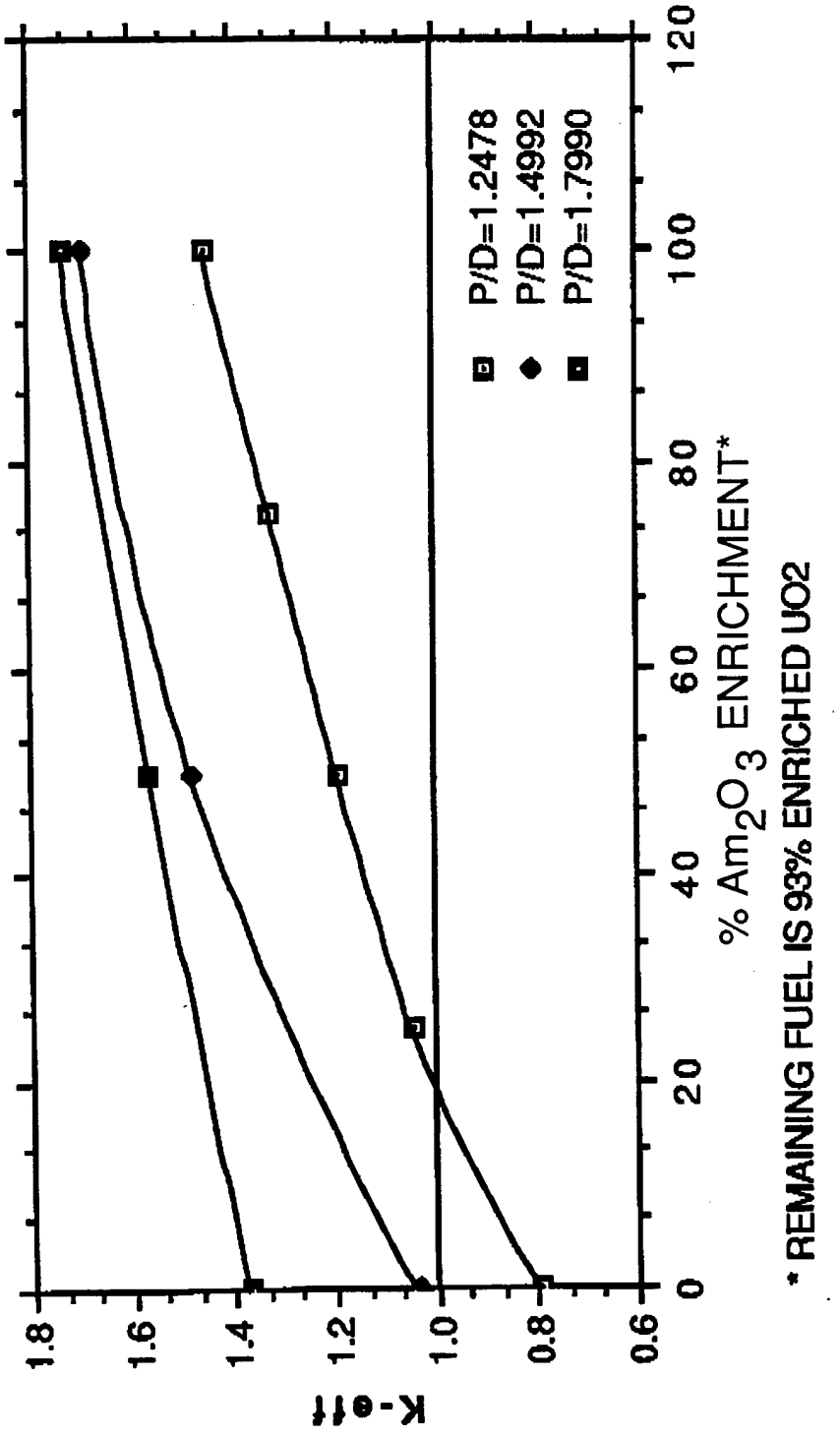

Figure 2.17. k_{eff} vs. Enrichment for 61 Rods

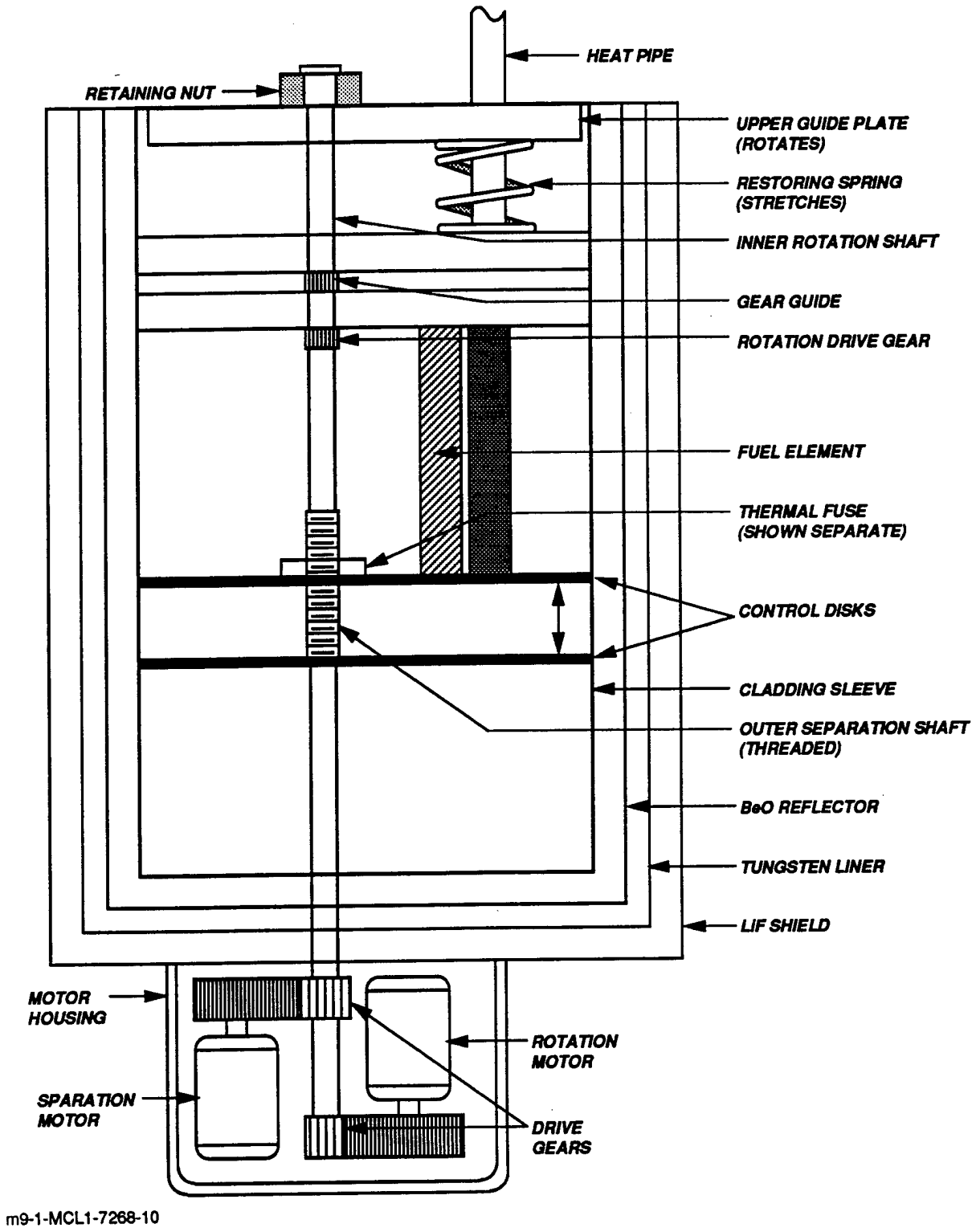

Figure 2.18 Am_2O_3 Fueled Reactor Core with No Energy Storage (Concept C)

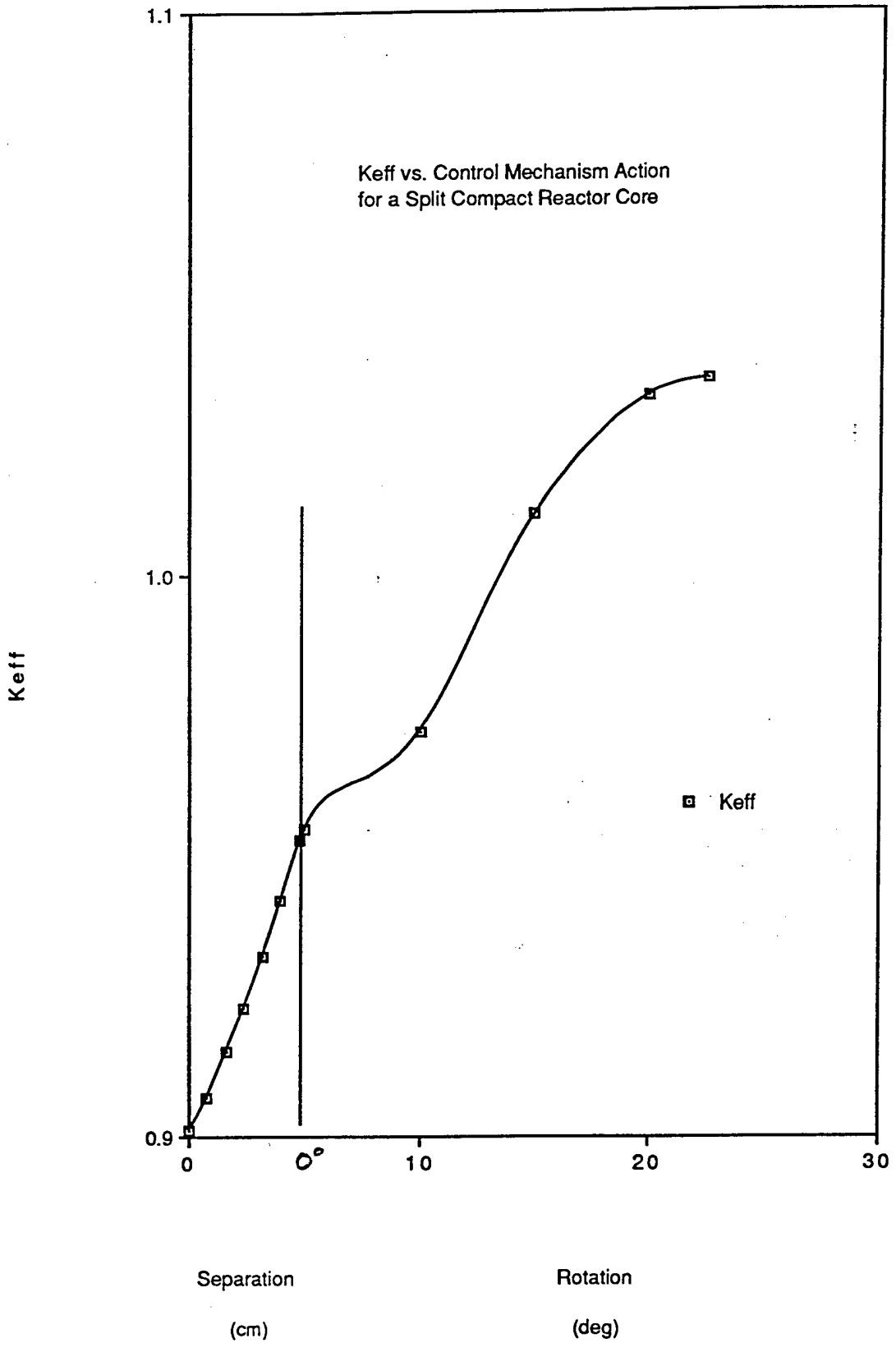

Figure 2.19. Variation of k_{eff} with Separation and Rotation

2.3 CONCEPT DEVELOPMENT

2.3.1 Reactor Neutronics & Control

A preliminary study of the neutronics and control characteristics of the off-the-shelf (Concept A) and advanced (Concept B) concepts has been carried out. All of the cross-sections for the calculations were obtained from the Los Alamos National Laboratory with the exception of Am-242 cross-sections which were provided by the Lawrence Livermore Laboratory. The spectrum used in generating these cross-sections was that of the Godiva critical assembly (a 93 percent enriched metallic U^{235} bare critical assembly). Therefore, these calculations should be considered as being very conservative. The fission cross-section of the lower energy neutrons is not appropriately weighted as a direct result of using very fast cross-sections. Consequently, the use of cross-sections with softer spectrum weighting should result in a more reactive core configuration for each of the two concepts presented. It is believed that the required fuel loading for each of the designs will be less then the figures presented in this document. All of the results presented in this section have been performed using 16 energy groups. At this stage, these results should be viewed as exploratory with the main purpose of demonstrating concept feasibility. A more indepth analysis will be performed in the studies that follow.

The neutronic calculations were performed using the TWODANT computer code, a two-dimensional Discrete-Ordinates Diffusion-Accelerated Transport Computer Code developed by the Los- Alamos National Laboratory. Two major categories of neutronics calculations were performed for both of the proposed designs - cell calculations and quarter care calculations. The cell calculations were performed in order to investigate the various trade-offs involved in optimizing the core lattice configurations. Variables such as pitch to diameter ratio and fuel enrichment were analyzed in order to investigate the criticality characteristics of the entire core under various configurations, such as maximum reactivity shutdown and water immersion.

These neutronic studies clearly support the feasibility for both the off-the-shelf and advanced concepts for the missions under consideration. They also provide a well-defined reference core design concept for future development, and a procedural methodology for the required engineering design calculations.

2.3.2 Off-the-Shelf-Concept Calculations

A quarter-core reactor configuration for the reference Off-the-Shelf system is shown in Figure 2.20. This is a square lattice core which is neutronically equivalent to the hexagonal lattice system described in the previous section. This neutronic equivalence was preserved by keeping the moderator and fuel volumes constant when transforming the hexagonal lattice to square lattice. The

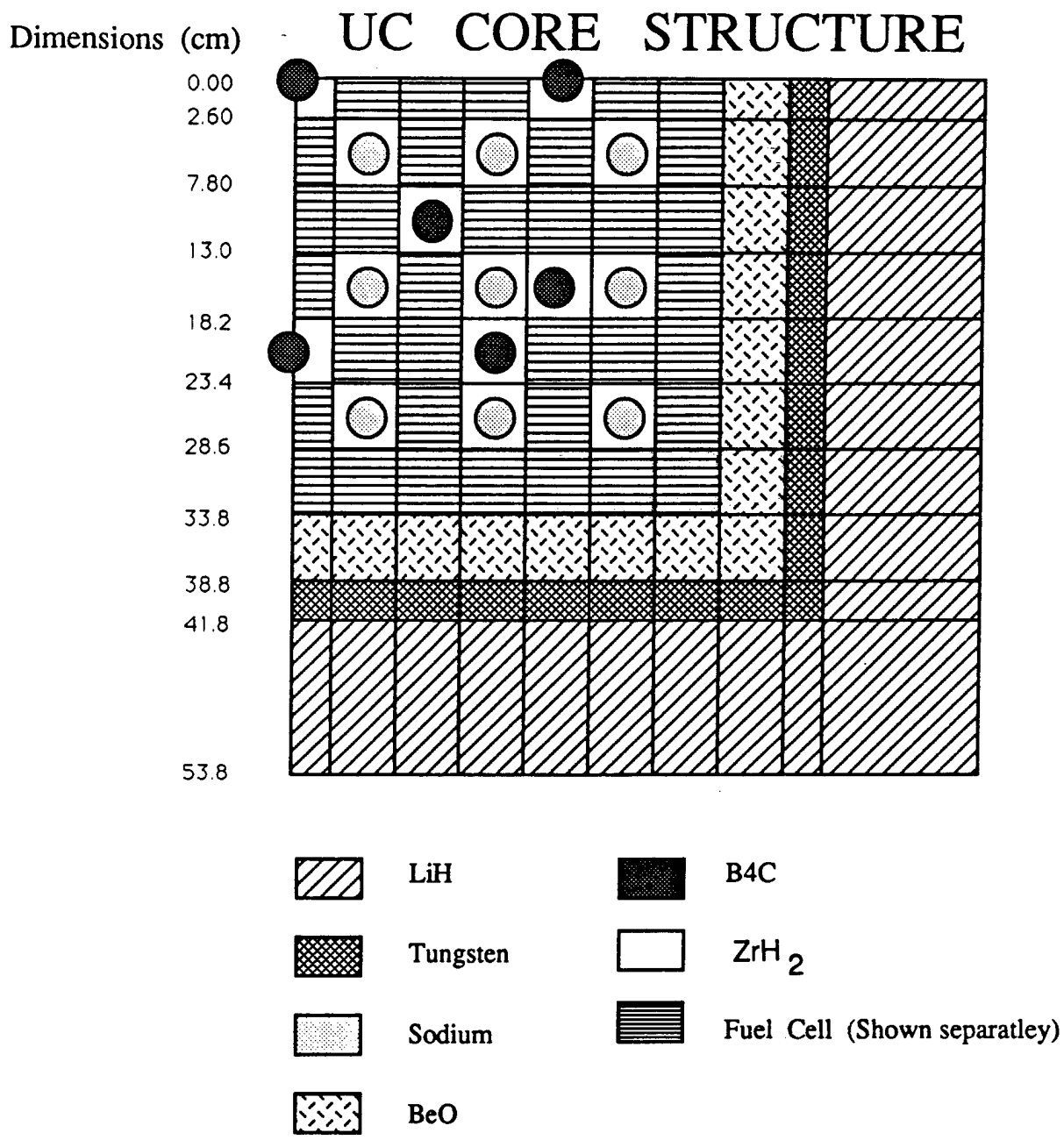

Figure 2.20. Off-The-Shelf Technology Core Configuration

use of Cartesian geometry considerably reduced the modeling effort that was required in performing the quarter core calculations with the TWODANT code. A typical fuel cell for the 169-element reference design is shown in Figure 2.21.

Parametric Cell Calculations

In order to investigate the feasibility of the proposed design and in order to optimize the reactor core configuration, several parametric studies were performed using the fuel cell shown in Figure 2.21. These were one dimensional (r only) calculations using the TWODANT code and sixteen neutron energy groups. One of the major outcomes of these calculations was the set of homogenized cell cross-sections to be used in the quarter-core calculations described in the following paragraphs. No neutron energy group collapsing was performed since both the local (cell) and global (quarter-core) calculations were performed using the same number of energy groups. The number densities of the various materials used in these cell calculations are summarized in Table 2.3. The densities of the various materials were taken at room temperature.

The one-dimensional UC or UO_2 cell calculations were performed using white boundary conditions all around the cell, thus simulating the neutronic behavior of an infinite lattice. Figure 2.22 summarizes these parametric calculations as a function of the U^{235} enrichment for different values of the cell pitch to fuel diameter ratio. The target k-effective, which is the same as the k-infinity in these calculations, was chosen to be in the range 1.13 to 1.15. From Figure 2.22, it can be seen that the desired excess reactivity can be obtained for pitch to diameter ratio ranges of 1.105 to 1.045 for U^{235} with enrichments as low as 55 percent. For all of these calculations, a major fraction of the available neutrons have energies in the 0.5 to1 Mev range.

Quarter Core Calculations

Quarter Core calculations were performed in order to determine the criticality characteristics of the proposed system under different operating scenarios. Homogenized 16 group cross-sections for the fuel cell were used in performing these calculations which resulted from the detailed heterogeneous cell calculations. The core configuration which was analyzed using TWODANT is shown in Figure 2.20. In this quarter core analysis, there were 116 thermionic fuel elements (with energy storage), 36 heat pipe elements and 17 control rod elements. A 5cm BeO reflector, a 3cm W gamma shield and a 12cm LiH neutron shield are also utilized in this analysis.

Four different core scenarios were investigated: (1) Maximum Reactivity Configuration, (2) Shutdown Configuration, (3) Water Immersion, and (4) Water Floodings. The desired and achieved values of the effective multiplication for these four cases are summarized in Table 2.4. The maximum reactivity configuration is as desired. The k-effective for the shutdown launch configuration

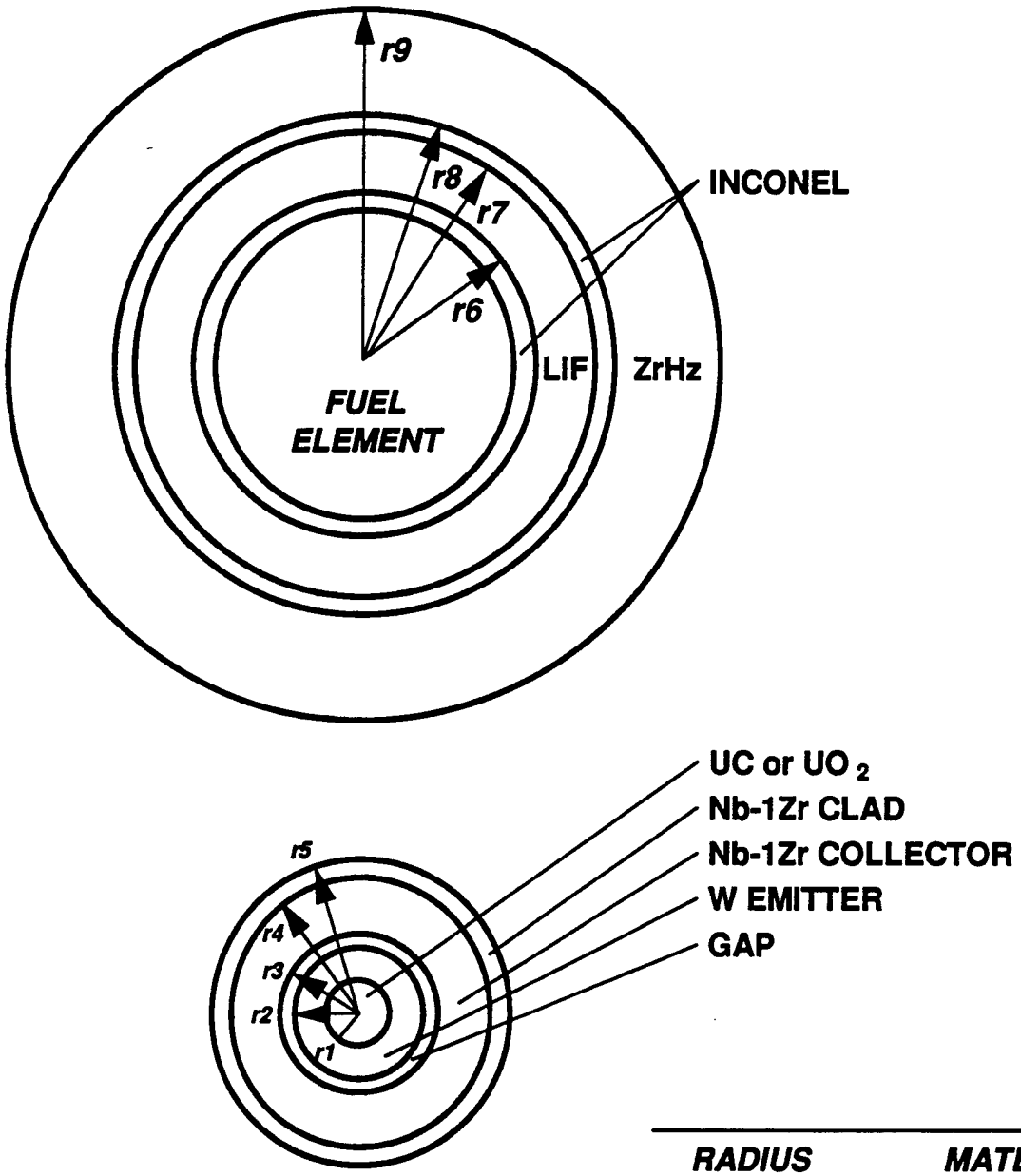

m9-1-MCL1-7268-11

RADIUS	MATERIAL
r1	UO_2 or UC (93%)
r2	W
r3	GAP
r4	Nb-1Zr
r5	Nb-1Zr
r6	INCONEL
r7	LIF
r8	INCONEL
r9	ZrHz

Figure 2.21. Equivalent UC or UO_2 Fuel Cell

TABLE 2.3. FUEL CELL ATOM DENSITIES

ZONE	ELEMENT	$N \times 10^{-24} cm^{-3}$
1	U^{235}	0.0309
	U^{238}	0.0023
	C	0.032
2	W	0.0634
3	Gap	0.0
4, 5	Nb	0.05506
	Zr	0.000556
6, 8	Ni	0.06385
	Cr	0.01432
	Mo	0.002685
	Fe	0.007159
7	Li	0.06082
	F	0.06082
9	Zr	0.06105
	H	0.1038

m9-1-MCL1-7268-12

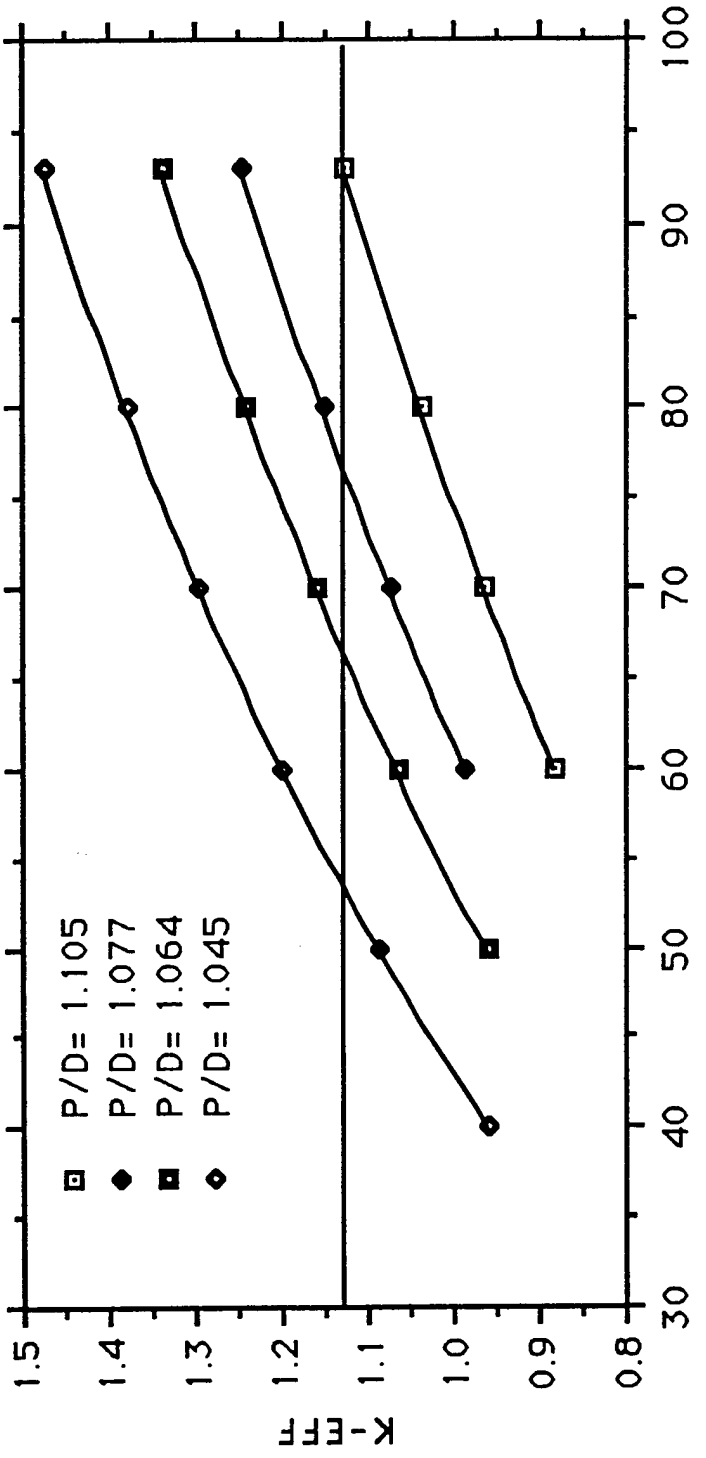

Figure 2.22. k_{eff} vs. Enrichment for UC Cell

TABLE 2-4. UC CORE SCENARIOS

CASE	*KEFF*	*DESIRED RANGE*
MAXIMUM REACTIVITY	**1.07**	**1.05 - 1.09**
LAUNCH CONFIGURATION	**0.922**	**<0.9**
WATER IMMERSION	**0.922**	**<0.95**
WATER FLOODING	**0.923**	**<0.95**

m9-1-MCL1-7268-17

is already fairly close to the desired value, and with some additional design, it is believed that it can be reduced to below 0.9. The water immersion configuration was analyzed by adding an infinite (~50cm) water reflector around the core. The water flooding was accomplished by replacing the ZrH_2 in the core with water, in addition to the surrounding infinite reflector. However, it was assumed that the control rods are in the fully inserted position during the core floodings. As can be seen from Table 2.4, the water immersion and water flooding does not add a significant amount of positive reactivity to the core. However, further investigation of these scenarios with softer spectrum weighted cross-sections will be necessary.

Reactor Control

Reactor Control for the Off-the-Shelf concept is achieved via the 17 B_4C control rod elements located in the core, as shown in Figure 2.20. From the preliminary calculations, summarized in Table 2.4, it appears that reactivity control via these 17 control rod elements is sufficient for the entire core operating range.

2.3.3 Advanced Concept

A quarter-core advanced reactor configuration for the reference system is shown in Figure 2.23. This is a square lattice core which is equivalent to the hexagonal lattice system described in Figure 2.16. This neutronic equivalence was preserved by keeping the moderator and fuel volumes constant when transforming the hexagonal lattice to a square lattice. The use of Cartesian geometry considerably facilitated the modeling effort that was required in performing the quarter-core calculation with the TWODANT code. A typical fuel cell for the 37 element reference design is shown in Figure 2.24.

Parametric Cell Calculations

In order to investigate the feasibility of the proposed design and in order to optimize the reactor core configuration, several parametric studies were performed using the fuel cell shown in Figure 2.24. These were one dimensional (r only) calculations using the TWODANT code and sixteen neutron energy groups. One of the major outcomes of these calculations were set of homogenized cell cross-sections to be used in the quarter-core calculations described in the following paragraphs. No neutron energy group collapsing was performed since both the local (cell) and global (quarter-core) calculations were performed using the same number of energy groups. The number densities of the various materials used in these cell calculations are summarized in Table 2.5. The densities of the various materials were taken at room temperature.

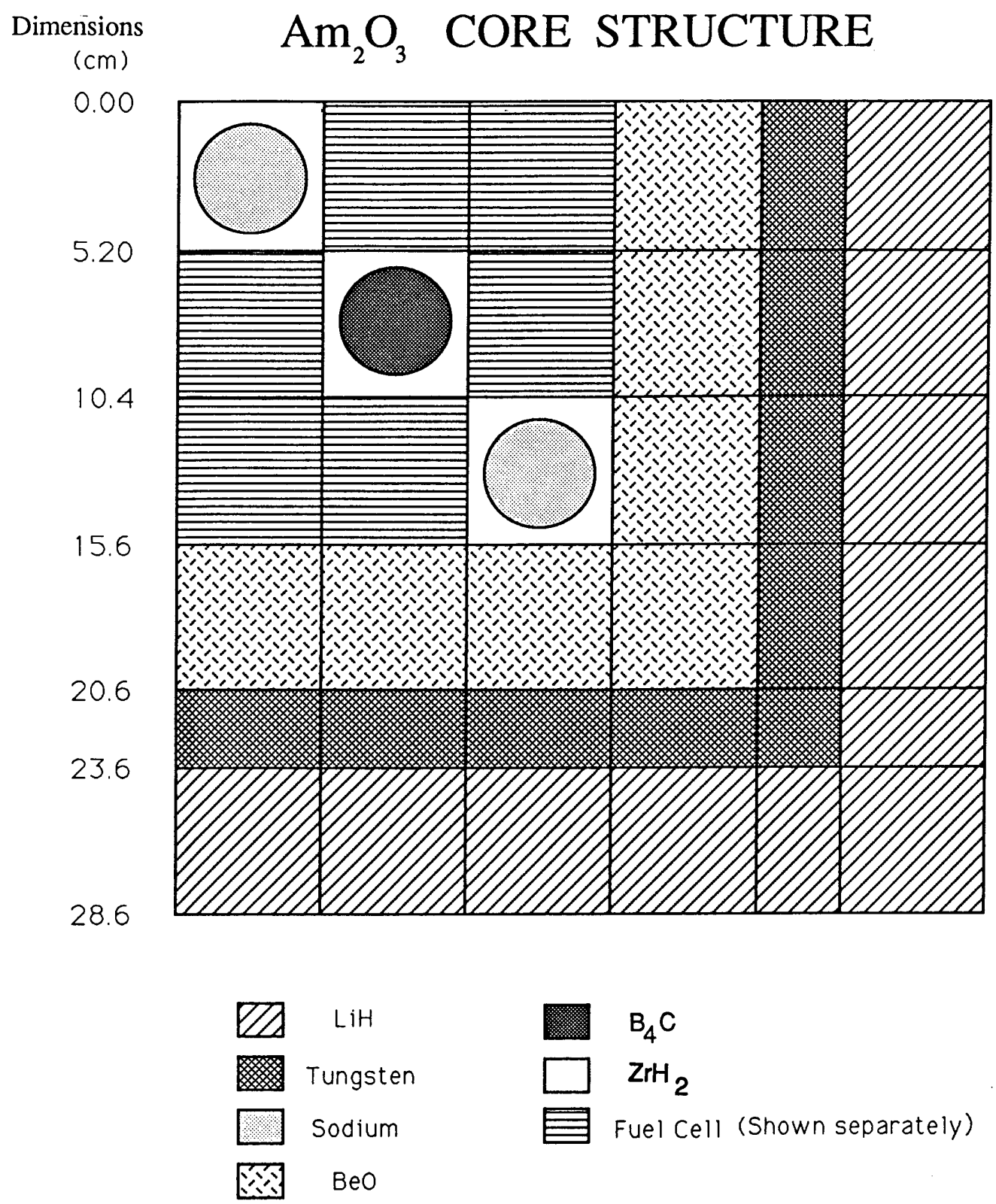

Figure 2.23. Advanced Energy Storage Core Configuration

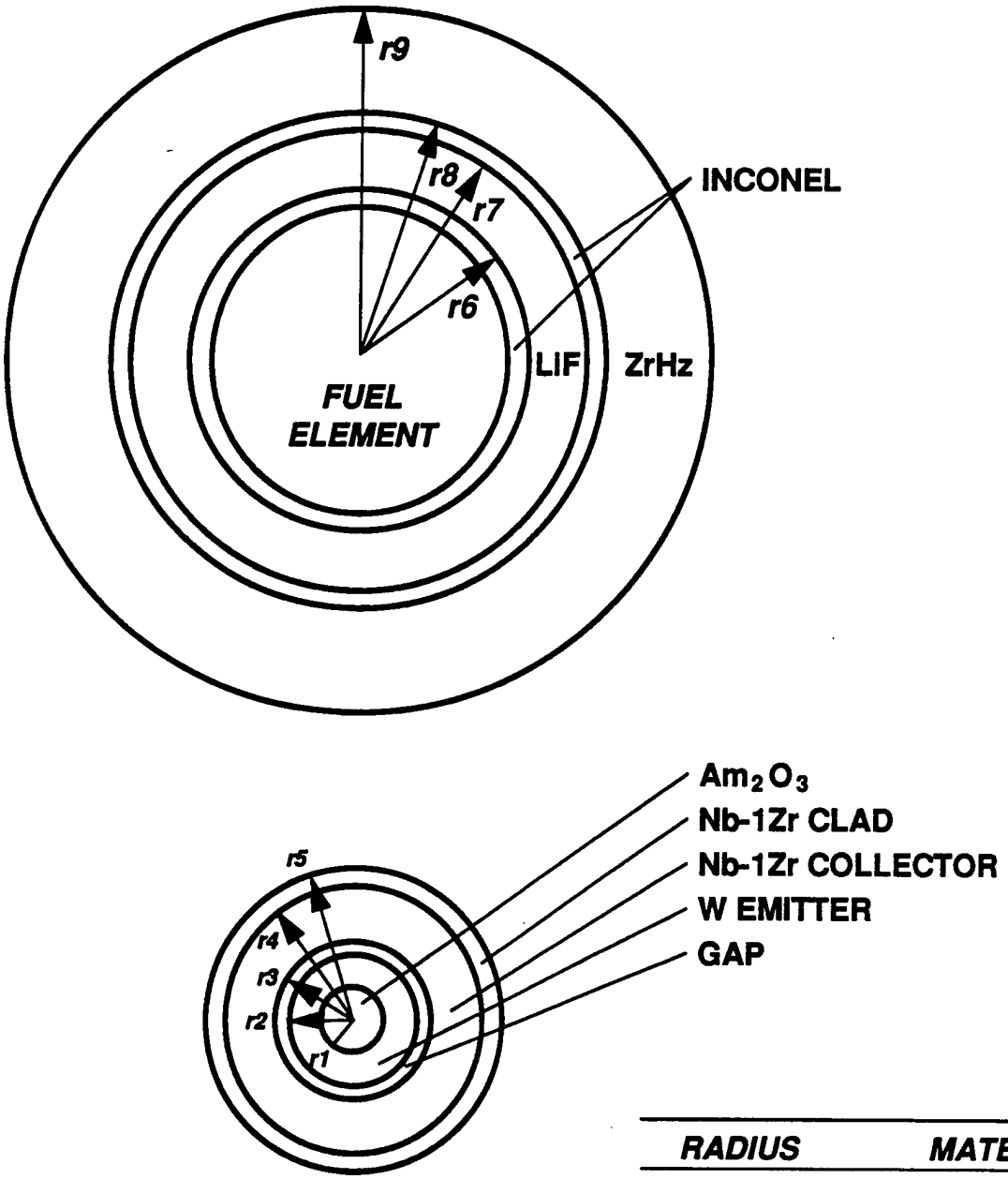

m9-1-MCL1-7268-13

RADIUS	MATERIAL
r1	Am_2O_3
r2	W
r3	GAP
r4	Nb-1Zr
r5	Nb-1Zr
r6	INCONEL
r7	LiF
r8	INCONEL
r9	ZrHz

Figure 2.24. Equivalent Am_2O_3 Fuel Cell

TABLE 2.5. FUEL CELL ATOM DENSITIES

ZONE	*ELEMENT*	*N x 10^{-24} cm^{-3}*
1	Am^{242}	0.026434
	O	0.039651
2	W	0.0634
3	Gap	0.0
4, 5	Nb	0.05506
	Zr	0.000556
6, 8	Ni	0.06385
	Cr	0.01432
	Mo	0.002685
	Fe	0.007159
7	Li	0.06082
	F	0.06082
9	Zr	0.06105
	H	0.1038

m9-1-MCL1-7268-14

The one-dimensional Am_2O_3 cell calculations were performed using white boundary conditions all around the cell, thus simulating the neutronic behavior of an infinite lattice. Figure 2.25 summarizes these parametric calculations as a function of the Am^{242} enrichment for different values of the cell pitch to fuel diameter ratio. The target k-effective, which is the same as the k-infinity in these calculations, was chosen to be in the range of 1.25 to 1.30. From Figure 2.25, it can be seen that the desired excess reactivity can be obtained for pitch to diameter ratio ranges of 1.198 to 1.162 for Am^{242} enrichments as low as 63 percent. For all of these calculations, a major fraction of the available neutrons have energies in the 0.5 to 1 Mev range.

Quarter Core Calculations

Quarter Core calculations were performed in order to determine the criticality characteristics of the proposed system under different operating scenarios. Homogenized 16 group cross-sections for the fuel cell were used in performing these calculations which resulted from the detailed heterogeneous cell calculations. The core configuration analyzed using TWODANT is shown in Figure 2.23. In this quarter core analysis, there were 23 fuel elements, 8 heat pipe elements and 6 control rod elements. In addition, a 5cm BeO reflector, a 3cm W gamma shield and a 12cm LiH neutron shield is utilized.

Four different core scenarios were investigated: (1) the maximum reactivity configuration, (2) Shutdown Configuration, (3) Water Immersion and (4) Water Floodings. The desired and achieved values of the effective multiplication for these four cases are summarized in Table 2.6. The maximum reactivity configuration is as desired. The k-effective for the shutdown launch configuration is not close to the desired value. Therefore, an alternate control mechanism is required. The water immersion configuration was analyzed by adding an infinite (~50cm) water reflector around the core. The water flooding was accomplished by replacing the Zr_1H_2 in the core with water, in addition to the surrounding infinite reflector. However, the control rods were assumed in the fully inserted position during the core floodings. As can be seen from Table 2.6, the water immersion and water flooding does not add a significant amount of positive reactivity to the core. However, further investigation of these scenarios with softer spectrum weighted cross-sections will be necessary.

Reactor Control

The results of the quarter core calculations for the advanced core indicate the inadequacy of the control rod element to effectively control the core. The reason for this effect is the high core leakage that is characteristic of a small core. Therefore, novel control mechanisms are proposed. One alternative that has been used in other space reactors are control drums. However, recent drum swelling problems required a design change in the SP-100 reactor and, therefore, this alternative has been rejected. Two other alternatives are proposed for effective control of compact reactors, as

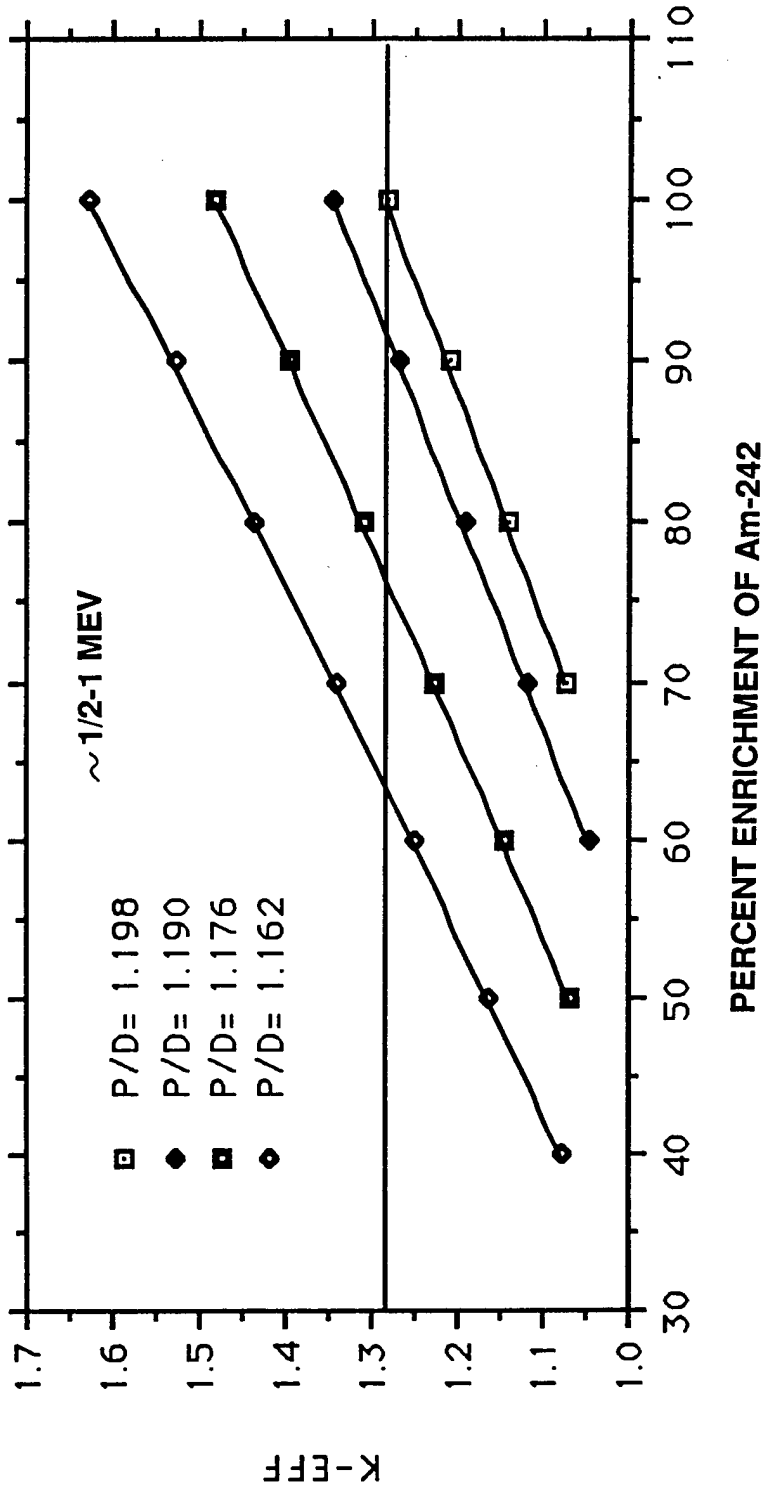

Figure 2.25. k_{eff} vs. Enrichment for Am_2O_3 Cell

TABLE 2.6. AMERICIUM CORE SCENARIOS

CASE	*KEFF*	*DESIRED RANGE*
MAXIMUM REACTIVITY	**1.078**	**1.05 - 1.09**
LAUNCH CONFIGURATION	**0.978**	**<0.9**
WATER IMMERSION	**0.978**	**<0.95**
WATER FLOODING	**0.975**	**<0.95**

m9-1-MCL1-7268-16

follows: (1) Control via separation of subcritical assemblies and (2) Control via rotating control disks. These concepts, which will be used in combination with one another are now briefly described:

(1) Control via separation of two core halves

It is proposed to use the separation distance between the two core halves as one of the mechanisms to control the core reactivity. Each core half is by itself a subcritical assembly. The overall core becomes critical and provides the required excess reactivity as the two halves come closer together.

The variation of the effective multiplication factor as a function of the separation distance for the advanced technology concept is shown in Figure 2.26. As an additional safety feature, it is proposed to include a thermal fuse as shown in Figures 2.27 and 2.28. These figures show the top and side views of the thermal fuse, respectively.

(2) Control via Disk Rotation

An alternate control strategy is the use of the control disk concept. This concept, first conceived by Scott Negron, a student at Texas A&M University, uses the relative rotation of two disks located at the core mid-plane to control the ratio of moderated neutrons to absorbed neutrons that are allowed to leave each core half of the core and enter the other. Both control disks have symmetrically located holes which allow neutron transmission when the two disks are properly aligned. A top view of the control disks is shown in Figure 2.29. In this configuration, which by no means represents an optimal hole pattern, a 22.5° relative rotation of the two disks reveals the least and most reactive core configurations. The variation of the effective multiplication as a function of the relative rotation angle of the disks is given in Appendix 1. It is believed that a combination of the above control mechanisms will be required to effectively control the advanced technology reactor. This will allow the development of a very compact overall reactor system.

In order to demonstrate feasibility of control, using the first of the above two control strategies, some of the previously reported scenarios are repeated as shown in Table 2.7. This table indicates that use of the separation distance provides a more effective control strategy for a wide range of operating scenarios. However, use of both alternate control strategies is needed to provide adequate control for all conditions.

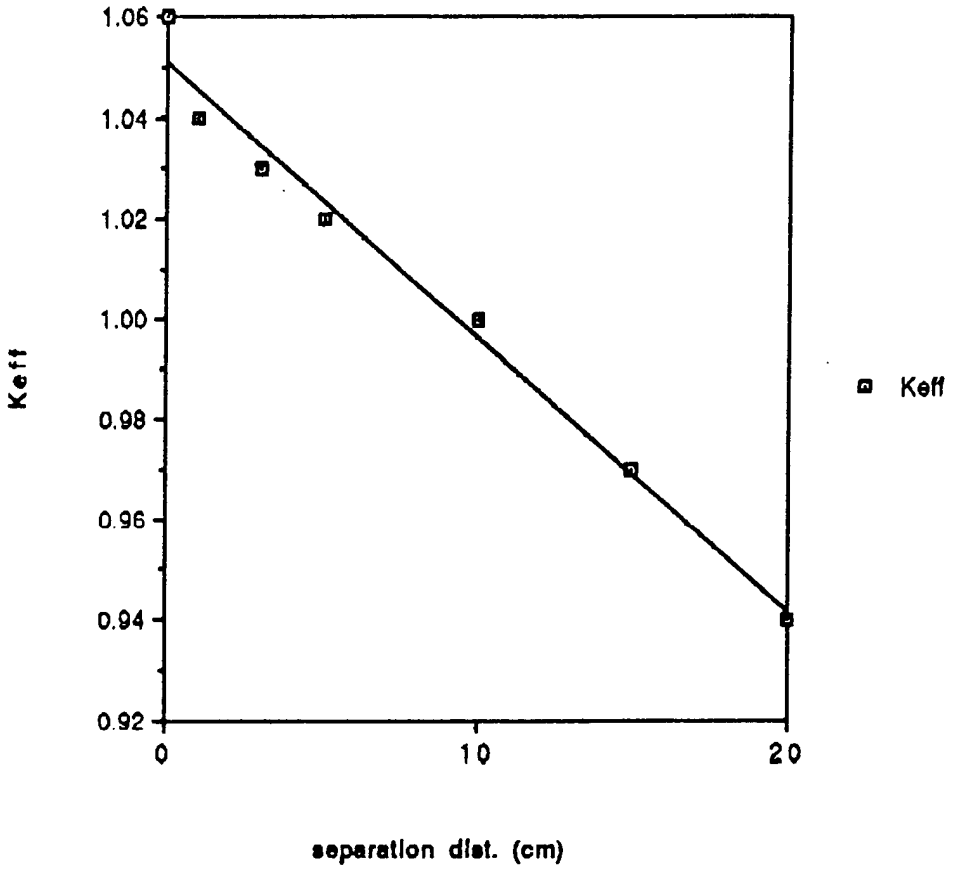

Figure 2.26. k_{eff} vs. Separation Distance for Advanced Am_2O_3 Core

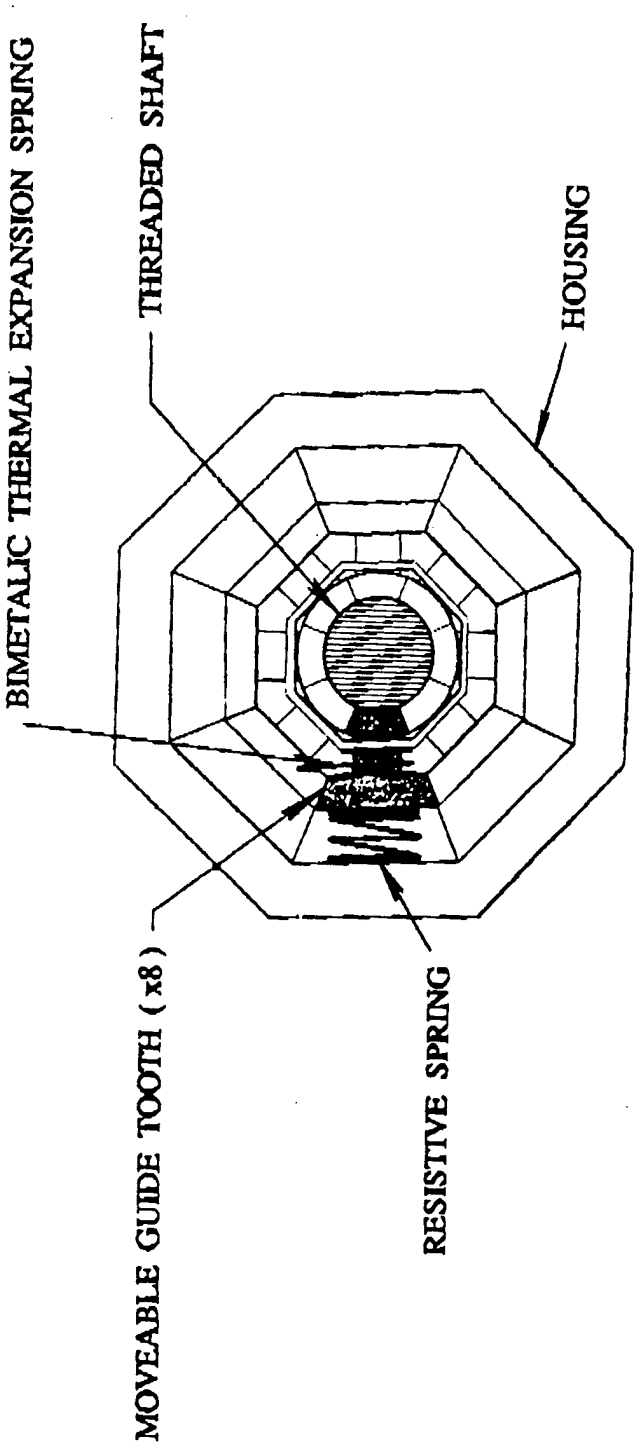

Figure 2.27. Thermal Fuse

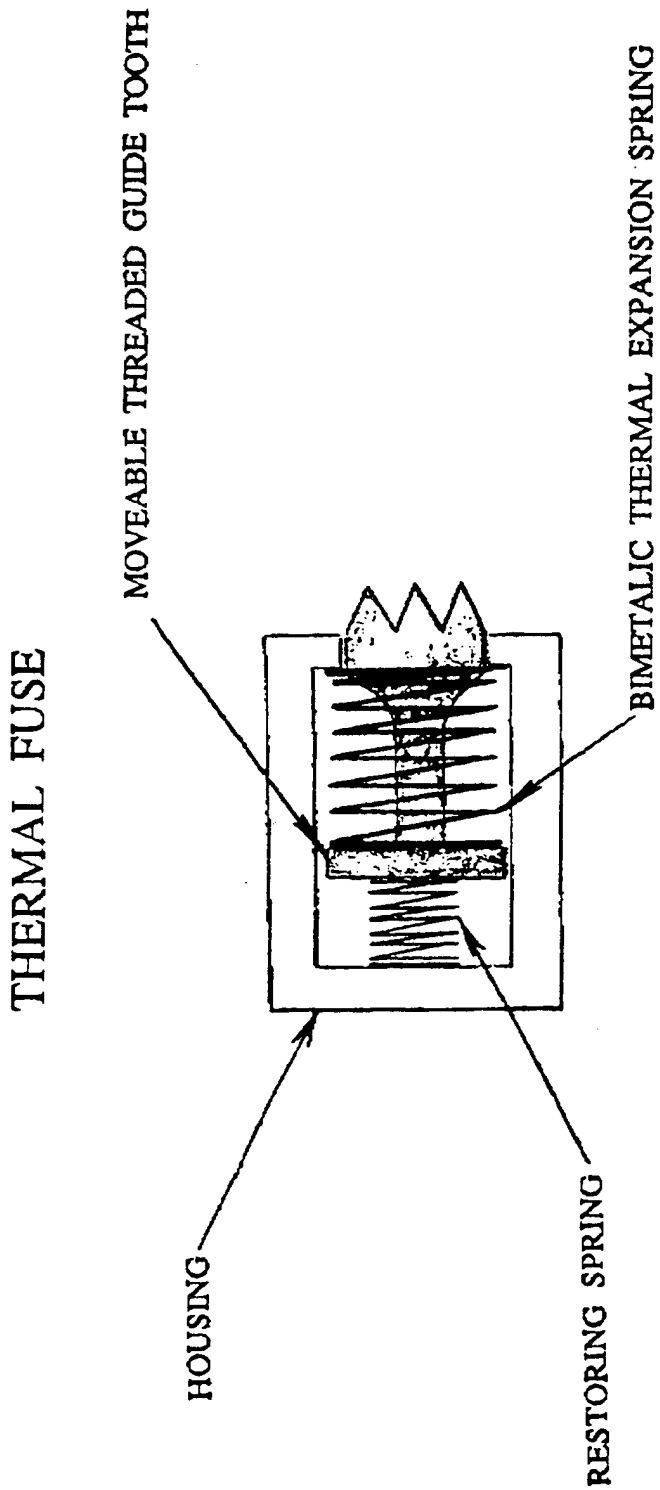

Figure 2.28. Side Cutaway View

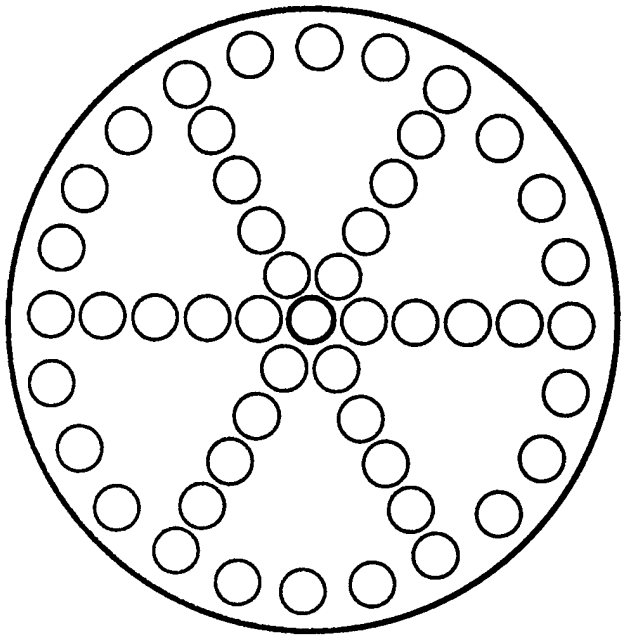

m9-1-MCL1-7268-17

Figure 2.29. Schematic of a Neutron Control Disk

TABLE 2.7. AM_2O_3 ADVANCED CORE CONTROL USING SEPARATION

	CASE	*DESIRED RANGE*	*KEFF*
1	**MAXIMUM REACTIVITY**	**KEFF=1.05 - 1.09**	**1.061**
2	**WATER FLOODING**	**KEFF<0.95**	**0.95**
3	**WATER IMMERSION**	**KEFF<0.95**	**0.95**
4	**LAUNCH CONFIGURATION**	**KEFF<0.90**	**0.943**

m9-1-MCL1-7268-18

2.3.10 Advanced Reactor Fuel

A number of transuranic fuels were considered for use in a compact space reactor. Two of these fuels are Curium and Americium in their oxide form, Cm_2O_3 and Am_2O_3. Some of the properties, availability and irradiation experience for these two fuels are given in Figures 2.30 through 2.33. Based on extensive discussions with personnel at Oakridge National Laboratory, Los Alamos National laboratory and Lawrence Livermore National laboratory, it was concluded that the choice fuel for making compact reactors is $Am_2^{242}O_3$, primarily because of relative ease of production and lower cost. The natural radioactive behavior of Am^{242} involves alpha decay with a 141 year half life emitting a 5.2 Mev particle. The relative alpha activity of 1 kg of Am^{242} with respect to 1 kg of P_u^{238} is

$$\frac{A(Am)}{A(PU)} = \frac{238}{242} \cdot \frac{T_{1/2}^{Pu}}{T_{1/2}^{Am}} = \frac{238}{242} \cdot \frac{88(yr)}{141(yr)} = 0.61$$

The Am_2O_3 fuel's natural activity is about 60% that of P_u^{238} based fuel.

It is interesting to note that Am^{241} will act as a poison in these reactor neutron spectra. Since Am^{242} is produced by neutron irradiation of Am^{241}, one can derive a double benefit by introducing some Am^{241} in the Am^{242} fuel. First Am^{241} could serve as a burnable poison and secondly it could breed Am^{242}. It is proposed that this reactor control technique should be explored in greater detail.

2.3.11 Energy Conversion

In-core thermionic energy conversion was selected as the energy conversion process for thermionic reactors because it directly converts thermal energy to electricity at reasonably high (10-15 percent) conversion efficiency, and has no moving parts. Its high temperature operation allows for heat rejection at a high temperature (a very desirable feature for space applications) and its thermionic converters can easily be accommodated around a reactor fuel rod without occupying much space - a necessary feature for compact reactors. Figures 2.34 through 2.39 show the basic principles of operation of thermionic converters and the schematics of a thermionic fuel element. In 1985, a Thermionic Fuel Element (TFE) Verification program was initiated by the Department of Energy. The purpose and goals of the program are displayed in Figure 2.40. Figure 2.41 describes the technical approach and Figures 2.42 and 2.43 illustrate the types of tests that are being conducted consistent with the technical approach. Figure 2.44 shows a summary of the key technology findings to date.

AVAILABILITY

- **CURRENT STATUS & PRICES NOT REPRESENTATIVE (TARGETS)**
- **DOD PROGRAMS COULD SUPPLY 10'S TO 100'S OF KG**
- **SPENT FUEL REPROCESSING COULD ALSO BE EMPLOYED**

IRRADIATION EXPERIENCE

- **EXTREMELY LIMITED**
- **JOINT US/UK PROGRAM (ONGOING)**
- **TUI/KFK PROGRAM (CANCELED PRIOR TO IRRADIATION)**

m9-1-MCL1-7268-50

Figure 2.30. Availability and Irradiation Experience

SESQUIOXIDE (Cm_2O_3)

- **MOST STABLE HIGH-TEMPERATURE PHASE**
- **CAPABLE OF DISSOLVING EXCESS OXYGEN UP TO Cm-01.7**
- **T<1600° C, MONOCLINIC, 11.2 GM/CM^3**
- **T>1800° C, HEXAGONAL, 11.4 GM/CM^3**
- **MELTING POINT APPOXIMATELY 2175° C**

SESQUIOXIDE (Am_2O_3)

- **MOST STABLE HIGH-TEMPERATURE PHASE**
- **CAPABLE OF DISSOLVING EXCESS OXYGEN UP TO Am-01.67**
- **T<700° C, (BCC), 10.57 GM/CM^3**
- **T>700° C, HEXAGONAL, 11.779 GM/CM^3**
- **MELTING POINT APPOXIMATELY 2205° C**

m9-1-MCL1-7268-25

Figure 2.31. Americium and Curium Phase Relationships

- **Thermal Conductivity (@ 1300°C)**
  - * Cm_2O_3 = 1.6 (W/m-K) (& decreasing slightly)
  - * UO_2 = 2.6 & UN = 25
- **Thermal Expansion (@ 1000°C)**
  - * Cm_2O_3 = 10 (x10^-6 1/K)
  - * UO_2 = 11 & UN = 8

Figure 2.32. Curium (Cm_2O_3) Material Properties

- **Fairly Extensive Testing Program @ ORNL**
- **Good Compatibility with Mo Alloys**
  - * TZM (Mo - 0.5 Ti - 0.1 Zr), Tm = 2610°C
- **Fair Compatibility with W & W-Re Alloys**
  - * Some W mass transfer
- **Incompatible with Ta Alloys**

Figure 2.33. Curium (Cm_2O_3) Compatibility

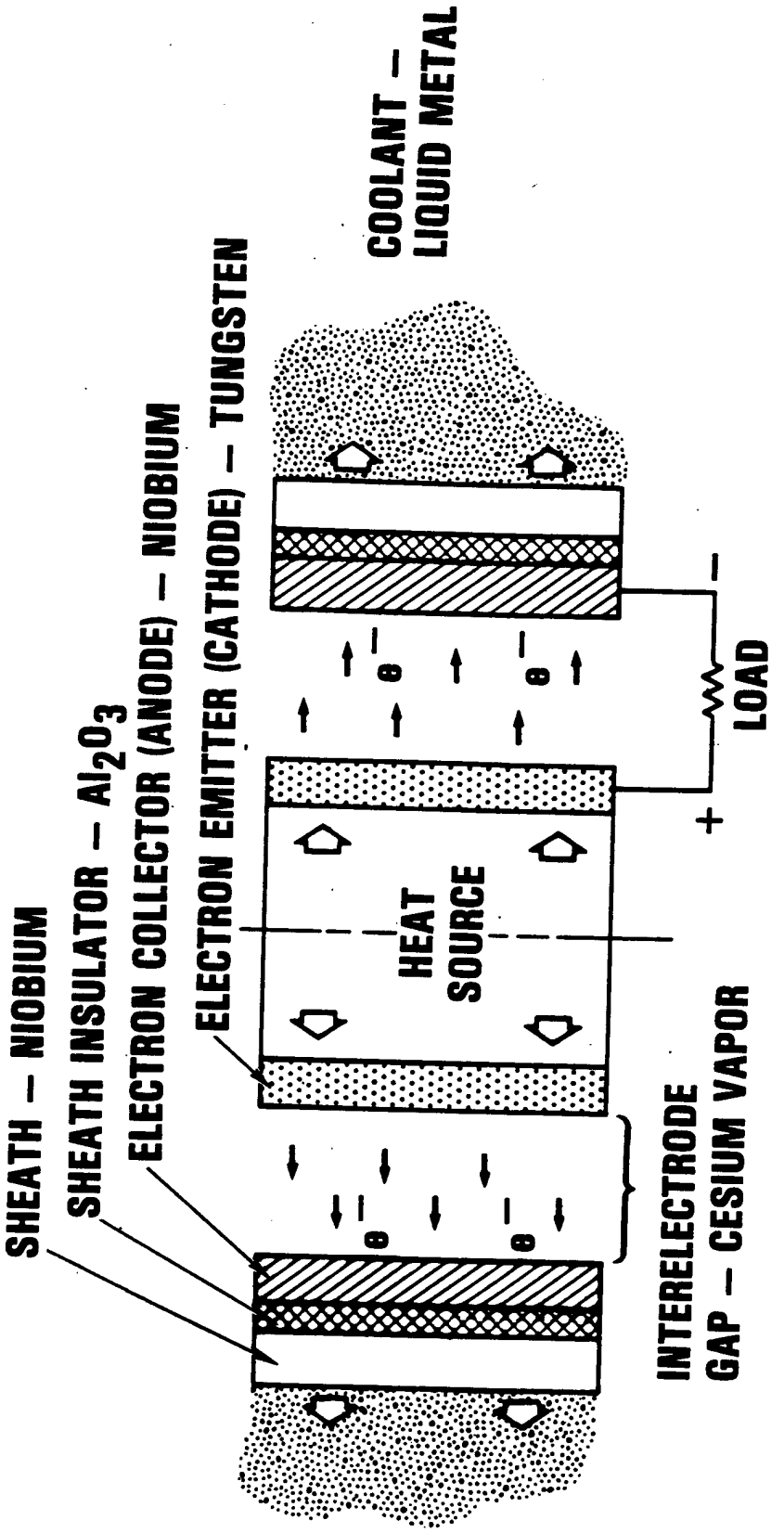

Figure 2.34. Thermionic Energy Conversion Principles

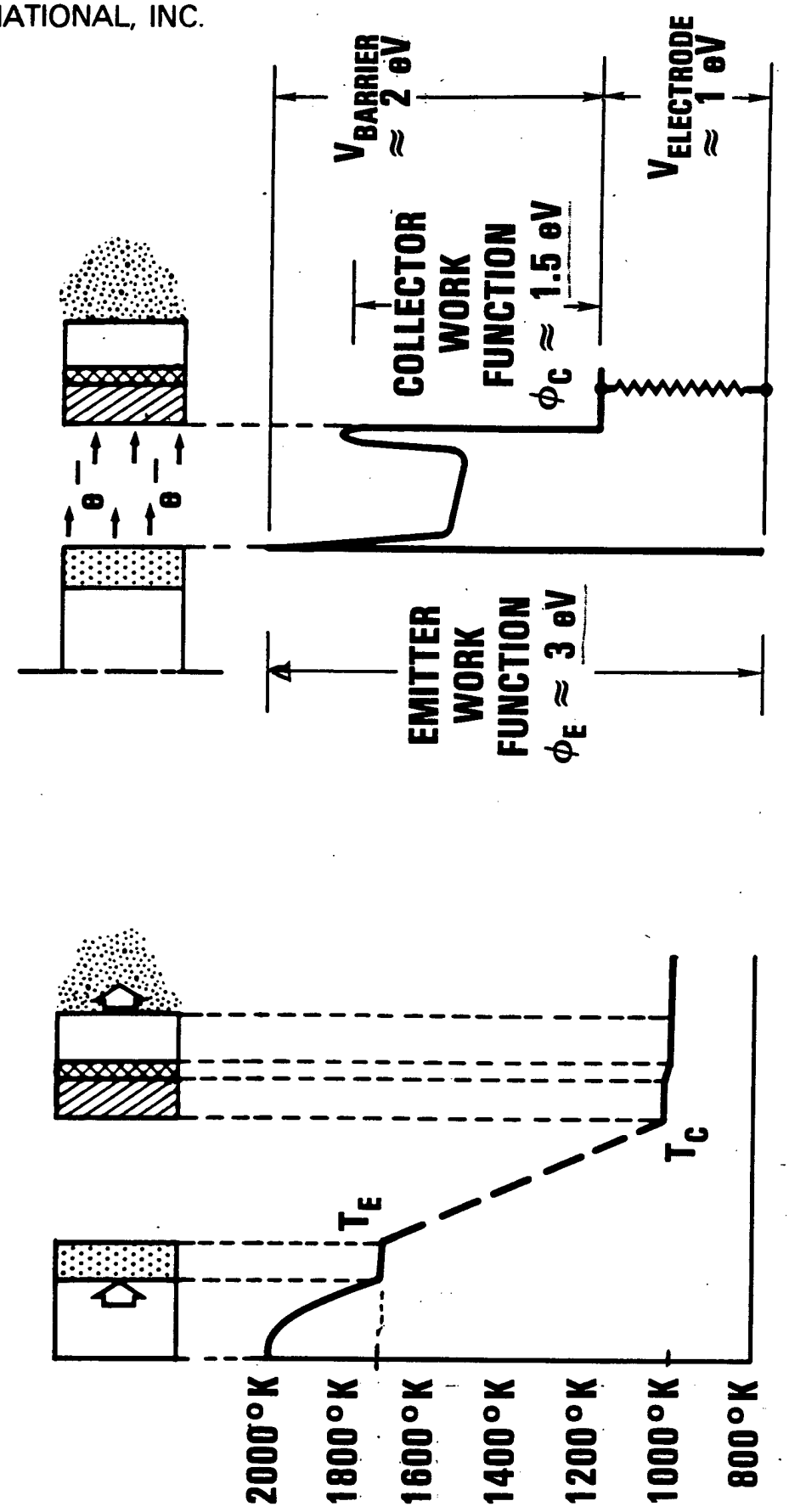

Figure 2.35. Thermionic Energy Conversion Characteristics

$$\eta_e = \frac{P_e}{Q} = \frac{\text{ELECTRIC POWER GENERATED BY ELECTRODES}}{\text{THERMAL POWER OF HEAT SOURCE}}$$

$$P_e \sim \bar{J}\,(\phi_E - \bar{V}_B) \text{ WHERE } J \cong AT_E^2 e^{-e\phi_E/kT_E}$$

$$Q = Q_e \text{ (EMITTER ELECTRON COOLING)} + Q_r \text{ (RADIATION COOLING)} + Q_K \text{ (CONDUCTION COOLING)}$$

Figure 2.36. Thermionic Energy Conversion Efficiency

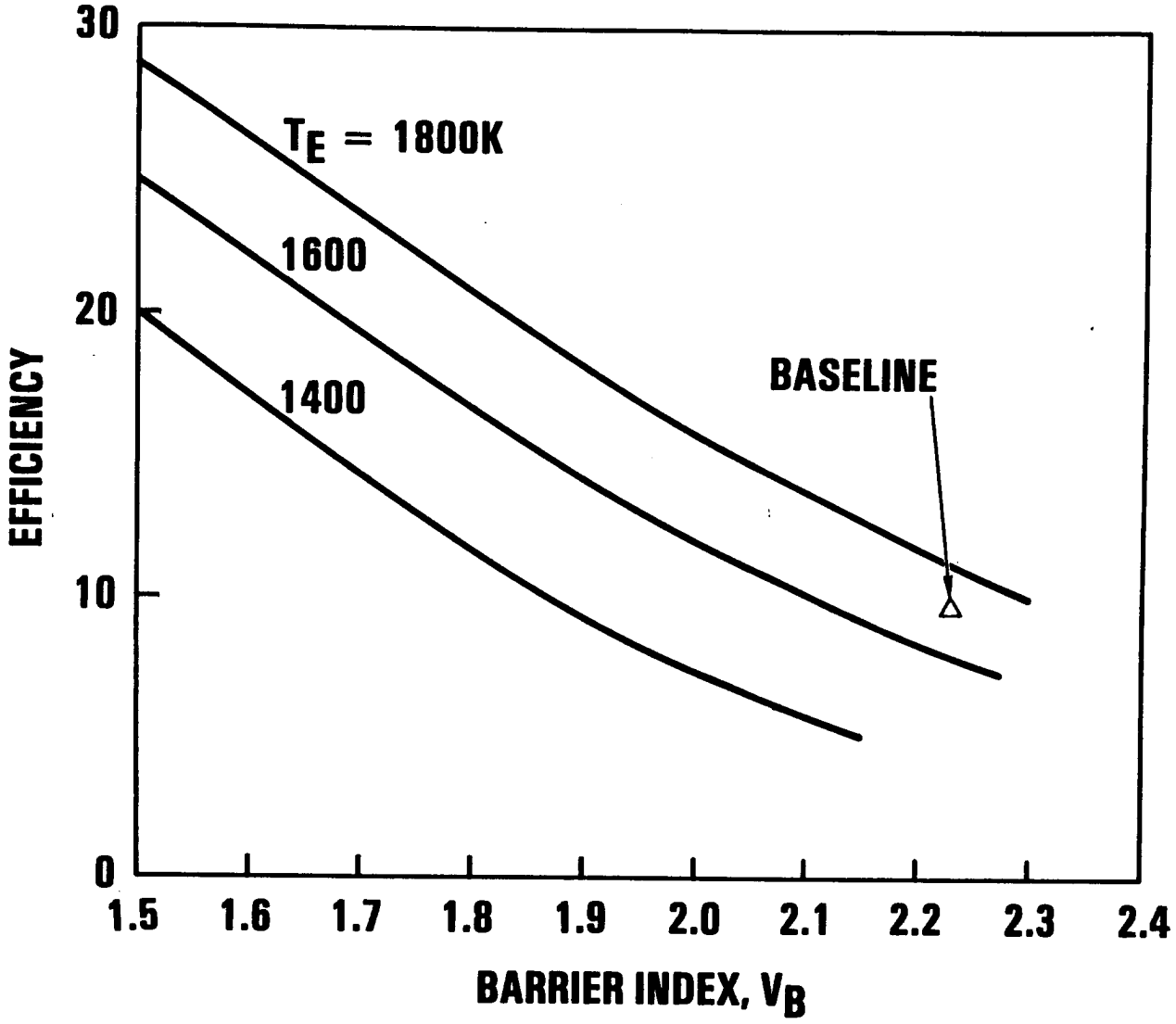

Figure 2.37. Efficiency Improvement for Lower Barrier Index

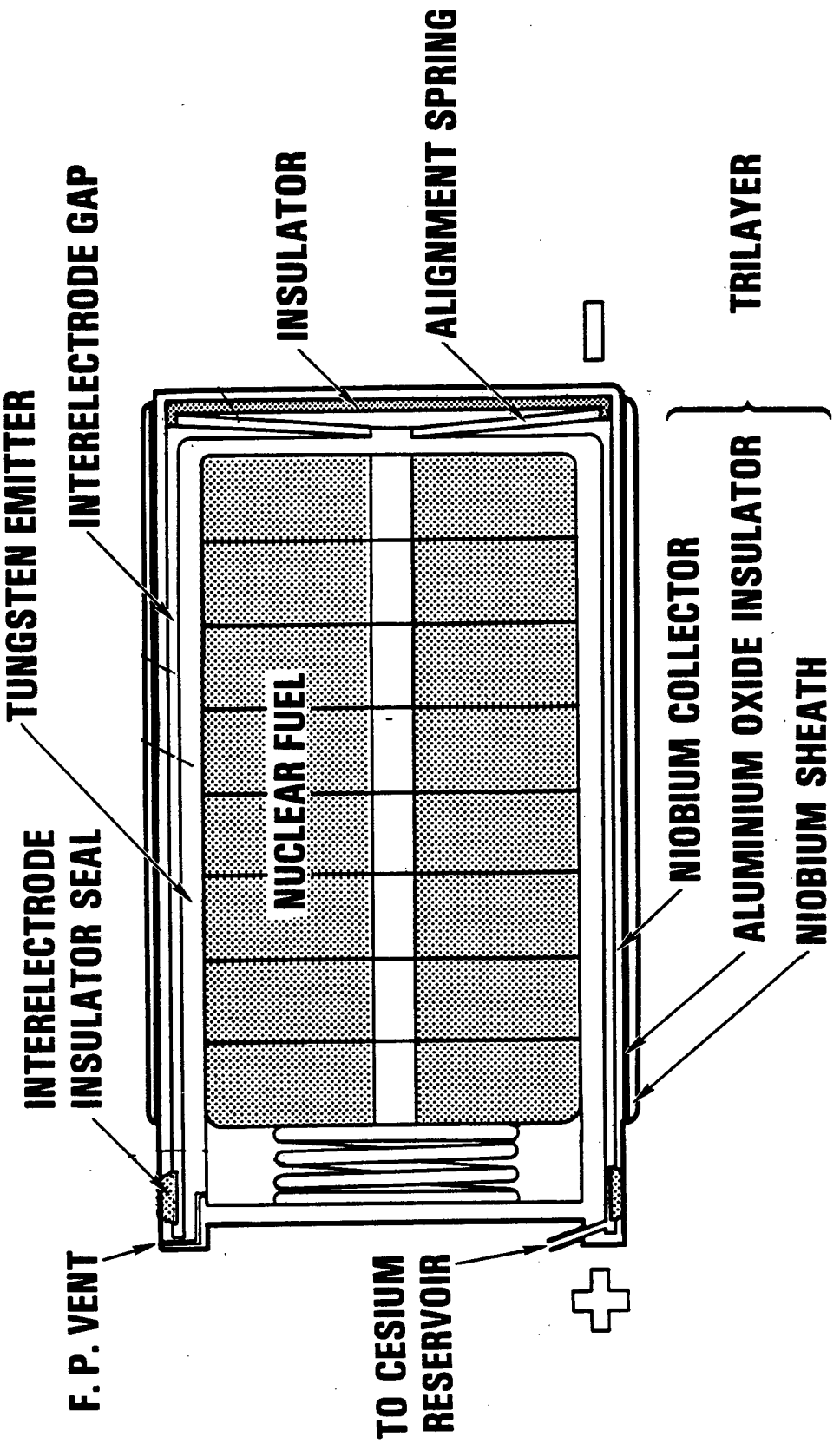

Figure 2.38. Schematic of In-Core Thermionic Cell

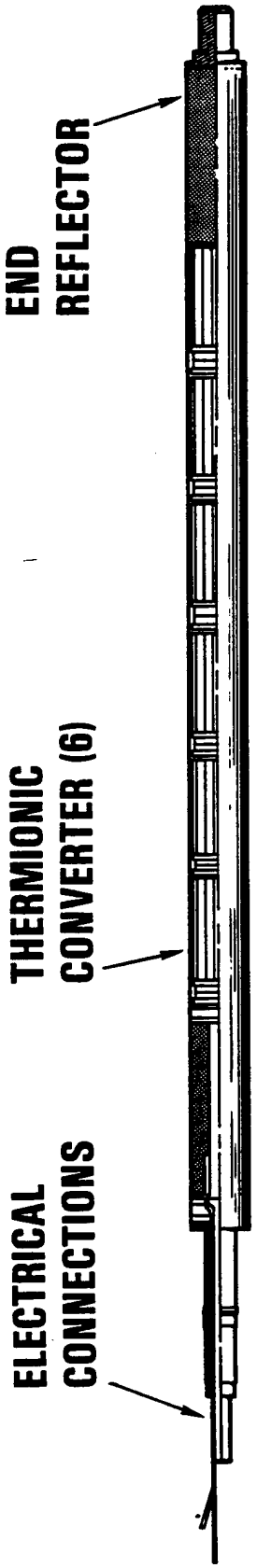

Figure 2.39. Schematic of In-Core Thermionic Fuel Element (TFE)

PURPOSE:

To Demonstrate and Verify the Technology Readiness of a Thermionic Fuel Element (TFE) Suitable for Use as a Basic Element in Advanced Thermionic Reactor Concepts with Electrical Power Output in the 0.5-5.0 kW(e) Range and a 7 Year Lifetime

GOALS:

- **Verify, Through Iterative, Accelerated Irradiation Testing and Analytical Modeling, a 7-Year Operational Lifetime for TFE Components**
- **Demonstrate TFE Performance Capabilities by Testing a Prototypic TFE Assembly in an Environment Representative of a Thermionic Reactor**

Figure 2.40. Thermionic Fuel Element (TFE) Verification Program

TECHNICAL APPROACH:

- **Design a Conceptual 2.0 MW(e) Thermionic Reactor System with a 7-Year Operational Lifetime as a Baseline for Developing Prototypic TFE Components**
- **Iteratively Fabricate and Test Various Sheath Insulator Designs to Assess Dimensional Stability and Interlayer Thermal Contact in Accelerated Irradiation Environments**
- **Iteratively Fabricate and Test Fueled Emitters to Assess Fuel Swelling at 6-7 Atom % Burnup in Real Time and Accelerated Irradiation Environments**
- **Verify the Performance Characteristics and Reliability of Insulator Seals, Cesium Reservoirs and Interconnective Components**
- **Based on Component Test Results, Fabricate and Test Partial and Prototypic Length TFE Assemblies in Real Time Irradiation Environments**

Figure 2.41. Thermionic Fuel Element (TFE) Verification Program

Accelerated Testing of Critical Components

Acceleration Variables	Acceleration Factors
• Flux	1 to 8 times the Real-Time Rate
• Burnup Rate	1 to 8 times the Real- Time Rate
• Voltage	3 times the Voltage
• Temperature	+ 100 K in Temperature

Planned Accelerated Tests

- Uninstrumented Tests in FFTF Using a Shared MOTA (UCA-1, -2, -3)
  - Multiple Specimens for Each Critical Component
  - 3 Sequential Irradiation Cycles to Allow Iterative Design/Downselection
- Instrumented Test in FFTF (IFAC-SI)
  - Tests Sheath Insulator Performance with Applied Voltage
- Uninstrumented Tests in EBR-II (UFAC-1, -2, -3)
  - Continuous Irradiation on 3 Sets of Fueled EmitterSpecimens
- Instrumented Test in EBR-II (IFAC-FE)
  - Instrumented Fueled Emitter Test Will Provide Benchmark Data

Figure 2.42. TFE Verification Program Technical Approach

Real Time Testing of Partial Length, Integral TFEs in TRIGA....

One and Three Cell TFE String Tests in TRIGA Will Verify:

- Emitter Performance and Swelling Relationships
- Intercell Insulation Performance
- Performance of Support, Alignment and Interconnective TFE Components
- Fission Product Vapor Barrier and Fission Gas Vent Performance

in FFTF....

- Prototype Six Cell TFE String Test Will be Tested Above Core To Provide a "Correct" Irradiation Environment

Analytical Modeling Support

- Provides Combined Physical/Empirical Models
- Rate Variation Modeling
- Verified by Benchmarking with Experimental Data
- Allows Extension to Real Time Performance

Demonstration of TFE Fabrication Capability

Figure 2.43. TFE Verification Program Technical Approach (Continued)

FUELED EMITTER EQUIVALENT LIFETIME OF 7 YR AT 1800 K INDICATED.

SATISFACTORY PERFORMANCE OF CS/GRAPHITE RESERVOIRS FOR FAST NEUTRON EXPOSURE EQUIVALENT TO ~15 YR DEMONSTRATED.

HERMETICITY OF TRILAYER DESIGN SEAL INSULATORS APPEARS ADEQUATE FOR:

7 YR	EQUIVALENT	FAST	NEUTRON	FLUENCE	(2MWe DESIGN).
18 YR	"	"	"	"	(100 KWe DESIGN).
100 YR	"	"	"	"	(10 KWe DESIGN).

GRADED AL_2O_3 AND Nb/AL_2O_3 CERMET SHEATH INSULATORS WITHSTAND 7 YR EQUIVALENT FAST NEUTRON FLUENCE.

STRESS RELIEVING END DESIGN DISCOVERED THAT ELIMINATES END DISTORTION OF GRADED AL_2O_3 AND Nb/AL_2O_3 CERMET SHEATH INSULATORS.

AL_2O_3, Y_2O_3, AND YAG INSULATOR COATINGS ON Nb ADHERENT AND CRACK FREE AT VERY HIGH FAST NEUTRON FLUENCE.

>8000 HR OPERATION OF SINGLE CELL PROTOTYPICAL TFE WITHOUT DEGRADATION. TEST CONTINUING.

Figure 2.44. TFE Verification Program Summary of Technology Findings

SECTION 3.0
IDENTIFICATION OF KEY FEASIBILITY ISSUES AND PROGRAM PLAN FOR CONCEPT DEVELOPMENT

This section identifies the key technical feasibility issues for the Off-the-Shelf Thermionic Reactor Power System with energy storage (Concept A) and the advanced thermionic reactor power system without energy storage (Concept C (Table 3.1)). Since work for Concept C has only recently been initiated, a detailed program plan for Concept A is delineated here.

Development of the thermionic reactor power system is strongly aided by several unique and inherent features of thermionic fuel elements (TFEs). These TFEs contain the fuel that generates the heat, energy transfer from fuel to the energy conversion system and thermionic energy conversion. All these functions are tested in individual TFEs along with all the interfaces.

The TFE's allow a high degree of redundancy and hence reliability because only a small fraction of the electrical output is produced in each TFE. An attractive feature of the thermionic reactor is the confinement of the high temperature of operation region to the fuel emitter which is essentally thermally isolated from the remainder of the TFE and the power system. The reactor vessel, controls, shield, power conditioning, and the space frame all operate at relatively low temperatures.

A unique feature of the OTS reactor is the energy storage system around the TFE and the passive heat pipe, heat transport, and heat rejection system. The energy storage system, in principle, is very similar to the heat receiver module that is being developed for the solar dynamic power generation system. The major difference is that the TFE replaces the internal tube that is used in the heat receiver module for heating the Brayton cycle working fluid.

Table 3.2 shows some of the previous reactor programs that aid the thermionic reactor development program. Figure 3.1 shows a generic program plan for development of the OTS reactor. It is assumed that flight components can be tested in parallel with the ground testing of the flight system. It is also assumed that parallel technical approaches are taken for those areas where feasibility issues need to be resolved.

Figure 3.2 shows the critical technology phase schedule for the OTS Space Reactor Program for a 1996-1997 launch. This table should be viewed in parallel with Figure 3.1 in order to develop a complete understanding of the schedule.

TABLE 3.1. KEY TECHNICAL FEASIBILITY ISSUES FOR CONCEPTS A AND C

CONCEPT A	CONCEPT C
UO_2 IS THE BASELINE FUEL; HOWEVER IF UC IS USED, IT WILL BE IN THE FORM OF TRISO PARTICLES WITH A SiC COATING *LIFE TESTING OF THE TFE WILL BE REQUIRED*	*FUEL FEASIBILITY DEMONSTRATION* *Am_2O_3 FUEL* *Am_2O_3 /UO_2 FUEL MIXTURES* *Am^{241} AND Am^{241} FUEL MIXTURES* *Am^{241} , Am^{242} , UO_2 FUEL MIXTURES* TESTING FOR — COMPATIBILITY — FABRICABILITY — STABILITY
EFFECT OF THERMAL CYCLING OF TFE's ON LIFE	*ZrH - CONTAINMENT*
ZrH - CONTAINMENT	*SEPARATING AND ROTARY DISC CONTROL SYSTEMS*

m9-1-MCL1-7268-24

TABLE 3.2. EARLIER PROGRAMS AIDING OTS THERMIONIC REACTOR PROGRAM

- *TFE VERIFICATION PROGRAM (STARTED IN 1985)*
- *SNAP REACTOR PROGRAM*
  - *x LiH shield*
  - *x ZrH_x experience*
- *FAST REACTOR TECHNOLOGY PROGRAM*
- *REFRACTORY METAL TECHNOLOGY*
- *HEAT RECEIVER TECHNOLOGY*
- *HEAT PIPE TECHNOLOGY*

m9-1-MCL1-7268-23

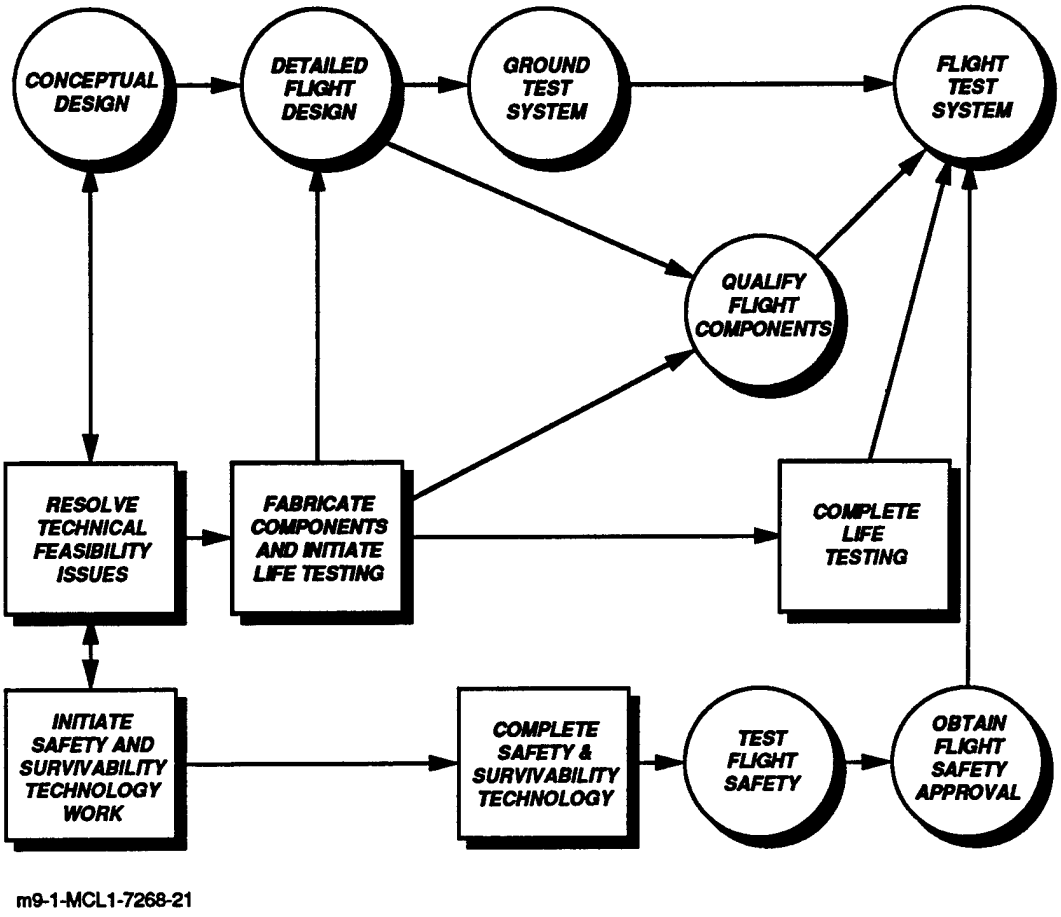

Figure 3.1. Generic Program Development Plan

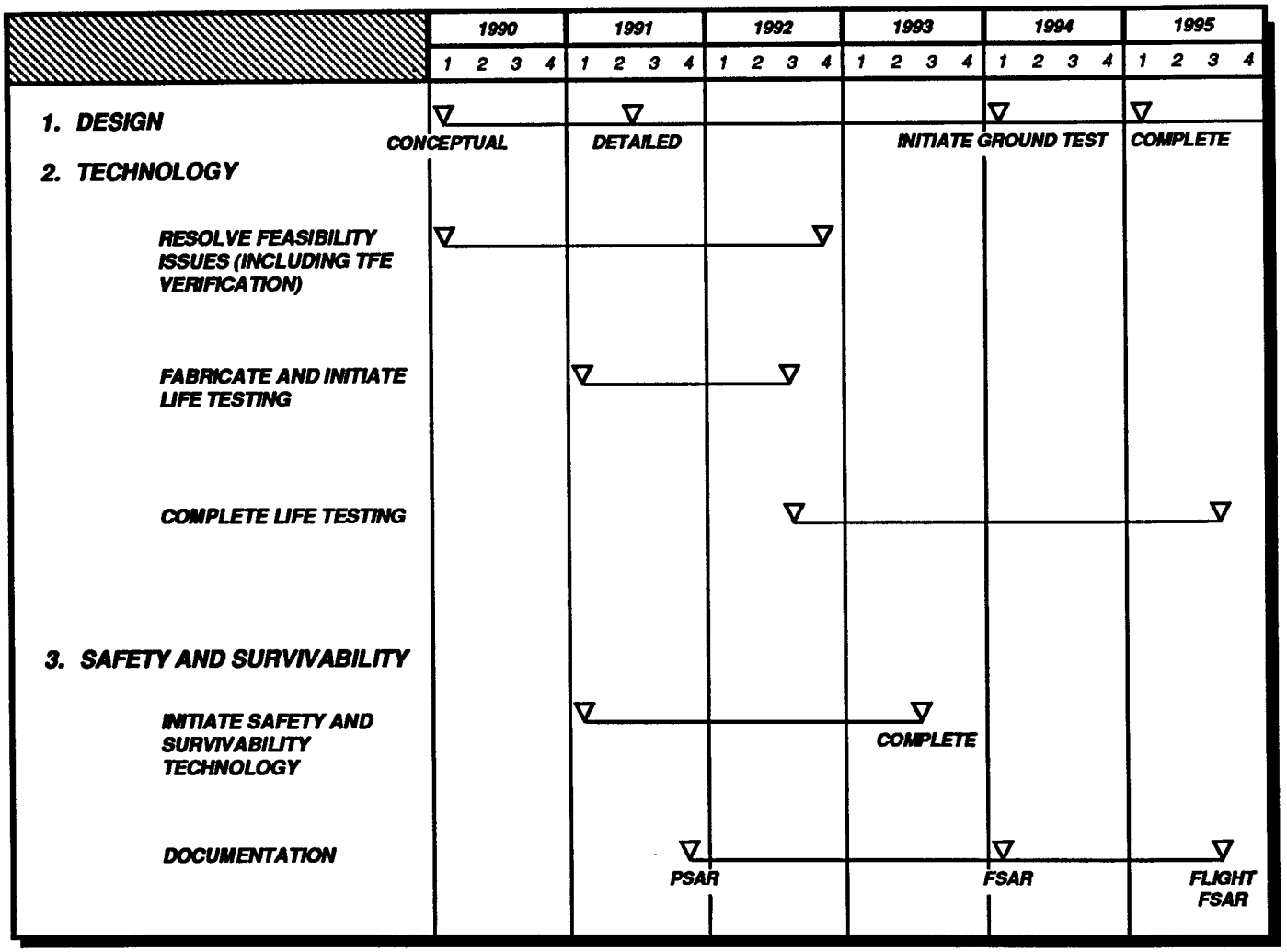

m9-1-MCL1-7268-22

Figure 3.2. Development Schedule For OTS Reactor (Concept A)

APPENDIX A
(SCOTT NEGRON – TEXAS A&M)

I. Introduction

A control device is necessary to safely regulate power in a nuclear fission reactor. Fission is the process in which a fissile atom, such as U-235 or Pu-239, absorbs a neutron and splits into two or more fragments producing an average of 2 - 3 neutrons. These neutrons may go on to produce further fissions in other fissile atoms. In a critical reactor core, the neutron population level (hereafter referred to as flux) remains constant, that is, as many neutrons are produced from fission as are lost. The power level of reactor core is directly proportional to the neutron flux level, and may be regulated by varying the fission reaction rate. Fission rate may be varied in several ways, which are each described separately.

Absorption: Elements such as boron and cadmium possess very high neutron absorption cross sections. These "absorber" materials can be used to regulate a fission reaction by parasitically absorbing the neutrons which cause the fissioning to occur. Control rods are fabricated from B_4C or similar material. Insertion of control rod thus decreases the fission rate while removal increases it.

Reflection: Neutrons which leave the boundary of the core are considered "leaking" neutrons. Reflection, which is essentially 180° scattering, causes an influx of neutrons which may again contribute to the reaction. Variable reflection can thus be used to vary reactor power to some extent.

Fuel: Addition or removal of fissile material within a reactor core may also be used to regulate reactor power. Addition of fuel almost always causes the reaction rate to increase. Some existing control rods are made of fuel, and are inserted to increase the fission rate.

Geometry: Changing the geometry of a reactor core can drastically alter the fission rate. Separation of fissile material decreases the reaction

rate due to an increase in neutron leakage. Fissile cores are generally quite sensitive to geometric changes.

All power fission reactors employ one or several control mechanisms to safely regulate power output over a broad range of power. Like most devices, each has its own advantages and disadvantages. For instance, while control rods may effectively control power in a large light-water reactor, such a device may prove impractical in a compact core. Drastic flux shifts may occur due to the presence of an absorber material at one extremity. Figure 1 illustrates the changes in flux when a control rod is inserted into a small homogeneous fissile core. Asymmetric flux profiles are undesirable due to the uneven fuel burnup and power distribution.

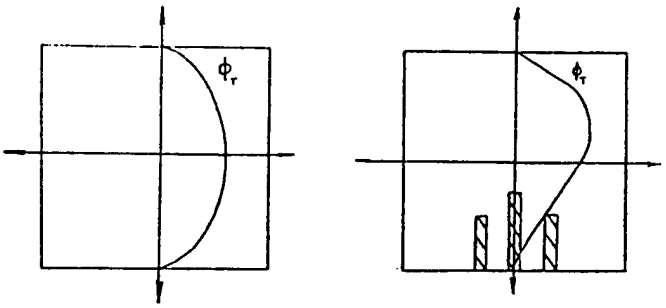

Figure 1
Neutron Flux Profiles With and Without a Control Rod

II. Detailed Description of Neutron Control Disks

The intention of neutron control disks is to offer a compact means of power regulation over a wide range of power. Additionally, control disks are centrally located within the core to insure symmetric flux profiles. Two disks made of an absorber material and having identically machined surface hole patterns are coupled such that rotation of one causes the holes to open and close. This may act to variably attenuate neutrons incident to the disk surface. Figure 2 shows a typical control disk design. Hole sizes and patterns were picked for simplified analysis and are so far not optimized.

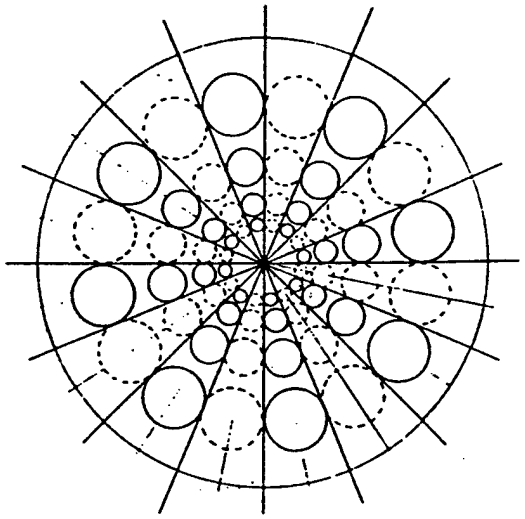

Figure 2
Control Disk Design

In order to determine the neutron attenuation as a function of angle, a scale control disk was fabricated from cadmium for experimental measurements. A collimated neutron beam from a port of the Texas A&M AGN-201M nuclear reactor was used for the incident neutron source. A BF_3 neutron detector was used to measure count rate as the disk assembly was rotated open. the resulting polynomial transmission obtained is shown in Figure 3.

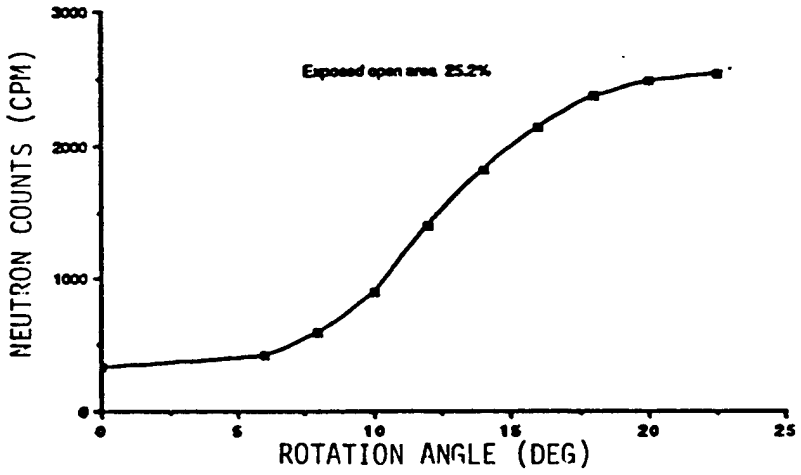

Figure 3
Polynomial Neutron Transmission of Model Control Disk

III. Modeling of Control Disks and Relevant Results

In order to evaluate the performance of a control disk in a reactor core, a numerical analysis is necessary. The Los Alamos National Laboratories computer code TWODANT was used to simulate the neutronics for a small PuC core containing a control disk. Figure 4 shows an expanded view of the basic geometry.

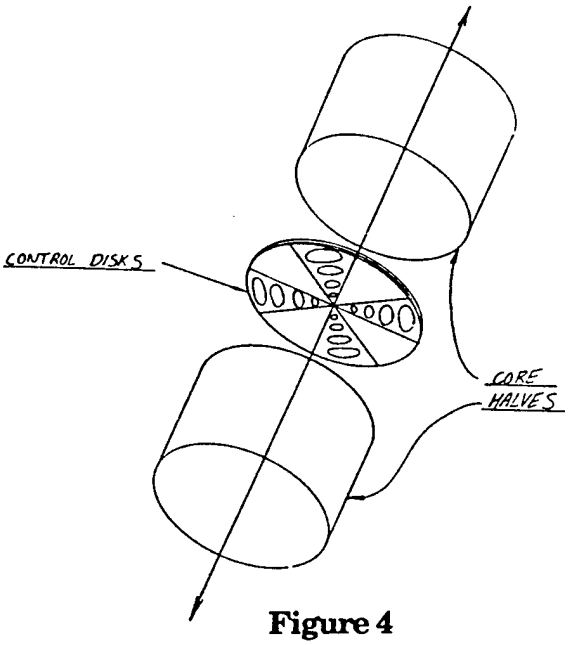

Figure 4
Control Disk Core Configuration

The main problem in modeling such a system is going from a 3-D geometry problem to a 2-D problem, which could be solved using TWODANT.

Figure 5. shows how hole coordinates in the 45° sector of action are mapped into the vertical plane. This "cutaway" view shows the hole positions as well as disk thickness. Regions containing a hole may thus be varied in material concentrations to simulate hole opening and closing.

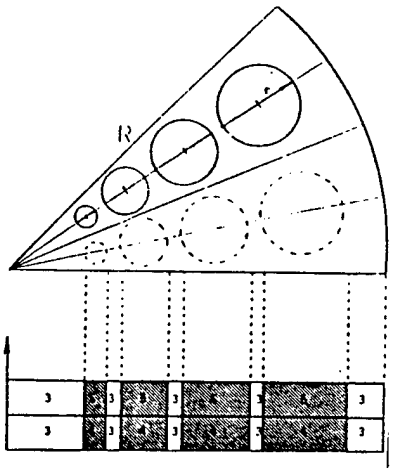

Figure 5

Mapping of Sector Coordinates into x-y Plane

The numbers in each region are assigned by TWODANT using the ASSIGN= and MATLS= arrays. Coarse geometric mesh points are used to describe the zones and dimensions. Figure 6 shows the arrays used in assigning materials to the regions in the problem. Each material is assigned a number in descending order of the list.

```
/ * * * * BLOCK IV (MIXING) * * * *
/
   MATLS=PUC      "PU-239" .032     C   .032/
         SODIUM   "NA-23"  .025/
         B4C      "B-10"   .087     C   .022/
         STEEL    FE       .079     C   .026/
         UO2      "U-235"  .0232    "U-238" .001     0   .049
/
   ASSIGN=CORE    PUC      1.00/
         COOLANT  SODIUM   1.00/
         DISK     B4C      1.00/
         HOLE     PUC      1.00/
         MIX      PUC      1.00    B4C       0.00     T
```

Figure 6

TWODANT Material Assignment Arrays

A core map is generated each time TWODANT is run. Figure 7 shows the core map containing fuel, disk, and reflector regions. The map is symmetric about the left vertical axis, that is only the right core half is shown. Materials which make up the disk region are (3) B_4C absorber and (4) PuC fuel inserts in the holes. The PuC fuel inserts are intended to further increase performance by causing additional fissioning as the holes are opened. This is analogous to fuel-followed absorber rods. Region (5) is a mix of B_4C and PuC which is varied in the top disk set of holes. Variation of PuC concentration in the hole regions was related to angular dependence by normalizing the attenuation polynomial in Figure 3. Although this may

not be strictly correct, it is believed to closely model the absorption angular dependence. Since scattering takes place within the disk absorber material, actual experimental data may prove more accurate in this situation.

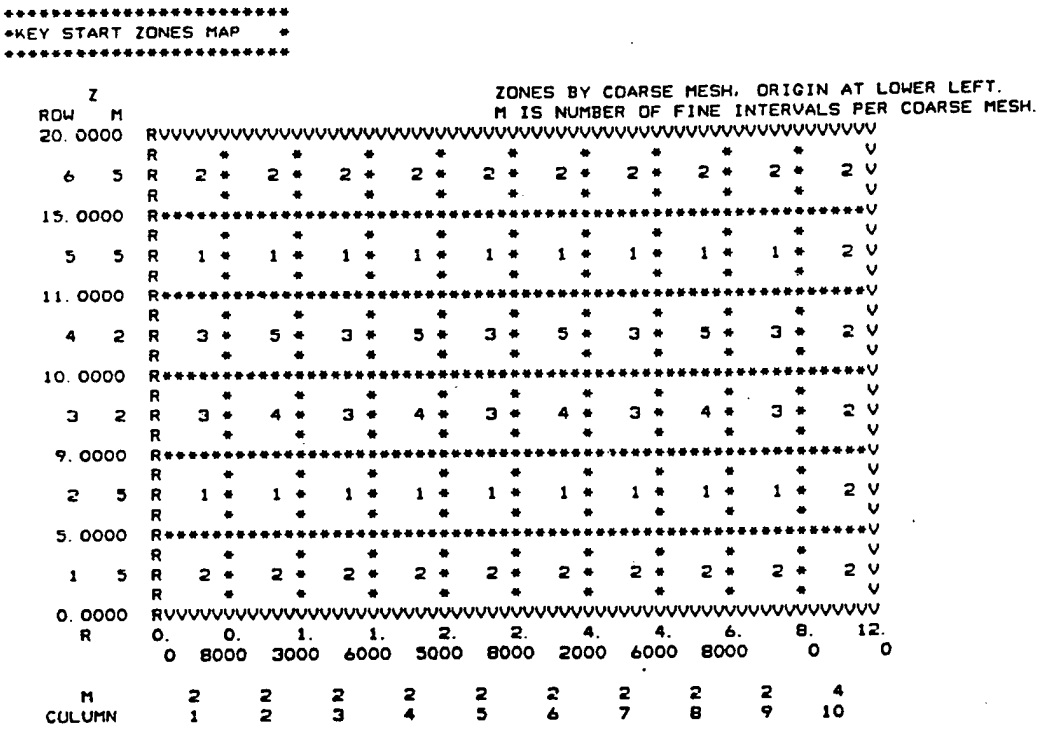

Figure 7
TWODANT Core Map

Figure 8 shows the vertical neutron flux profile of all eight energy groups used. As expected the vertical flux is symmetric about the horizontal axis. This may be a valuable attribute as most irregularities become extenuated in smaller systems. The central flux depression is caused by the presence of the absorber material. As the total flux decreases this depression may become more pronounced.

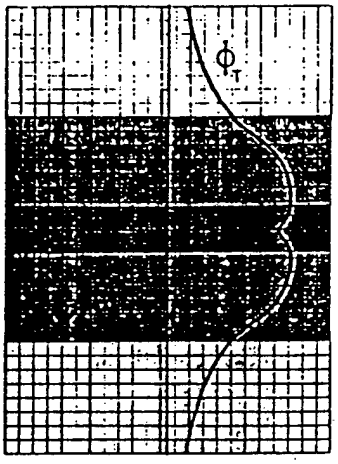

Figure 8
Vertical Neutron Flux

In addition,Keff eigenvalues obtained from TWODANT were used to generate a differential reactivity worth curve as a function of angle of rotation. In calculating reactivity, Equation (1) was used with ß eff = 0.0021 for Pu-239

Equation 1. $$\frac{\Delta\rho(\$)}{\Delta\theta} = \frac{\left[\frac{1}{k_1} - \frac{1}{k_2}\right]}{\theta_2 - \theta_1}$$

Keff eigenvalues were obtained from successive TWODANT runs. Table 1 shows the values obtained, for each normalized PuC concentration]

Table 1
Keff Values for Various Angular Positions

0 (deg)	% PuC	Keff
0	0.000	0.953
5	0.025	0.955
7.5	0.100	0.960
10	0.260	0.972
12.5	0.525	0.992
15	0.750	1.011
17.5	0.900	1.025
20	0.975	1.032
22.5	1.00	1.035

The resulting differential worth curve is shown in Figure 9. Because of the sensitivity of the system, fairly large reactivity changes can occur over the full 22.5° of rotation. Larger reactivity changes may be obtained by use of a greater hole pattern area. For the disk as modeled, the maximum hole surface area may be easily found to be 24.5%. This may be increased to up to 50% using two disks or 66.7% for three disks.

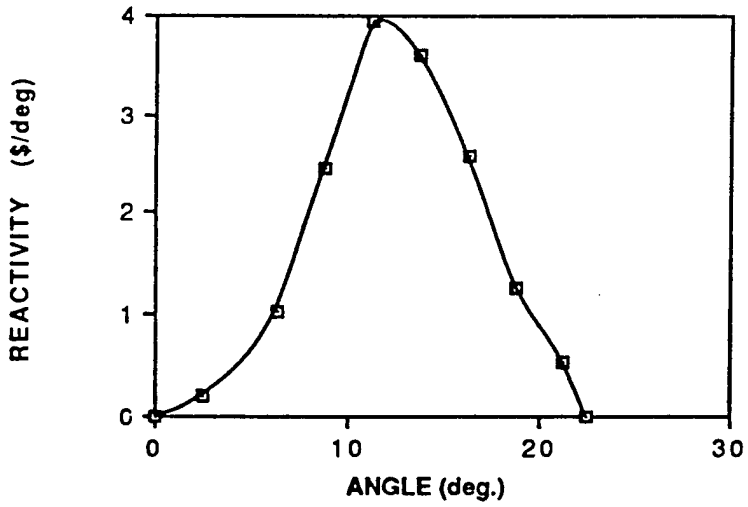

Figure 9

Differential Reactivity Worth of Control Disk

The differential rod worth curve of Figure 9 can be integrated to obtain the integral rod worth for use in transient simulations.

IV. Conclusions

Constant disks may offer many advantages over existing control devices, because of compactness, ease of operation, flux symmetry, as well

as significant reactivity worth. These advantages may lend themselves well to a new generation of advanced compact fast reactor cores. Such reactors could be feasible power sources for many future space missions and eventual colonization of the solar system.

References

1. Scott B. Negron, Steve Nance, "Neutron Attenuation by Control Disks" -Experiment performed as a requirement for NUEN 405 by Dr. G. A. Schlapper, Spring 1989.
2. Dr. Alexander G. Parlos, Department of Nuclear Engineering, Texas A&M University. Personal communication (Summer 1989); lecture notes from NUEN 404.
3. Dr. Forrest Brinkley, Los Alamos National Laboratories. Personal communication (July 1989).
4. Dr. R. Douglas O'Dell, Los Alamos National Laboratories, Personal communication (Summer 1989).
5. Argonne National Laboratory, United States Atomic Energy Commission, 1963. ANL-5800.

APPENDIX B

RELEVANT PROPERTIES OF ZIRCONIUM HYDRIDE AND OTHER METAL HYDRIDES

B.1 INTRODUCTION

BDM has conducted a literature review to examine the relevant properties of zirconium hydride and other potential candidate metal hydrides as moderator materials in nuclear reactors for space power applications.

Hydrogen is a highly desirable moderator material. Because of its mass, hydrogen, in elastic collisions with high energy neutrons, rapidly slows these neutrons. Metal hydrides are capable of containing higher densities of hydrogen than liquid or solid hydrogen itself. Table 1 lists some hydrogen containing materials and the associated density in number of atoms of hydrogen per cubic centimeter.

In addition to their high hydrogen content, metal hydrides have other characteristics such as thermal stability and mechanical strength that are of interest for reactor design. This is particularly true for compact reactors. Reference 1 briefly summarizes information from several efforts investigating the use of metal hydrides for moderators during the 1950's and 60's. Key findings from these efforts will be discussed with the associated physical properties later. Additional references to more current reactor design programs are identified in the list of references (Ref 5&6) but have not been reviewed for this discussion.

This review focused principally on zirconium hydride and while no effort has been made to comprehensively gather all detailed information on the numerous candidate metal hydrides and perform any detailed trade-off analysis for their applicability as moderators, Reference 1, W. M. Mueller Metal Hydrides, provides a good comprehensive reference on these materials; however, it is somewhat dated and out of print. One possible alternative material which was briefly examined was titanium hydride. Like zirconium hydride, titanium hydride has good thermal stability and mechanical properties and is capable of high hydrogen densities. However, Reference 1 infers that titanium has a significantly higher neutron absorption cross section than zirconium, making zirconium hydride the better moderator material. Most of the discussion in Reference 1 regarding metal hydride modulators addressed zirconium hydride and zirconium hydride/uranium fuel mixtures. The focus of the remainder of this Appendix will be on the properties of zirconium hydride, particularly for temperatures in the range of 500-1000^{o}K (227-727^{o}C or 440-1340^{o}F).

TABLE 1. HYDROGEN DENSITIES IN SOME HYDROGEN-CONTAINING COMPOUNDS

Compound	Number of H atoms/$cm^3 x 10^{-22}$
Liquid hydrogen (20°K)	4.2
Solid hydrogen (4.2°K)	5.3
Water	6.7
LiH	5.9
TiH_2	9.2
ZrH_2	7.3
$VH_{0.8}$	5.1
GdH_2	5.4
GdH_3	6.4
YH_2	5.7
UH_3	8.2

B.2 PHASE DIAGRAM

The work to establish phase diagrams for the zirconium-hydrogen system is reviewed in References 1 and 2 and the authors construct temperature vs. composition phase diagrams based on the compilation of their reviewed work. While the major features of these phase diagrams are in agreement, some minor questions remain from the experimental results. For a discussion of these experimental details see Reference 1.

Figure 1 shows the temperature vs. composition phase diagram from Reference 1. Superimposed on the figure are dashed isobars at different pressures. Regions for the α and β phases are shown in the figure. In these regions a solid solution is formed with hydrogen "dissolving" in the respective α and β phases of zirconium. There are three nonstoichiometric zirconium hydride phases:

- γ described as a metastable phase occurring in the α-δ mixed phase region,
- δ existing in the composition range of approximately $ZrH_{1.4}$ to $ZrH_{1.65}$ and has a face centered cubic crystal structure, and
- ε existing for compositions $ZrH_{1.65}$ - ZrH_2 with a face centered tetragonal crystal structure.

The δ and ε phases become miscible at a temperature of approximately 750°C.

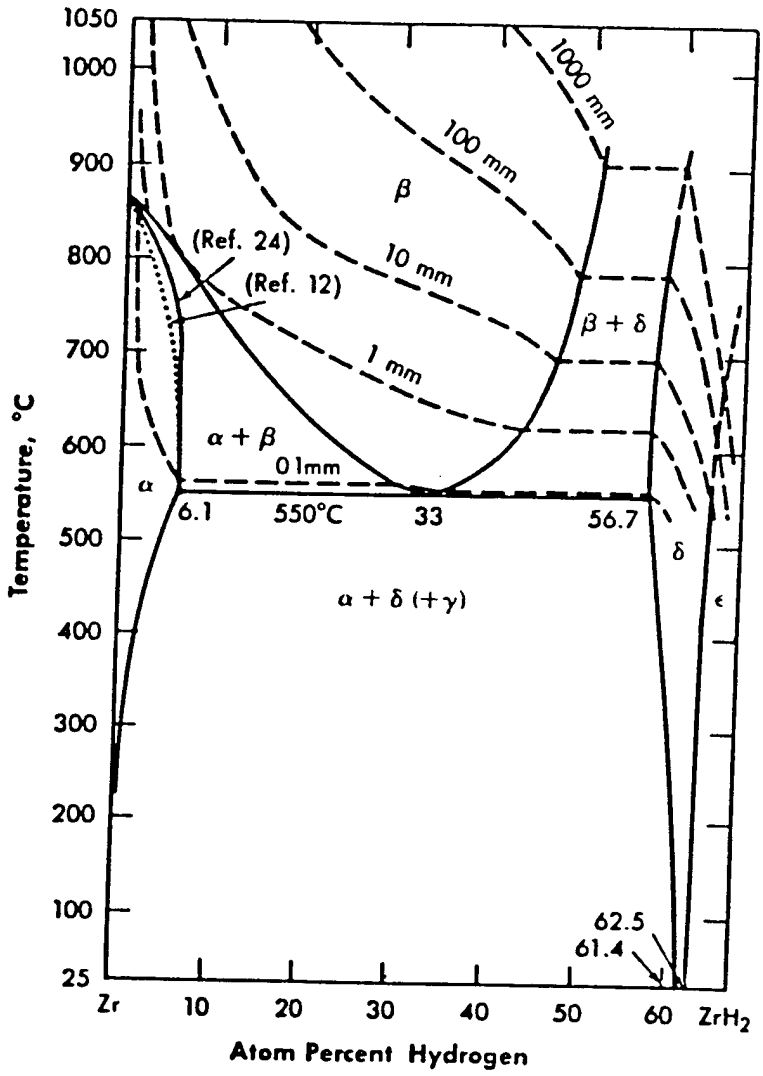

Figure 1. Zirconium-hydrogen Phase Diagram (from Ref 1)

For use as modulator materials, the higher hydrogen composition hydrides are of most interest, particularly the δ and ε phases. The information in Figure 2 (Ref 1) showing pressure/composition isotherms is of interest. The isotherms show the equilibrium hydrogen vapor pressure versus H/Zr atom composition. The two-phase plateau regions show typical constant pressure as the material shifts from one phase to the other associated with the absorption or desorption of hydrogen. Figure 2 presents information relevant to the selection of composition for ZrH_X for modulator use. For example use of $ZrH_{1.6}$ (δ phase) at 750°C will require a H_2 vapor pressure of 100's of mmHg to keep it in equilibrium otherwise it will lose H_2 and the composition the hydride will move to the left along the isotherm line until the equilibrium conditions are met.

Earlier investigations of ZrH_X as a modulator material indicated (Ref 1) swelling and distortion of ZrH_X components due to phase changes associated with hydrogen diffusion driven by thermal gradients. Those studies recommended that a composition of $ZrH_{1.6}$ that is centered in the δ phase region be used to mitigate the problem.

In conclusion it can be seen from the phase diagram of Figure 1 that the ZrH_X δ phase can exist over the temperature range of interest; however, the associated equilibrium vapor pressure can vary over several orders of magnitude.

B.3 DENSITY AS A FUNCTION OF COMPOSITION

Figure 3 shows the density of ZrH_X at room temperature for X greater than 1.22 (55 atom %) base on X-ray diffraction. This includes the α+δ(+γ), δ, and ε phases. The density at higher temperatures can be calculated using information below on thermal expansion coefficients (Table 2).

B.4 THERMAL PROPERTIES

Summarized information is provided below on thermal expansion, thermal conductivity and heat capacity.

B.4.1 Thermal Expansion Coefficient

The thermal expansion coefficients for various zirconium hydride compositions over the indicated temperature range are summarized in Table 2. Some of the values, given in angular brackets, are averages over the entire temperature range.

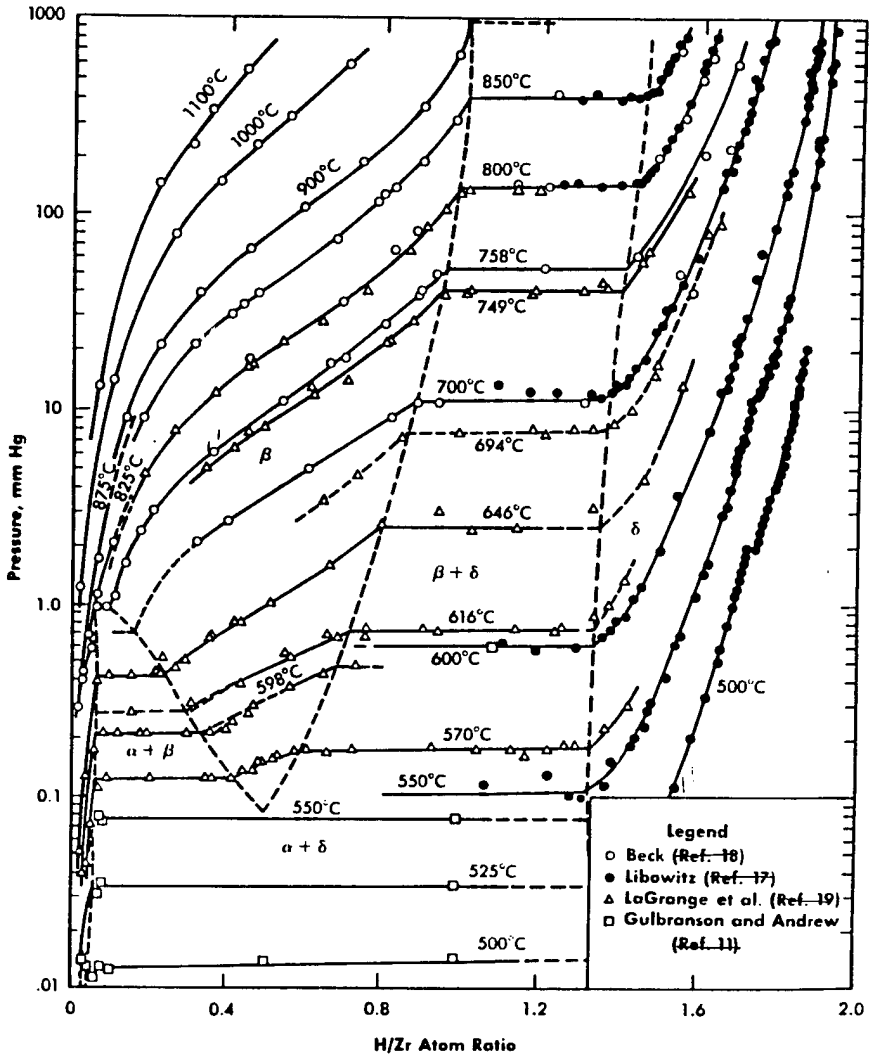

Figure 2. Pressure-composition Isotherms (Composite Data) (from Ref 1)

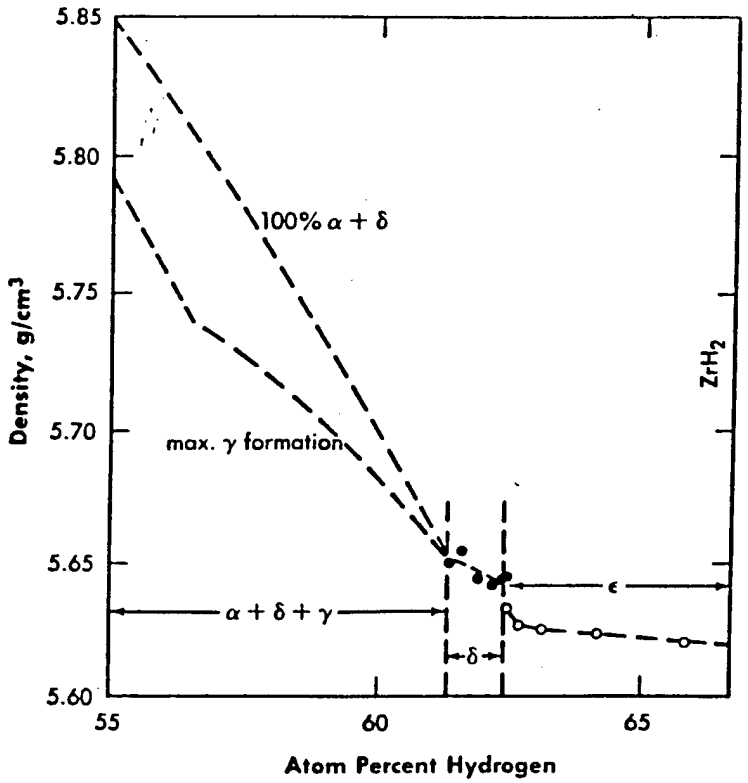

Figure 3. Density vs. Composition (Ref 1)

B.4.2 Thermal Conductivity

Accurate measurement of thermal conductivity of zirconium hydride is complicated by the diffusion and rearrangement in the structure being measured. Figures 4 and 5 provide information on the alpha plus delta, beta plus delta phase regions and the beta phase region respectively. Experimental evidence (Ref 1) suggests that thermal conductivity should increase with increased hydrogen content. This would at least bound an estimate for thermal conductivity of the δ and ε phases.

B.4.3 Heat Capacity

Figure 6 plots heat capacity C_p as a function of temperature for various compositions of zirconium hydride, including the δ phase ($ZrH_{1.58}$) and the ε phase ($ZrH_{1.78}$). Additional information is provided with thermodynamic data in Table 3.

TABLE 2. THERMAL EXPANSION COEFFICIENTS (REF 1)

COMPOSITION	*TEMP RANGE*	*COEFFICIENT THERMAL EXPANSION* $\frac{\Delta l}{l\ °C}$
$ZrH_{1.83}$	27° - 550° C	< 9.15×10^{-6} >
$ZrH_{1.92}$	27° - 427° C	< 9.03×10^{-6} >
$ZrH_{1.96}$	24° - 300° C	< 9.3×10^{-6} >
$ZrH_{1.83}$	550° C	19×10^{-6}
Zr (α PHASE)	24° - 362°	$5.5\text{-}6.5 \times 10^{-6}$
ZrH_x (PURE δ PHASE)	200° - 850° C	14.2×10^{-6}
ZrH_x (β PHASE)		
x = 0.60	650° - 760° C	10.6×10^{-6}
= 0.74	650° - 760° C	12.2×10^{-6}
= 0.77	650° - 760° C	11.2×10^{-6}

m9-1-MCL1-7268-20

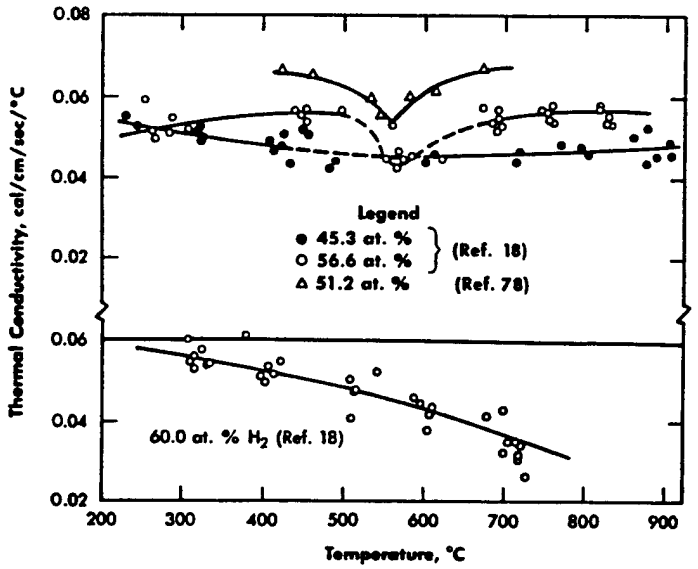

Figure 4. Thermal Conductivity of Zirconium-Hydrogen Alloys ($\alpha+\delta$, and $\beta+\delta$ Phase Regions) [Ref 1]

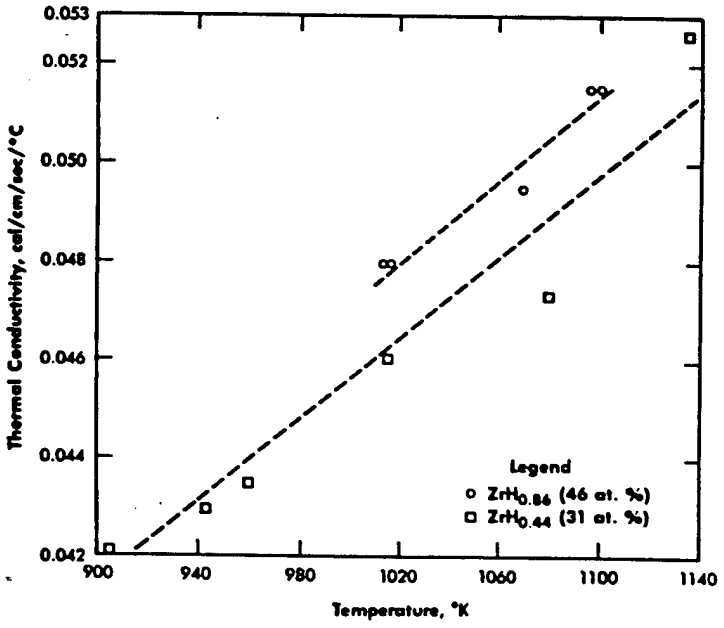

Figure 5. Thermal Conductivity of Beta Zirconium Hydride

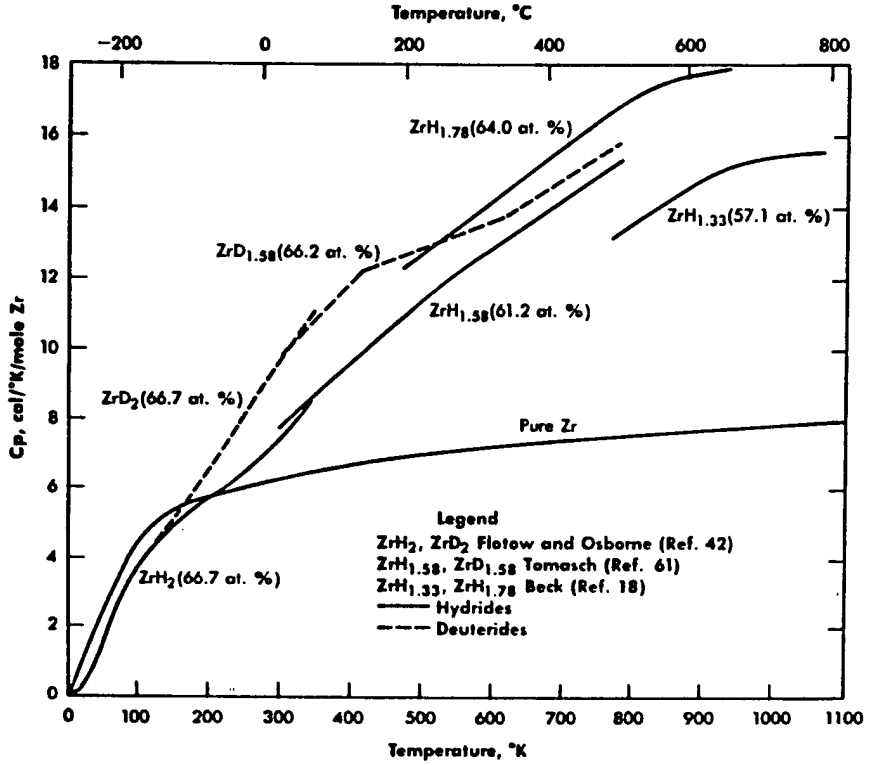

Figure 6. Heat Capacity vs. Temperature for Zr and Various Hydrides and Deuterides (Ref 1)

TABLE 3. THERMODYNAMIC FUNCTIONS OF ZRH_2

Temperature (°K)	C_p (cal/°K/mole)	S^o (cal/°K/mole)	$H^o - H^o$ (cal/°K/mole)	$-(F^o - H^o)/T$ (cal/°K/mole)
5	0.0068	0.0055	0.015	0.0026
10	0.0252	0.0149	0.087	0.0062
15	0.0706	0.0326	0.314	0.0117
20	0.1528	0.0631	0.853	0.0205
25	0.2863	0.1105	1.927	0.0334
30	0.469	0.1781	3.795	0.0516
35	0.700	0.2672	6.702	0.0757
40	0.964	0.3776	10.85	0.1063
45	1.246	0.5073	16.37	0.1435
50	1.540	0.6538	23.33	0.1871
60	2.117	0.9860	41.64	0.2920
70	2.648	1.353	65.54	0.417
80	3.116	1.738	94.40	0.558
90	3.519	2.129	127.64	0.711
100	3.848	2.517	164.52	0.872
110	4.130	2.898	204.45	1.039
120	4.374	3.268	247.00	1.210
130	4.568	3.626	291.82	1.381
140	4.768	3.973	338.60	1.554
150	4.930	4.308	387.11	1.727
160	5.078	4.630	437.16	1.898
170	5.219	4.943	488.65	2.069
180	5.354	5.245	541.52	2.237
190	5.490	5.538	595.74	2.403
200	5.630	5.823	651.33	2.566
210	5.775	6.101	708.35	2.728
220	5.925	6.373	766.84	2.887
230	6.082	6.640	826.87	3.045
240	6.250	6.903	888.52	3.201
250	6.430	7.161	951.91	3.353
260	6.617	7.417	1017.1	3.505
270	6.812	7.670	1084.3	3.654
280	7.014	7.922	1153.4	3.803
290	7.221	8.172	1224.6	3.949
300	7.435	8.420	1297.9	4.094
310	7.656	8.667	1373.3	4.237
320	7.880	8.914	1451.0	4.380
330	8.110	9.160	1530.9	4.521
340	8.342	9.406	1613.2	4.661
350	8.579	9.651	1697.8	3.702
273.15	6.875	7.750	1105.8	3.702
298.15	7.396	8.374	1284.1	4.067
	±0.015	±0.02	±2.0	±0.01

From H. E. Flotow and D. W. Osborne, Heat Capacities and Thermodynamic Functions of ZrH_2, *J. Chem, Phys.*, 34: 1423-1424 (1961).

B.5 THERMODYNAMIC DATA

The entropy and free energy of formation at 298°K are listed in Table 4 for delta and epsilon phase compositions of zirconium hydride. Table 3 contains values of thermodynamic functions calculated from heat capacity measurements over a range of low temperatures for the stoichiometric compound ZrH_2.

TABLE 4. ENTROPIES AND FREE ENERGIES OF FORMATION OF DELTA AND EPSILON ZIRCONIUM HYDRIDES (FROM REF 1)

	$\Delta S_{f(298)}$ (cal/°C/gram atom hydrogen)	$\Delta F_{f(298)}$ (kcal/gram atom hydrogen)
$ZrH_{1.5}$ (δ)	-24.1	-15.3
ZrH_2 (ε)	-16.1	-14.7
ZrH_2 (ε)	-17.4	-15.0

B.6 MECHANICAL PROPERTIES

The mechanical properties of zirconium are significantly effected as hydrogen content is increased. The ultimate tensile rapidly decreases as hydrogen content increases from 40 to 60 atom percent as shown in Figure 7. The δ phase is particularly brittle as shown in Figure 7.

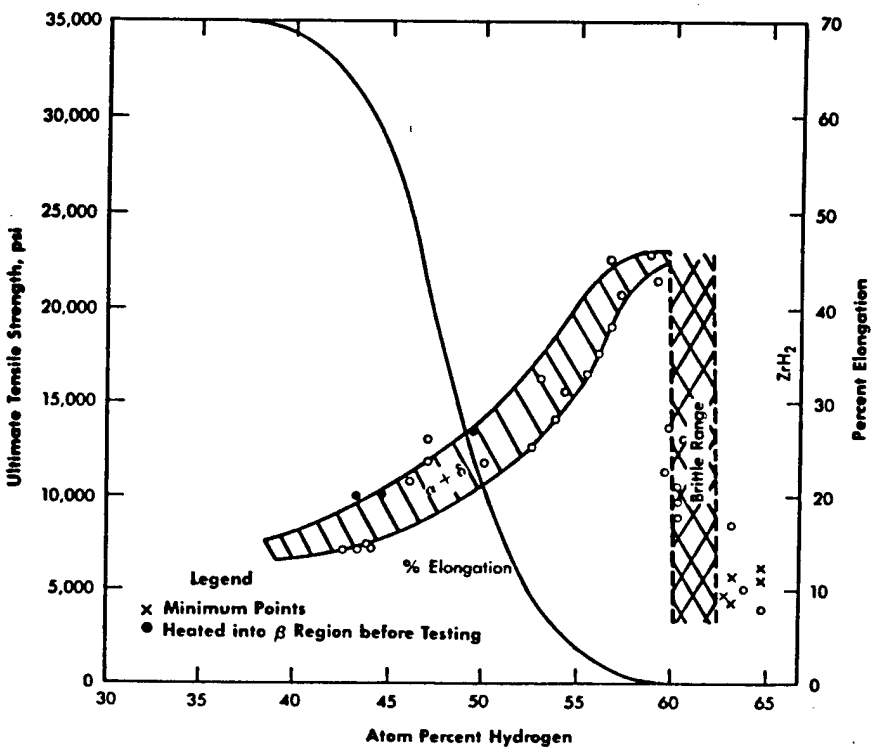

Figure 7. Ultimate Tensile Strength and Percent Elongation of Zirconium Hydride at 600°C. From R. L. Beck and W. M. Mueller, Mechanical Properties of Solid Zirconium Hydride, in *Nuclear Metallurgy, A Symposium on Metalic Moderators and Cladding Materials, Philadelphia, Oct. 19, 1960*, Vol. VII, p. 65, American Institute of Mining, Metallurgical, and Petroleum Engineers, New York, 1960.

The addition of small amounts of other metals alloying with the zirconium hydride have shown significant enhancements in the tensile strength. Table 5 compares the ultimate tensile strength and elongation for the alloyed and pure hydrides for ranges of atom percentages of H associated with the beta plus delta and delta region.

TABLE 5. MECHANICAL STRENGTH AND ELONGATION OF ALLOYED ZIRCONIUM HYDRIDE AT 600°C (REF 1)

ALLOYED HYDRIDE				COMPARISON TO PURE HYDRIDE	
Alloy Addition	Hydrogen (at%)	UTS (psi)	Estimated Elongation (%)	UTS (psi)	Estimated Elongation (%)
1 at.% Se	55.6	21.000	5	16,000 to 21,000	3.0
1 at.% Pr	54.7	14.620	25	15,000 to 20,000	4 1/2
1 at.% Y	55.5	16.300	29	16,000 to 21,000	6.0
	57.8	16.970	16	22,000 to 23,000	1/2
	62.6	12.560	Nil	~5,000	Nil

The diamond pyramid hardness (DPH) of zirconium hydride over a range of compositions is summarized in Figure 8. Reference 1 attributes the rapid decrease at 62-65 atom % H to a less brittle ε phase than δ phase.

B.7 CHEMICAL REACTIVITY

The information on chemical reactivity of ZrH_2 is summarized from Reference 2 in Table 6.

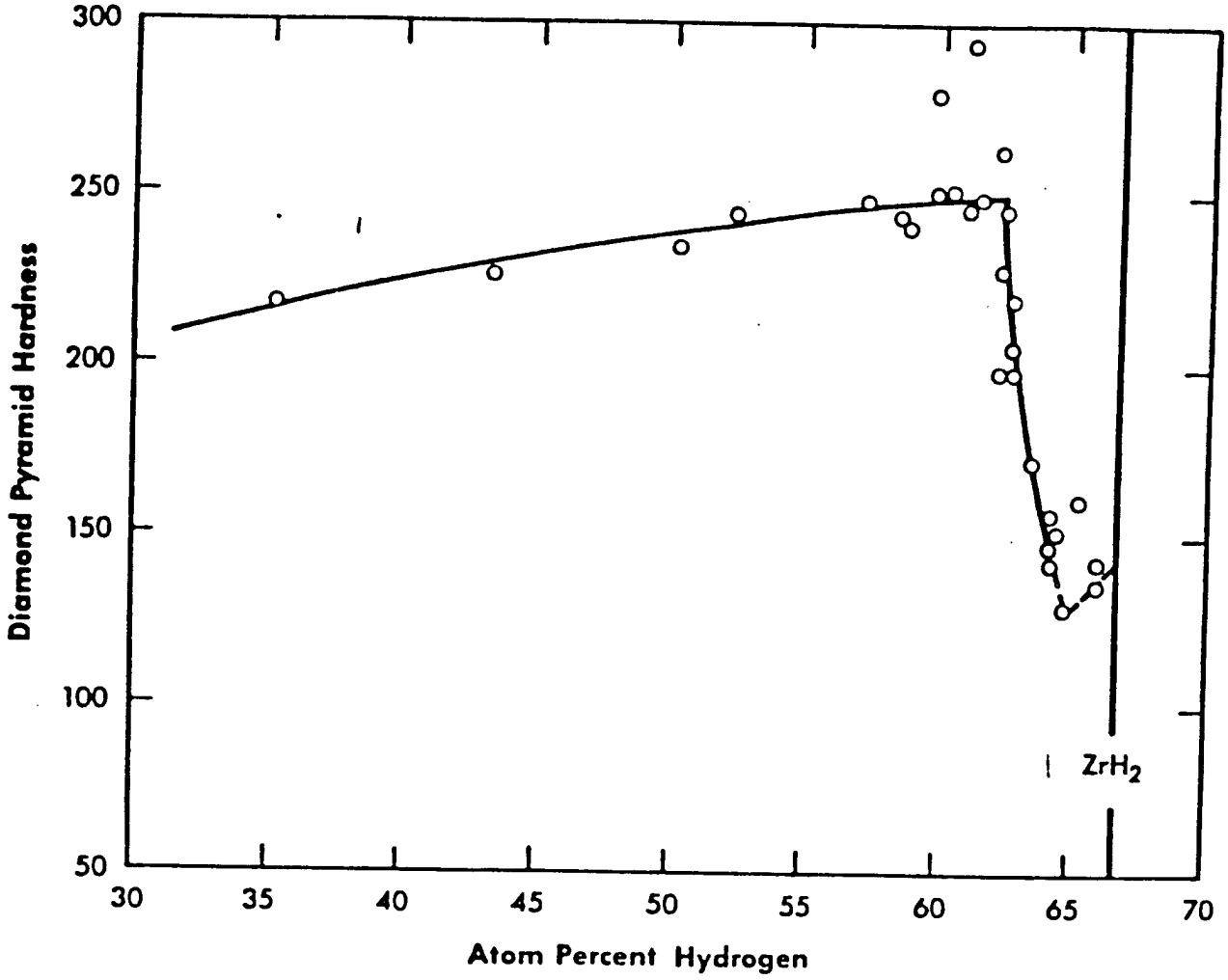

Figure Figure 8. Room-Temperature Hardness of Zirconium-Hydrogen Alloys. From R. L. Beck, Zirconium-Hydrogen Phase System, *Amer. Soc. Metals, Trans. Quart.*, 55: 550 (1962).

TABLE 6. ZrH_2 REACTIVITY

Material	Temperature	Environment	Reactivity
bulk ZrH_2	Room	air, water, H_2 inert gases	stable
bulk ZrH_2	to 440°C	vacuum	stable
bulk ZrH_2	430°C	air	combasts
Powdered ZrH_2 (3-18u)	260-440°C	air	spontaneously combusts
Powdered ZrH_2 (3-18u)	260-440°C	CO_2	stable
Powder as dust	560°C	CO_2	will combust
Powder	to 850°C	N_2 Ar, He	does not combust

In addition to this information Reference 1 describes experiments with δ $ZrH_{1.5}$ in CO_2 at temperatures of 1200°F (649°C). The hydride lost as much as 20% of its hydrogen and was severely corroded.

B.8 SUMMARY

The above discussion summarizes the information available on key properties of zirconium hydride, particularly for the δ and ε phases in the temperature range of 500 to 1000°K. Most of the information was obtained from a few comprehensive references published in the late 1960's. While more research has, no doubt, been conducted, the information does not yet appear to be compiled in comparable references. The δ and ε phases are of particular interest because of their high H content relative to other phases and the associated impact for a moderator material. These phases are stable over the temperature range of interest in that they do not undergo phase transitions (Figure 1) if maintained with equilibrium hydrogen pressure for constant composition. The equilibrium hydrogen pressure at 1000°K is less than 1 atmosphere.

REFERENCES

1. Mueller, W. M., Blackledge, J. P., and Libowitz, G. G., Metal Hydrides Academic Press, New York, 1968

2. Vol, A. E. Handbook of Binary Metallic Systems Structures and Properties, 1967

3. Kirk-Othmer Encyclopedia of Chemical Technology Wiley-Interscience 3rd Edition, 1978

4. A. F. Andresen, and A. J. Maeland, Hydrides for Energy Storage, Proceedings of an International Symposium held in Geilo, Norway, 14-19 August, 1977, Pergamon, 1978.

5. "SNAP reactor reflector control systems development" Proc. 23rd Intersoc. Energy Convers. Eng. Conf. 1988, p. 239-44

6. "Multikilowatt Space Power System using zirconium hydride-moderated reactor and organic Rankine power conversion," Proc. 22nd Intersoc. Energy Conversion Eng. Conf. 1987, p. 444-8.